Investigation into Mechanisms of Functional Mitral Regurgitation by Advanced Echocardiographic Technologies - Dyssynchrony and Beyond

LIANG, Yujia

A Thesis Submitted in Partial Fulfillment
of the Requirements for the Degree of
Doctor of Philosophy
in
Medical Sciences

The Chinese University of Hong Kong
October 2009

To my dearest husband, Zeng Jian

To my sweat little girl, Zeng Zi-Tong

To my open-minded parents, Tian Qing-Cheng and Liang Zeng-Jun

whose love and understanding made this dissertation possible

ACKNOWLEDGEMENTS

I would like to express my sincerely appreciation to all the people who have helped me during the whole period of my study.

My gratitude first goes to my supervisor, Professor Yu Cheuk-Man, for giving me this precious opportunity to study here, for his inspiring ideas in clinical research in echocardiography, invaluable guidance, helpful and constructive advice in my research work, and for his encouragement, support and confidence over the whole period of my study.

My sincerely gratitude also goes to my co-supervisors, Professor Qing Zhang and Professor Gabriel Yip, for their invaluable guidance, helpful and creative suggestions, and tremendous encouragement.

I would like to sincerely thank my colleagues in cardiac team for their support and advice: Dr. YY Lam, Dr. PW Lee, Ms. Pearl Ho, Ms. Dico Tse, Ms. Cramen Chow, Ms. Skiva Chan, Ms. Leata Yeung, Ms. Sheung Poon, Miss Kidius Tam and Miss. Tracy Lam.

Last, but not least, I would like to express my sincere thanks to my good friends for their enthusiastic help, countless encouragement and warmly friendship: Chunyan-Ma, Fang-Fang, Qing-Shang, Rickie Lee, Jean Dong, Mango Zhang, Yueyi-Wen and Maple Xie.

PUBLICATIONS AND PRESENTATIONS

Full Papers

1. Yu-Jia Liang. Qing Zhang, Jeffrey Wing-Hong Fung, Joseph Yat-Sun Chan, Gabriel Wai-Kwok Yip, Yat-Yin Lam, Cheuk-Man Yu. Impact of reduction in early- and late-systolic functional mitral regurgitation on reverse remodeling after cardiac resynchronization therapy. (submitted)

2. Yu-Jia Liang. Qing Zhang, Jeffrey Wing-Hong Fung, Joseph Yat-Sun Chan, Gabriel Wai-Kwok Yip, Yat-Yin Lam, Pui-Wei Lee, Cheuk-Man Yu. Improvement of early- and late-systolic mitral regurgitation contributed by global reverse remodeling and improvement of mitral deformation after cardiac resynchronization therapy. (submitted)

3. Yu-Jia Liang. Qing Zhang, Gabriel Wai-Kwok Yip, Yat-Yin Lam, Pui-Wei Lee, Cheuk-Man Yu. Incremental value of left ventricular mechanical dyssynchrony in predicting significant functional mitral regurgitation in patients with left ventricular systolic dysfunction. (submitted)

4. Yu-Jia Liang. Qing Zhang, Jeffrey Wing-Hong Fung, Joseph Yat-Sun Chan, Gabriel Wai-Kwok Yip, Yat-Yin Lam, Pui-Wei Lee, Cheuk-Man Yu. Differential changes in left ventricular myocardial deformation in patients with and without significant functional mitral regurgitation. (submitted)

5. Qing Zhang, Fang Fang, Gabriel Wai-Kwok Yip, Joseph Yat-Sun Chan, Qing Shang, Jeffrey Wing-Hong Fung, Anna Kin-Yin Chan, Yu-Jia Liang, Cheuk-Man Yu. Difference in prevalence and pattern of mechanical dyssynchrony in left bundle branch block occurring in right ventricular apical pacing versus systolic heart failure. ***Am Heart J*** 2008;156:989

6. Chin-Pang Chan, Qing Zhang, Gabriel Wai-Kwok Yip, Jeffery Wing-Hong Fung, Yat-Yin Lam, Pui-Wai Lee, Eugene B. Wu, Qing Shang, Yujia Liang, Cheuk-Man Yu. Relation of left ventricular systolic dyssynchrony in patients with heart failure to left ventricular ejection fraction and to QRS duration. ***Am J Cardiol*** 2008;102:602.

Abstracts

1. Y.J. Liang , Q. Zhang, J.W.H. Fung, J.Y.S. Chan, G.W.K. Yip, C.M. Yu. Impact of cardiac resynchronization therapy on phasic change of mitral regurgitation. ***International Journal of Cardiology*** 2008; 125 (suppl): 56. Poster presentation.

2. Y.J. Liang, Q. Zhang, G.W.K. Yip, P.W. Lee, H. Meng, J.M. Xie, C.M.Yu. Effect of left ventricular dyssynchrony on the severity of ischemic mitral regurgitation in patients with ischemic left ventricular systolic dysfunction. Poster presentation at **Euroecho 2008**.

3. Y.J. Liang, Q. Zhang, J.W.H. Fung, J.Y.S. Chan, G.W.K. Yip, Y.Y. Lam, C.M. Yu. Impact of functional mitral regurgitation on left ventricular reverse remodeling after cardiac resynchronization therapy. Accepted for poster presentation at **Euroecho 2009**

LIST OF ABBREVIATIONS

2D = two-dimensional

2DSTE = two-dimensionaLl speckle tracking echocardiography

3D = three-dimensional

ACEi = angiotensin-converting enzyme inhibitor

APM-PPM delay = the absolute difference in time to peak systolic velocity between the mid lateral and mid inferior left ventricular segments

ARB = angiotensin receptor blocker

AUC = area under curve

AV = atrioventricular

AVO = aortic valve opening

AVC = aortic valve closure

CRT = cardiac resynchronization therapy

CW = continuous wave Doppler

+dp/dt = pressure rise in systole

EROA = effective regurgitant orifice area

JA/LAA = ratio of mitral regurgitant jet area to left atrial area

LA = left atrium

LBBB = left bundle branch block

LV = left ventricle

LVEDV = left ventricular end-diastolic volume

LVESV= left ventricular end-systolic volume

LVOT = left ventricular outflow tract

MAA = mitral annular area

MLWHF = Minnesota Living with Heart Failure

MVC = mitral valve closure

MVO= mitral valve opening

MR = mitral regurgitation

NYHA = New York Heart Association

PISA = proximal isovelocity surface area

PW = pulse wave Doppler

RA = right atrium

RBBB = right bundle branch block

ROC = receiver operating characteristics

Rot = peak rotation

RV = right ventricular

TDI = tissue Doppler imaging

Tor = left ventricular torsion

Ts = the time from the beginning of the QRS complex to peak systolic velocity in the ejection phase

Ts-dif = the maximal difference in time to peak systolic velocity in ejection phase of the 12 LV segments by TDI, i.e. dyssynchrony index

Ts-SD = the standard deviation of time to peak systolic velocity in ejection phase of the 12 LV segments by TDI, i.e. dyssynchrony index

TVI = time-velocity integral

ε-circum = peak systolic circumferential strain

ε-long = peak systolic longitudinal strain

ε-radial = peak systolic radial strain

TABLE OF CONTENTS

ABSTRACT

Functional mitral regurgitation (MR) is a common complication of left ventricular (LV) systolic dysfunction, which conveys adverse prognosis. There are multiple factors interact in causing functional MR, whereas the basic mechanism is believed to be the mismatch between increased mitral leaflet tethering due to the outward displacement of papillary muscles and reduced closing force in systolic dysfunction. Both conditions can be attributed by global and regional LV remodeling. LV mechanical dyssynchrony, which illustrates discoordinated contraction of the LV segments, has been suggested to occur in heart failure with a high prevalence and implies a poor prognosis. It has been postulated that the presence of regional LV mechanical dyssynchrony between the papillary muscle attaching sites would participate in the pathogenesis of functional MR as an additional factor. However, the contribution of LV global mechanical dyssynchrony has not been evaluated.

On the other hand, functional MR is increasingly recognized as a ventricular disease, in which the primary problem exists in the LV myocardium rather than in the mitral valve itself. During the development of congestive heart failure, the LV undergoes complex change in geometry and function, accompanied by alterations of individual myocardial deformational component. The presence of functional MR may further burden the failing LV with additional volume overload. However, it is unknown whether there is any difference in myocardial deformation between heart failure patients with and without functional MR.

Cardiac resynchronization therapy (CRT) is an established therapy for patients with advanced congestive heart failure and prolonged QRS duration, aiming at correcting

dyssynchrony in the LV. Apart from the beneficial effects on cardiac function and LV reverse remodeling, reduction in functional MR has been observed by Doppler echocardiography after CRT. On the other hand, functional MR in fact varies over the cardiac cycle that a biphasic pattern has been reported, i.e. early- and late-systolic peaks with a mid-systolic decrease in regurgitant flow. Nevertheless, it remains to be explored whether (1) the improvement of MR leads to a greater extent of LV reverse remodeling; (2) the different components (i.e. early- and late-systolic) of MR improve and their predictors if any.

Echocardiography has a prominent role in assessing MR severity, local geometric changes in mitral apparatus, LV remodeling/reverse remodeling, cardiac function and mechanical dyssynchrony, in particular by use of advanced techniques such as tissue Doppler imaging (TDI) and two-dimensional (2D) speckle tracking echocardiography (2DSTE).

We performed echocardiography with TDI and 2DSTE in 147 patients of both ischemic and non-ischemic etiologies with LV systolic dysfunction (defined as LV ejection fraction <50%) and 45 normal controls. MR severity, displacement of papillary muscle, mitral annular dilation and dysfunction, mitral leaflet tenting, LV remodeling and function were assessed by 2D and Doppler echocardiography. LV mechanical dyssynchrony indices were derived from TDI velocity. Myocardial strain (i.e. amount of deformation) in longitudinal, circumferential and radial directions and torsion (opposite rotational movement between apex and base of the heart) were measured by 2DTSE.

We also recruited a group of 83 patients with chronic heart failure who received CRT. Serial echocardiographic assessments were performed at baseline and three months after CRT, where MR measures included ratio of MR jet area to left atrial area, total MR volume, early- and late-systolic MR flow rate. Parameters of mitral valve deformation, LV reverse remodeling, function and dyssynchrony (both global and regional) were also obtained.

The main findings were as follows:

LV global systolic dyssynchrony served as an independent predictor for the presence of significant functional MR in patients with LV systolic dysfunction. Although mitral valvular tenting area was the most powerful predictor, LV global systolic dyssynchrony added incremental value to mitral valve tenting area in predicting the presence of significant functional MR.

Despite comparable ejection fraction, higher degree of functional MR was associated with further impairment in short-axis myocardial deformation (circumferential and radial), but not with long-axis myocardial deformation. The degree of LV basal rotation was also lower in the MR patient group. Furthermore, the decrease in myocardial deformation was associated with greater extent of LV remodeling.

The improvement of functional MR was an independent predictor of LV reverse remodeling after CRT. The extent of LV reverse remodeling (reduction of LV end-systolic volume) was greatest in patients with improvement of MR, followed by those with "mild or no" MR at baseline, and was least in those without improvement of MR.

CRT reduced functional MR by reducing both its early- and late-systolic components in heart failure patients. The reductions in LV end-systolic volume and dyssynchrony were related to the improvement of early-systolic MR, while the improvement of late-systolic MR was attributable to the reductions in mitral leaflet tenting and LV dyssynchrony.

In conclusion, LV global mechanical dyssynchrony play a role in determining the severity of functional MR in addition to mitral leaflet tenting in patients with LV systolic dysfunction. Functional MR is associated with further impairment of myocardial deformation, but with differential change in individual component of myocardial deformation. CRT reduces functional MR in both early- and late-systolic phases, by way of improvement in LV remodeling, LV dyssynchrony and mitral leaflet tenting. Meanwhile, the improvement of MR contributes to LV reverse remodeling after CRT.

摘要

功能性二尖瓣返流常见于缺血性和非缺血性心肌病所导致的左室收缩功能不全患者。它的出现往往提示患者预后不良。功能性二尖瓣返流的机制复杂，涉及多种因素。但乳头肌移位导致二尖瓣受牵拉以及左室收缩功能不全引起的关闭力量减弱被认为是其基本机制。而左室整体和局部重构是引起乳头肌移位和左室收缩功能不全的原因。左室机械收缩不同步（左室各节段的不协调收缩）在心力衰竭患者中的发生率很高。有研究证实左室两组乳头肌附着部位局部的机械收缩不同步参与了功能性二尖瓣返流的发生机制，但目前尚不清楚左室整体机械收缩不同步在功能性二尖瓣返流发生中的作用。

功能性二尖瓣返流被认为是左心室的疾病而非二尖瓣结构本身的问题。在充血性心力衰竭的发生发展过程中，左室的几何形态和功能以及心肌的形变都发生了一系列的变化。二尖瓣返流的发生会进一步加重心力衰竭患者左室的容量负荷，但它对左室各方向心肌形变的影响如何目前尚无研究报道。

心脏再同步化治疗(CRT)是一项针对伴有QRS波延长的充血性心力衰竭患者的治疗方法。它可以纠正左室收缩不同步。CRT 可改善心力衰竭患者的心功能状况并引起左室逆转重构。此外它还能明显减少功能性二尖瓣返流。功能性二尖瓣返流的严重程度在一个心动周期中呈双向型变化：收缩早期和收缩晚期返流量较多，而收缩中期返流量较少。目前尚不清楚：（1）CRT 术后功能性二尖瓣返流的减少是否会影响左室逆转重构的程度；（2）收缩早期和收缩晚期二尖瓣返流对 CRT 治疗的反应及其相关机制。

超声心动图，尤其是一些新兴的超声技术如组织多普勒成像和二维斑点追踪技术，在评价二尖瓣返流的程度、二尖瓣结构的几何形状变化、左室重构和

逆转重构、心脏功能及同步性方面具有优势。

本研究纳入了 147 例患有缺血性和非缺血性心力衰竭（定义为左室射血分数低于 50%）的患者。我们运用二维和多普勒超声对这组患者的二尖瓣返流程度、乳头肌移位、二尖瓣环扩张、瓣叶膨出程度、左室重构及其收缩功能进行了评价。同时我们还运用组织多普勒技术，通过检测左室 12 个节段中达到峰值收缩速度的时间差异对左室整体和两组乳头肌附着部位局部的机械收缩不同步进行了评价。此外我们还运用了二维斑点追踪技术测量了左室长轴、圆周、径向应变及左室扭转，对左室各方向的形变进行了评价。

同时，本研究还纳入了 83 例接受 CRT 治疗的患者，并且分别在植入起搏器前和植入后三个月对这些患者进行超声心动图检查。测量指标包括：二尖瓣返流束面积与左房面积之比值，二尖瓣总返流量，收缩早期和收缩晚期的二尖瓣返流流率，以及反映左室重构、收缩功能和机械收缩同步性的指标。

以下是本研究的主要发现：

在左室收缩功能不全的患者中，左室整体机械收缩不同步，而非两组乳头肌附着部位局部的机械收缩不同步是功能性二尖瓣返流的独立预测因素。尽管二尖瓣叶的膨出面积是功能性二尖瓣返流的最强独立影响因素，左室整体机械收缩不同步再此基础上对功能性二尖瓣返流具有额外的预测价值。

左室不同方向的形变也与功能性二尖瓣返流的严重程度有关，，但不同方向形变的变化程度不同。在左室射血分数无显著性差异的情况下，随着二尖瓣返流程度加重，左室短轴方向的形变（径向应变和圆周应变）降低，但左室长轴方向的应变不随二尖瓣返流程度变化。左室基底段的旋转角度随着二尖瓣返流程度的加重而减少，但左室心尖段的旋转和左室扭转不随二尖瓣返流程度变化。

而且，以上左室形变的差异与左室重构的程度相关。

CRT 植入后功能性二尖瓣返流的改善程度与左室逆转重构的程度有关。在多因素回归分析中，CRT 植入后功能性二尖瓣返流的减少程度是左室逆转重构的独立预测因素之一。左室逆转重构的程度在 CRT 术后二尖瓣返流减少的患者中最高，在 CRT 术前没有或仅有少量二尖瓣返流的患者中次之，在 CRT 术后二尖瓣返流未减少的患者中最低。

在心力衰竭患者中，CRT 可同时减少收缩早期和收缩晚期的功能性二尖瓣返流。左室收缩末期容积的减少和机械收缩不同步的改善与收缩早期功能性二尖瓣返流的减少有关；而二尖瓣膨出面积的减少和左室机械收缩不同步的改善与收缩晚期功能性二尖瓣返流的减少有关。

总之，功能性二尖瓣返流的发病机制涉及多种因素，其中二尖瓣叶的受牵拉变形是左室局部和整体重构作用于二尖瓣的最后共同通路。除此之外，左室整体机械收缩不同步也是影响心力衰竭患者功能性二尖瓣返流程度的重要因素。左室不同方向的形变也与功能性二尖瓣返流的严重程度有关，但不同方向的形变所发生的变化不同。CRT 可同时减少收缩早期和收缩晚期的功能性二尖瓣返流。其作用机制是通过左室逆转重构，改善机械收缩不同步和减少二尖瓣叶膨出。另一方面，CRT 术后二尖瓣返流的减少也会影响左室逆转重构的程度。

SECTION I

INTRODUCTION

CHAPTER 1 INTRODUCTION

1.1 Normal Anatomy and Function of Mitral Valve

Mitral valve is a dual-flap valve in the heart located between the left atrium (LA) and the left ventricle (LV). Normally, mitral valve only allows blood to flow from LA to LV during the diastolic period while it closes completely to prevent blood from back flowing into the LA during the systolic period. The mitral valve apparatus is a complex anatomical structure formed by the following components: mitral annulus, two leaflets (anterior and posterior), chordae tendineae (primary, secondary and tertiary), two papillary muscles (anterolateral and posteromedial), as well as the basal and mid LV free wall which bears papillary muscles and in continuity with mitral annulus (Figure 1.1). Competent mitral valve function requires a proper interaction of all these components.

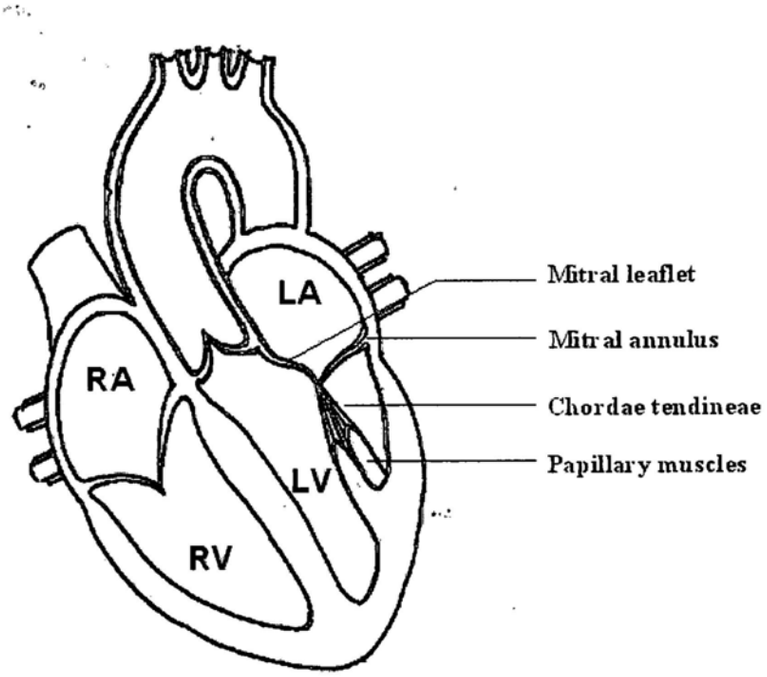

Figure 1.1 Schematics of the mitral valve which is located between the left atrium (LA) and the left ventricle (LV).

1.1.1 Mitral Annulus

Mitral annulus is a flexible junctional zone that separates the muscles of LA and LV that gives attachment to the mitral valve leaflets. It consists of discontinuous fibrous and muscular tissue and becomes a part of the fibrous skeleton of the heart. The anterior one-third of annular ring is formed by fibrous tissue shared with aortic annulus. The fixed portion between anterior mitral annulus and aortic annulus is called "fibrosa", which serves as a landmark for assessing the apical displacement of papillary muscles (i.e. papillary-fibrosa distance). The posterior two-thirds of annular ring is basically formed by muscular tissue with little fibrous tissue. It has the ability to contract that is responsible for the major changes in the circumference of mitral annulus during the cardiac cycle (1-4).

The normal mitral annular ring is roughly "D-shaped". The anterior part of mitral annulus shared with aortic annulus is straighter than the other parts. The intercommissural dimension is longer than the septal-lateral dimension. Furthermore, mitral annulus is a nonplanar, saddle-shaped structure from a three-dimensional view. The higher points (far from the LV apex) of the annulus are located near the midpoints of anterior and posterior annular segments, whereas the lower points are located posteromedially and anterolaterally near the commissure (3-8).

The complex deformation of mitral annulus throughout a cardiac cycle has been revealed by tracing the annular motion and its shape. Firstly, the whole annulus moves upward into the atrium in diastole and toward the ventricular apex during systole. Secondly, the distance between the two higher points of the annulus lengthens during diastole and shortens during systole while the annular height

decreases during diastole and increases during systole. Thirdly, the annular region adjacent to the posterior leaflet moves toward the relatively immobile anterior annulus during systole and moves away during diastole, resulting in the change of annular shape from more circular in diastole to elliptical in systole. Therefore, the circumference and cross-sectional area of the annulus vary during a cardiac cycle due to the complex geometric changes. The maximal annular area occurs in late diastole, while the minimal annular area occurs in early- to mid-systole. The systolic contraction of mitral annulus has an important contribution to mitral valve closure where the magnitude of change in mitral annular area is 20 to 40% in normal subjects (3, 4, 7-12).

1.1.2 Mitral Leaflets

Mitral valve has two major leaflets: the anterior (also known as aortic or septal) leaflet and the posterior (or mural) leaflet. The two leaflets arise from mitral annulus attached to papillary muscles by primary and secondary chordae tendineae. They are separated by the posteromedial and anterolateral commissure from the annular ring. The anterior mitral leaflet is roughly triangular in shape and occupies approximately one-third of the circumference of mitral annulus. It is in direct continuity with the fibrous skeleton of the heart. The posterior mitral leaflet is rectangular in shape and occupies approximately two-thirds of the annular circumference. The free margin of the posterior mitral leaflet has two major clefts, which divide the posterior leaflet into three scallops: the largest or middle scallop, the posteromedial scallop, and the anterolateral scallop. The anterior mitral leaflet is larger than the posterior mitral leaflet and the surface area of both leaflets together is about twice as large as that of

the mitral orifice (13, 14). This enables the two leaflets to coapt with a large coaptation area during systole, which is important for a complete valve closure.

1.1.3 Chordae Tendineae

Chordae tendineae are cords of connective tissue that arise from papillary muscles or LV free wall attached to mitral leaflets. They are divided classically and functionally into three groups: primary, secondary, and tertiary chordae (15). Primary chordae originate from the papillary muscle heads, divide progressively and attach to the free edge of the leaflets. They are useful for preventing the prolapse of valve edge during systole. Secondary chordae (including two or more larger and less branched "strut" chordae) also originate from the papillary muscle heads but attach to the ventricular surface of the leaflets. They are responsible for anchoring the mitral valve. The primary and secondary chordae attach to both anterior and posterior mitral leaflets, whereas the tertiary chordae are unique to the posterior leaflet. They originate directly from the trabeculae carneae of LV wall and attach to the posterior leaflet near mitral annulus (14-16).

1.1.4 Papillary Muscles and LV Wall

Papillary muscles are columns of myocardium that arise from the middle third of LV free wall and protrude into the LV cavity. Normally, there are two prominent papillary muscles located in the mid anterolateral and posteromedial segments of LV wall. The axes of two papillary muscles are perpendicular to the mitral annular plane. The chordae tendineae of either leaflet arise from the tips of both anterolateral and posteromedial papillary muscles (14).

The anterolateral papillary muscle has a double blood supply from branches of the circumflex and left anterior descending coronary arteries. In contrast, the posteromedial papillary muscle is only supplied by a single artery arising from the right coronary artery or terminal circumflex artery. This explains why infarction of the posteromedial papillary muscle is more commonly observed in myocardial infarction (16-19).

Papillary muscles shorten during LV ejection phase and lengthen during diastolic period while remain minimal changes during isovolumic periods. The shortening of papillary muscles during systole serves to facilitate mitral valve opening, while the elongation of papillary muscles during diastole contributes to proper mitral valve closure (20, 21).

1.1.5 Normal Closure of Mitral Valve

Both anterior and posterior mitral leaflets contribute to an effective mitral valve closure, though the movement of posterior leaflet is more restricted than that of anterior leaflet. The onset of mitral valve closure at end-diastole is actually initiated by atrial contraction, but the small pressure gradient between LV and LA is inadequate for a complete closure. Mitral valve closure is completed about 10 to 40 ms after the initial systolic rise in LV pressure. Therefore, a competent mitral valve closure requires an increase in LV pressure exceeding LA pressure by ventricular contraction which gives rise to enough closing force. In addition, a proper mitral annular size and adequate leaflet surface area available to cover the mitral orifice area are needed (22-26).

1.2 An Overview of Functional Mitral Regurgitation (MR)

1.2.1 What is Functional MR

MR is defined as a retrograde blood flow from LV to LA through mitral valve. Based on whether it is caused by intrinsic lesions of the mitral valve apparatus, MR can be divided into two categories: organic (or primary) and functional (or secondary) MR. MR is defined as "organic" when it is caused by intrinsic lesions of mitral valve leaflets and their immediate supporting apparatus such as papillary muscles and chordae tendineae. Otherwise, MR is "functional" as a result of the dilation of LV cavity and/or alteration of LV chamber geometry. Mitral valve leaflets, papillary muscles and chordae tendineae appear normal in structure by surgical inspection or echocardiographic examination in functional MR, though the leaflets fail to coapt properly. By Carpentier's classification (27) (Table 1.1) (28), the type IIIb is most commonly observed in functional MR, which is characterized by restricted mitral leaflet motion during systole and leaflet tethering due to papillary muscle displacement.

Table 1.1 Carpentier's Pathophysiological Triad in MR

Dysfunction	**Leaflet Motion**	**Lesions**	**Chronic vs. Acute**
Type I	Normal	Annular dilation	Chronic
Type II	Increased	Chordal rupture	Acute
	Increased	Papillary muscle rupture	Acute
	Increased	Papillary muscle elongation	Chronic
Type IIIa	Restricted during systole and diastole	Leaflet thickening/retraction Chordal thickening/shortening Commissural fusion	Chronic
Type IIIb	Restricted during systole only	Papillary muscle displacement/leaflet tethering	Acute or chronic

On the other hand, "ischemic MR" refers to MR that occurs only in ischemic heart disease. It may develop in the acute or chronic phase after myocardial infarction. The MR secondary to papillary muscle infarction and rupture during the acute phase is not included in functional MR. However, the MR mainly caused by the remodeling of LV wall during chronic phase is called "functional" where no lesions found in mitral leaflets, papillary muscles and chordae tendineae. In most cases, "ischemic MR" indicates the chronic functional ischemic MR.

1.2.2 Functional MR and LV Remodeling

Functional MR, as a complication of LV dilation and systolic dysfunction, can further aggravate LV remodeling with the increase in LV volumes and reduction in ejection fraction. During systole, the returning of blood from LV to LA results in

decreased forward blood flow and elevated LA filling pressure. During diastole, more blood enters LV from LA has given rise to LV volume overload. In the long term, LV systolic and diastolic wall stress are increased (29-31) which in turn can aggravate LV remodeling by activating matrix metalloproteinases for degrading extracellular matrix (32) as well as increasing neurohumoral and cytokine promoters of remodeling. Furthermore, the serial changes accompanying LV remodeling that include further papillary muscle displacement, leaflet tethering and annular dilation increase the severity of functional MR. Therefore, functional MR and LV remodeling set up a vicious circle where functional MR may beget functional MR in a self perpetuating manner.

1.2.3 Prevalence of Functional MR

Functional MR is quite common in patients with congestive heart failure, in particular those with LV systolic dysfunction. In a large study including >2,000 patients with symptomatic LV systolic dysfunction defined as ejection fraction <40%, the occurrence and severity of functional MR were assessed by angiography. It was shown that functional MR of any grade was present in about 60% of the patients. Among the patients with MR, most of them (70%) had a mild degree of regurgitation while the other 30% had moderate or severe regurgitation (33). Another study investigated 1,421 patients with LV ejection fraction $\leq$ 35% by color Doppler echocardiography showed that moderate or severe functional MR was observed in about half of the patients, including moderate MR in 30% and severe MR in 19% (34).

On the other hand, the prevalence of functional MR is difficult to estimate in patients after myocardial infarction due to several factors which include the diagnostic techniques being used, timing of examination after myocardial infarction and heterogeneity of the study population. It was reported to occur in 1.6% to 19.4% in angiographic studies (35-39) and from 8% to 74% by color Doppler echocardiography (40-49). Risk factors for developing functional MR after myocardial infarction include advancing age, female gender, history of inferior or a combined anterior-inferior myocardial infarction, multiple vessel coronary artery disease, congestive heart failure, recurrent ischemia as well as large infarct size.

1.2.4 Impact of Functional MR on Outcome

The adverse impact of functional MR on survival rate and exercise capacity has been confirmed in patients with congestive heart failure. Several studies revealed that the presence of functional MR in patients with congestive heart failure was an independent predictor of worse survival (33, 34). In a study of >2,000 patients with LV systolic dysfunction who were followed up for five years, functional MR was an independent predictor of long-term mortality. In addition, a dose-response relationship was observed between the severity of functional MR and survival. An increase risk of death by 23% was found to be associated with a change from no MR to mild MR as well as a change from mild to moderate or severe MR. This relationship between functional MR and survival was present in both patients with ischemic and non-ischemic cardiomyopathy (33). Nevertheless, sometimes even the presence of mild MR would have a detrimental effect. In a small study that included 30 patients with dilated cardiomyopathy, a significantly lower peak workload, peak

oxygen uptake and peak oxygen pulse were observed in patients with functional MR with compared to those without (50).

Similarly, in patients after myocardial infarction, the presence of functional MR is associated with an increased risk of heart failure and death (40, 51, 52). It is independent of all other clinical and LV characteristics such as age, sex, history of myocardial infarction, and ejection fraction. Moreover, the risk of congestive heart failure and cardiac death is closely related to the severity of MR. It was found that patients with effective regurgitant orifice area (EROA)$\geq$20mm^2 had four times higher the risk of congestive heart failure than patients without MR, with an absolute rate close to 70% at the end of five-year follow up (52). Similarly, EROA$\geq$20mm^2 was associated with a markedly excess mortality in another study in which the adjusted relative risk (RR) was 2.23 versus those without MR (51).

1.2.5 Diastolic MR

Functional MR not only occurs during systolic period, but also may occur during late-diastolic (or pre-ejection) period in some patients. Diastolic MR is often observed in patients with elevated LV end-diastolic pressure as well as in patients with prolonged atrioventricular (AV) interval such as first degree and complete AV block (53-56). In normal subjects, mitral valve closure is actually initiated by LA contraction, which induces a slightly higher LV diastolic pressure than LA pressure. This reversal of diastolic AV pressure gradient usually moves the mitral leaflets closer to each other before the onset of ventricular contraction, though it is insufficient to close the mitral valve completely. The subsequent ventricular contraction produces enough closing force for a complete closure of mitral valve.

Therefore, it is important to have a proper time interval between atrial and ventricular contraction for a complete closure. However, in patients with a prolonged AV interval, ventricular contraction may be very delayed after atrial contraction where the reversed AV pressure gradient in late-diastole may result in significant MR. This phenomenon could be more obvious in the presence of tethered mitral valve when a greater AV pressure gradient is needed to exert enough closing force to move the leaflets toward a complete closure (57).

1.2.6 Phasic Change of Functional MR

The severity of MR can be affected by many factors, including ventricular volume and shape, loading condition, transmitral pressure gradient and the geometry of mitral annulus and leaflets (58-60). Due to the dynamic changes in these factors during a cardiac cycle, the instantaneous severity of functional MR varies throughout the regurgitant period that has been observed in both in animal and human studies (61-64). In patients with LV systolic dysfunction and functional MR, a biphasic pattern was observed in instantaneous regurgitant flow rate and EROA change, including early- and late-systolic peaks with a mid-systolic decrease (62-64). This perhaps is attributed to the variation in the balance between two competing factors acting on the mitral leaflets, namely the tethering force and the closing force (62). However, the biphasic pattern of instantaneous MR flow could be different from patient to patient in the dominant component. In patients with globally dilated LV and severely impaired LV systolic function, the early-systolic peak was found to be greater than the late-systolic one (64). Whereas, in patients with acute localized inferior myocardial infarction where there was no obvious LV global remodeling but

significant local remodeling, the late-systolic peak was found to be greater than the early-systolic peak (65).

1.2.7 Exercise-induced Change in Functional MR

Exercise has been reported to cause changes in the severity of functional MR. In patients with LV dysfunction and at least mild functional MR, most patients showed an increase in MR severity without the evidence of inducible ischemia during semi-supine bicycle exercise, though the extent of change of MR varied between individuals (66-72). In a study of 70 patients with ischemic heart failure, EROA decreased in 13 but increased in the remaining 57 patients during exercise in which the increase was small ($<13mm^2$) in 38 and large ($>13mm^2$) in 19 patients. Furthermore, this exercise-induced changes in functional MR were not associated with the degree of functional MR at rest nor the changes in global LV function during exercise, but were related to the changes in local LV remodeling and mitral valve deformation (67). On the other hand, intraventricular mechanical dyssynchrony at rest (73) and its increase induced by exercise (66, 70, 72) have recently been suggested to contribute to the worsening of functional MR during exercise on top of other known factors. Interestingly, the exercise-induced increase in MR was related to the change in mitral valve deformation, as estimated by mitral tenting area in synchronous LV; whereas it was more specifically determined by the inadequate increase in mitral closing force in dyssynchronous LV, as estimated by LV pressure rise in systole (+dp/dt) (69).

Clinical outcome could be affected by the exercise-induced changes of functional MR. A large increase in functional MR during exercise was reported to be associated

with a higher mortality and hospitalization for decompensated heart failure where an increase in EROA of >13 mm^2 was an independent predictor for cardiac death (74, 75). In contrast, minor changes or even a sizeable decrease in EROA during exercise resulted in a better long-term prognosis. The relationship between exercise-induced increase in functional MR and worse outcome involves the following mechanisms: firstly, an intermittent increase in functional MR during life activities can induce flash pulmonary edema (76); secondly, an acute increase in systolic pulmonary artery pressure caused by acute increase in functional MR is an independent predictor of cardiac death (68); and lastly, an intermittent increase in functional MR and LV dyssynchrony may result in LV volume overload which increases myocardial stiffness and accelerates further LV remodeling in the long run.

1.3 Mechanisms of Functional MR

Since a competent mitral valve closure relies on the coordination among different components of the mitral apparatus, including the annulus, leaflets, chordae tendineae, papillary muscles and underlying LV walls, any abnormality of these structures may be involved in the pathogenesis of MR. Similarly, the occurrence of functional MR is a multifactorial process, though it remains unknown the exact mechanism and key parameters for determining the severity.

1.3.1 The Imbalance between Tethering Force and Closing Force

The position of the mitral leaflets and the coaptation zone during systole is determined by two superimposing and opposing forces acting on the leaflets: tethering force and closing force. The tethering force produced by chordae tendineae pulls mitral leaflets toward papillary muscles and prevents the leaflets from prolapsing into LA. At the same time, the closing force generated by LV systolic contraction acts to push mitral leaflets toward LA. Therefore, the systolic position of mitral leaflets is determined by the balance between these two forces.

Either kind of imbalance between the two forces, i.e. an increase in tethering force or a decrease in closing force, may lead to a poor coaptation of mitral valve leaflets resulting in functional MR. LV dilation, spherical LV geometry, papillary muscle displacement and systolic dyssynchrony are major reasons for the increase in tethering force, while the decrease in closing force is related to reduction in LV contractility and significant LV systolic dyssynchrony when the efficiency of LV contraction is depressed.

Ogawa and Godley have firstly reported that apical displacement of mitral leaflets and coaptation zone relative to mitral annular plane is an important morphological characteristic in patients with functional MR (77, 78). It could be caused by reduced closing force and/or increased tethering force. Due to the non-elastic nature of chordae tendineae, the tethering force is regulated by the position of papillary muscles. In normal subjects, papillary muscles are oriented parallel to the LV long axis and perpendicular to mitral annular plane where the tethering force is not more than the closing force generated by ventricular contraction. On the contrary, when LV global and/or local remodeling occurs, the apical, posterior and outward displacement of papillary muscles, caused by the posterior and outward bulging of the myocardial segments underlying papillary muscles, raises the tethering force remarkably. This increase in tethering pulls the leaflets away from the normal coaptation position and restricts their motion during both systole and diastole (57, 79), resulting in delayed coaptation, prolonged regurgitant period (80), incomplete closure (78) and malcoaptation of the two leaflets (81, 82) related to the development of functional MR. It has been suggested that the increase in mitral leaflet tethering could be the primary mechanism of functional MR since the severity of MR is closely correlated to the extent of tethering (83-87). In the absence of leaflet tethering, isolated LV contractile dysfunction or annular dilation may not be enough to produce significant functional MR (85-89).

The decrease in LV closing force resulting from reduced myocardial contractility and /or global LV systolic dyssynchrony is also attributable to the development of functional MR, though its role may not be as important as the counterpart, the increase in leaflet tethering. It has been observed in several studies that in the

absence of LV dilation, even severe LV systolic dysfunction does not induce clinically significant MR (85-87). In an animal model of severe systolic heart failure created by giving esmolol and phenylephrine, LV expansion was initially limited by increasing pericardial restraint when only trace MR was observed; then the pericardium was opened to allow LV dilation when moderate MR occurred with the increase in LV size (85). Another animal study conducted by the same group gave rise to similar findings in both acute and chronic ischemic segmental LV contractile dysfunction (86). Normally, a little force is required to close the thin leaflets, so it is understandable that LV systolic dysfunction without leaflet tethering is not able to produce important MR. However, a much greater closing force that could not be provided in the LV systolic impairment is wanted as the tethering increases during the displacement of papillary muscles in LV remodeling. Therefore, the reduced closing force acts as a supplemental factor contributing to functional MR in the presence of increased leaflet tethering. He et al. investigated in vivo the effects of LV pressure rise on the severity of MR by keeping the degree of papillary muscle displacement and mitral annular dilation unchanged using a special device. It was shown that the decrease in systolic LV pressure in this model increased the severity of functional MR (87). Intriguingly, the change of LV closing force within a cardiac cycle was hypothesized to explain the dynamic pattern in the instantaneous severity of functional MR with greater extent in early- and late-systole while minimal in mid-systole(62). Moreover, the increase in LV closing force after cardiac resynchronization therapy (CRT) as evidenced by the rise in +dp/dt contributed to the acute reduction in functional MR (90).

1.3.2 Global and Local LV Remodeling

The occurrence of local or global LV remodeling leads to the abnormalities in LV volume, shape and function. In both ischemic and non-ischemic dilated cardiomyopathy, LV remodeling has been regarded as the initial pathogenic factor for functional MR (91-94). First of all, LV dilation displaces papillary muscles apically and laterally which produces the tethering of mitral valve and poor coaptation of the two leaflets during systole. Secondly, ventricular dilation results in increased mitral annular circumference and area which further compounds the valve incompetence by increasing the area needed to be covered by the leaflets and the conversion of LV shape from elliptical to more spherical exacerbates the problem. Thirdly, LV dysfunction decreases ventricular closing forces, which further impairs the leaflets closure and causes more apical displacement of the coaptation zone. Therefore, the presence of local or global LV remodeling acts as the prerequisite for initiating the development of regurgitation.

When the relationship with functional MR was further compared between local and global LV remodeling, it is more prominent in the former situation. Although previous studies revealed a weak correlation between the degree of regurgitation and LV sphericity (91, 92, 94), both in vitro and in vivo studies demonstrated that excessive papillary muscle displacement was the main cause of functional MR (85-87). Another clinical study which included patients with a wide range of LV dilation and functional MR also confirmed that the apical and posterior displacement papillary muscles were an independent determinant of mitral leaflet tethering and hence MR severity (83). The papillary muscle displacement is caused by LV dilation and sphericalization, however, it is not necessarily proportional to the degree of LV dilation. In fact, the discrepancy between LV dilatation and the degree of associated

MR is frequently observed in clinical settings, such as a higher incidence of functional MR in patients with inferior myocardial infarction than those with anterior myocardial infarction and more LV global remodeling. In the animal model of anteroseptal myocardial infarction, no significant MR was observed when LV dilatation occurred in the absence of geometric changes in the mitral apparatus. In contrast, in the model of posterior myocardial infarction, more obvious functional MR was noted with geometric changes in the mitral annulus and posteromedial papillary muscle (95). It was also demonstrated in clinical study that inferior myocardial infarction resulted in less global LV dilatation but greater displacement of the posteromedial papillary muscle (96). Therefore, LV remodeling for any given LV volume may have different degree of local remodeling, i.e. papillary muscle displacement and leaflet tethering, which leads to different degree of regurgitation (85, 97).

1.3.3 Tethering of the Mitral Leaflets

The tethering of mitral leaflets by displaced papillary muscles has been proven to be the fundamental mechanism of functional MR (83-87). The outward and apical displacement of papillary muscle can cause the apical displacement of coaptation zone relative to mitral annulus; on the other hand, stronger tethering in the middle of the leaflet may result in its concave deformation and decrease in coaptation area. Two main patterns of leaflet tethering have been observed in functional MR (98, 99).

The first type is the symmetric pattern which is characterized by a predominant apical tethering of both mitral leaflets symmetrically into the LV cavity, which caused by the apical and outward displacement of both anterolateral and

posteromedial papillary muscles equally. The anterior leaflet is deformed, with a sharp bend created near its base, at a point where the secondary chordae tendineae insert (100, 101). This particularly restricts the motion of the distal anterior leaflet to coapt with the posterior leaflet. It is commonly seen in patients with anterior myocardial infarction or dilated cardiomyopathy where the LV is globally remodeled with severe impairment of myocardial contractility. A central MR jet is typical for this pattern.

The second type is the asymmetric pattern which is characterized by the predominant posterior tethering of both mitral leaflets. In this case, the motion of the posterior leaflet is highly restricted by remarkable displacement of the posteromedial papillary muscle, whereas the motion of the distal anterior leaflet is less restricted. The restriction on posterior leaflet prevents it from reaching the normal coaptation point. Instead, the coaptation point moves posteriorly creating the asymmetric tethering shape where the anterior leaflet tip coapts to the level of mid-posterior leaflet (98). This tethering pattern is frequently observed in patients with isolated inferior-lateral myocardial infarction where the ventricle is more locally remodeled in the inferior, posterior and lateral segments supporting the posterior papillary muscle. Consequently, mitral valve tenting is localized in the posterior region with less pronounced tenting area and volume than that seen in the symmetric pattern (99). The MR jet is generally eccentric that oriented toward the posterior wall of the LA.

1.3.4 Mitral Annular Deformation and Dysfunction

In patients with functional MR, changes in geometry and motion of the mitral annulus have been observed. Firstly, the mitral annulus is consistently dilated

compared to normal subjects, with increase in circumference and annular area (11, 102, 103). Secondly, it is flattened with decreased annular height and loss of the normal saddle configuration (104, 105). In addition, the contractile function of mitral annulus reflected by the annular area change during a cardiac cycle is reduced (11, 106).

Mitral annular dilation and loss of contractility increases the systolic mitral closure area to be covered by the anterior and posterior leaflets. The abnormal plannar shape of mitral annulus extends the distance between commissures and papillary muscle heads, which may increase mitral leaflet tethering. However, significant functional MR is seldom found in isolated mitral annular dilation without leaflet tethering (89), since the large surface area of mitral leaflets would compensate for the annular dilation. It has been observed in an experimental study that functional MR occurs when the annulus is dilated 1.75-fold in the absence of leaflet tethering, or dilated 1.50-fold with an apical leaflet tethering (107). In a clinical study conducted in patients with lone atrial fibrillation and LA enlargement, mitral annulus was dilated without LV dilation and leaflet tethering where no obvious functional MR occurred. On the contrary, in patients with dilated cardiomyopathy, the same degree of annular dilatation was frequently associated with significant MR when the leaflet tethering was present (89). Nevertheless, a normal mitral annulus size could not preclude the appearance of functional MR which demonstrated by a persistent or recurrent MR after surgical undersized annuloplasty (108-111). This might be caused by the persistence or progression of excessive mitral valve tethering and progressive LV remodeling after the procedure.

1.3.5 Papillary Muscle Dysfunction

In normal LV, papillary muscles shorten during ejection phase to maintain the distance between the tips and mitral annulus and hence prevent mitral valve prolapse. Therefore, MR was initially suggested as the result of leaflet prolapse due to reduced longitudinal contraction of papillary muscles secondary to ischemic dysfunction. However, this is not supported by both animal and human studies. Functional MR caused by mitral valve prolapse may occasionally develop in patients with ischemic heart disease or animal models (112, 113); at the same time, mitral leaflet prolapse in patients with ischemic MR is very rare (77, 78, 114). Furthermore, experimental studies have reported that isolated papillary muscle dysfunction is not related to significant MR (24, 115-117).

The central role of mitral leaflet tethering in the pathogenesis of functional MR has been emphasized by many studies and the tethering distance is believed to be the major factor determining the level of mitral leaflet coaptation (83, 85-87). The change in tethering distance is caused by displacements of the LV wall underlying papillary muscles as well as changes in papillary muscle length. Messas et al created an animal model of localized basal inferior myocardial infarction with wall bulging where significant MR occurred. When acute ischemia of the adjacent papillary muscle produced, elongation of the papillary muscle was present in response to ventricular forces which reduced the tethering distance and therefore the amount of MR (118). In another study of 123 patients with LV ejection fraction <40%, it was shown that papillary muscle function reflected by myocardial velocity gradient correlated with mitral valve tenting in that patients with lower velocity gradient tended to have less severe MR (119). Therefore, the papillary muscle dysfunction

may contribute to the severity of functional MR by adjusting the tethering distance, though it may not be the primary cause of functional MR.

1.3.6 Mechanical Dyssynchrony

Immediate improvement of functional MR by biventricular pacing in heart failure patients were reported by a few studies (90, 120-122). In addition to the improvement in mitral valve geometry and LV reverse remodeling, the reduction in functional MR was found to be related with a better timing of mechanical activation in the regions of papillary muscle insertion, i.e. local mechanical dyssynchrony (120). Therefore, it has been suggested that LV mechanical dyssynchrony may play a potential role in determining the degree of functional MR in patients with advanced heart failure, adjunctive to aforementioned factors in LV and mitral apparatus, though the mechanism and impact remains to be explored.

1.3.6.1 Intraventricular Dyssynchrony and Resting Functional MR

In patients with LV dilation, both the degree and duration of functional MR are closely correlated with prolonged QRS duration (123). The presence of moderate or severe MR was more commonly observed in patients with wide QRS complex (≥130ms) than those with narrow QRS complex (<130ms). Among patients with wide QRS complex, functional MR was strongly associated with left bundle branch block (LBBB) but not right bundle branch block (RBBB). Not surprisingly, the right ventricular (RV) apical pacing where iatrogenic LBBB occurred was reported to cause functional MR as well. It was also illustrated in animal studies that pacing at the RV apex resulted in severe functional MR in dogs, whereas pacing at the LV base only produced mild MR (124).

In recent echocardiographic studies, mechanical dyssynchrony of the myocardial segments adjacent to papillary muscles was found to be an independent contributor of functional MR. This uncoordinated contraction may increase mitral leaflet tethering and cause mal-alignment of the leaflet scallops leading to incomplete closure. In 32 patients with dilated cardiomyopathy, Soyama et al. showed that the regurgitant fraction correlated with a significant delay in mechanical activity between the LV segment adjacent to the anterolateral papillary muscle and the segment adjacent to the posteromedial papillary muscle, as assessed by the difference in the time to peak systolic myocardial strain (125). This finding was confirmed in a prospective study of 74 patients with ischemic and nonischemic LV dysfunction where the contribution of regional dyssynchrony in determining MR was evaluated with respect to the deformation of mitral valve apparatus, global and local LV remodeling. Although the degree of functional MR was associated with the mitral deformation indices, the regional dyssynchrony assessed as the standard deviation of the time to peak systolic tissue velocity among the eight basal and mid LV free wall segments, also had an independent correlation with MR but to a lesser extent. However, it was not an independent determinant of MR in ischemic patients while in non-ischemic patients, regional dyssynchrony worsened MR regardless of LV geometry (84).

Furthermore, electromechanical dyssynchrony of the LV also has an impact on functional MR through changes in the mitral valve geometry and kinetics. A study using cardiac magnetic resonance imaging revealed that isolated LBBB in asymptomatic patients was associated with global mechanical dyssynchrony and

deformation of the mitral valve apparatus defined as a larger tenting area (126). The RV apical pacing resulted in a more widely opened mitral valve at end-diastole and leaflet dyssynchrony with delayed mitral valve closure in animal models (127). The dyssynchronous contraction of the LV basal segments may worsen MR, attributable to the loss of mitral annular contraction, increase in systolic annular area and the presence of mitral leaflet tethering (128). Furthermore, LV systolic dyssynchrony reduces the efficiency of contraction, resulting in decreased closing force which becomes unable to counteract the increased valve tenting.

1.3.6.2 Intraventricular Dyssynchrony and Exercise-induced Functional MR

Intraventricular dyssynchrony is related not only to resting but also to exercise-induced functional MR. In patients with LV systolic dysfunction, a significant correlation was observed between LV intraventricular mechanical dyssynchrony at rest and worsening of functional MR during exercise (73). In addition, a positive association between the change in LV dyssynchrony and change in MR severity during exercise were also reported in several studies (66, 70, 72, 129).

1.3.6.3 Atrioventricular Dyssynchrony and Diastolic MR

Besides intraventricular dyssynchrony, atrioventricular dyssynchrony is also related to functional MR. Diastolic MR, a special category of functional MR, often occurs in patients with prolonged AV interval (53-56). It is caused by the positive pressure gradient between the LV and LA which occurs in the prolonged period after atrial contraction and before the abnormally delayed ventricular contraction. Optimization

of the timing between atrial and ventricular contraction can reduce or even abolish diastolic MR (53, 57).

1.4 Current Therapeutic Options for Functional MR

The current therapeutic options for functional MR include medical therapy, surgical therapy and CRT, though none of them could totally abolish functional MR since the generation of this condition is a complex process involving multiple factors in the LV and mitral valve apparatus.

1.4.1 Medical Therapy

Several studies investigated the effect of medical treatment on functional MR, but the numbers of patients were small. In fact, heart failure therapy was targeted by medications which included diuretics, β-blockers, angiotensin-converting enzyme inhibitors (ACEi), angiotensin receptor blockers (ARB), nitrates as well as inotropic agents. Although the severity of functional MR could be reduced acutely (130-132) or in the long-term (133-136) by way of increasing ventricular closing force, reducing LV preload and provoking LV reverse remodeling, mild to moderate residual MR is commonly observed in heart failure patients despite the use of these medicines.

1.4.2 Surgical Therapy

Many surgical techniques have been developed for treating functional MR, of which the most commonly performed procedure is the undersized mitral annuloplasty. This procedure aims to correct the mitral annular dilation and restore the surface of coaptation between the two leaflets which would enable a complete valve closure. In

a study which included patients with ischemic MR treated by mitral annuloplasty combined with revascularization, significant improvement in MR severity from the grade 3.1±0.5 to 0.6±0.6 was observed in a 18-month follow up after the procedure, while 48% patients had no MR and 44% had only mild MR (137). However, a high rate of postoperative persistence or recurrence of MR have been reported in a number of studies, which is believed to be the results of continued or even worsened mitral valve tethering as well as ongoing ventricular remodeling after annuloplasty (108-111). Therefore, several alternative or concomitant surgical techniques directly targeting the causal mechanisms of the disease have been developed recently, which include second-order chordal cutting, Alfieri edge-to-edge repair, papillary muscle reposition, and infarct placation for patients after myocardial infarction. The papillary muscle repositioning, infarct plication and external constraint applied to reverse local LV remodeling (138-142) are aimed at correcting the unbalanced tethering, while the specific chordal modification might minimize the deformity of mitral leaflets (100). The long-term results on favorable clinical outcome are lacking, though beneficial effects on MR severity have been showed in some of these techniques.

1.4.3 CRT

1.4.3.1 An Overview of CRT

A high prevalence of electrical and/or mechanical dyssynchrony occurs in patients with advanced heart failure, which produces uncoordinated ventricular activation and contraction with further reduced efficiency in ejection (143-145). Atrial synchronous biventricular pacing or CRT is a non-pharmacological therapy for patients with advanced heart failure with electromechanical delay, currently defined as a

prolonged QRS duration of >120ms (146). The device consists of an impulse generator, one atrial lead and two ventricular leads, namely the conventional RV lead and an additional LV lead. The LV lead is placed into the lateral or postero-lateral cardiac vein through the coronary sinus to pace the LV lateral wall, a site consistently observed to have delayed electrical activation. The atrial lead is placed in the right atrium (RA) and the RV lead is placed either in the RV apex or in right ventricular outflow tract (RVOT). Therefore, different regions of the LV can be paced simultaneously to resynchronize ventricular activation and restore a coordinated contraction (147). The AV interval will also be shortened to maintain atrioventricular synchrony and abolish diastolic MR. It has been proved in numerous studies that CRT improves hemodynamic status, heart failure symptoms, exercise capacity, quality of life and cardiac function in heart failure patients (148-155). More importantly, CRT induces LV reverse remodeling with reduction in LV volume and LV mass (151, 152, 156, 157), which reverse remodeling has been shown to predict a better long-term prognosis after the therapy, in terms of reduced mortality and heart failure hospitalization (155, 158). According to the recent ACC/AHA and ESC guidelines on chronic heart failure, CRT can be considered in patients with LV systolic dysfunction (ejection fraction <35%) and wide QRS complex (QRS duration $\geq$ 120 ms) who remains symptomatic (NYHA class III or IV) despite optimal medical therapy (146).

1.4.3.2 Beneficial Effects of CRT on Functional MR

(1) CRT on Resting Functional MR

Data from the MIRACLE trial and others have shown a significant reduction in MR jet area and index of MR severity after CRT (152, 155, 159). An effective CRT can

reduce functional MR immediately by about 30% on average and continue to decrease by an additional 10-20% up to six months after device implantation (90, 120, 151).

However, the beneficial effect of CRT on functional MR seems to be associated with some pacing and disease factors. It was shown to be pacing dependent in that an immediate recurrence of MR occurred when the therapy was withheld (121, 160). The pacing modalities were also found to correlate with the magnitude of improvement in functional MR. Although in acute studies (161, 162) similar benefits on MR were seen for LV pacing and simultaneous biventricular pacing, a more recent multicenter trial with 306 patients with six-month follow up has suggested that biventricular pacing (either simultaneous or sequential) was better than LV pacing for the reduction of MR severity (163). With regard to the etiologies of heart failure, a lesser degree of reduction in MR was reported for CRT in ischemic than non-ischemic patients (164), which was likely due to the natural progression of coronary heart disease faster than the improvement in MR. On the other hand, the benefit on functional MR showed no difference between patients with sinus rhythm and atrial fibrillation (165), as well as between patients with wide and narrow QRS complexes provided a similar extent of systolic dyssynchrony was present (166).

(2) CRT on Exercise-induced Functional MR

Acute reduction in functional MR during exercise was reported with CRT in several studies (69, 71, 72). However, a recent study with only 28 patients suggested a different impact of CRT on exercise-induced functional MR between acute and chronic pacing. It was shown that CRT improved resting but not exercise-induced

MR immediately after the therapy, though reduction in both resting and exercise-induced MR was observed three months after CRT (167).

(3) CRT on Phasic Changes of Functional MR

Previous studies reported a biphasic pattern of functional MR with early- and late-systolic peaks and a mid-systolic decrease of regurgitation flow (62, 63). This phenomenon was also evaluated before and three months after CRT in one study of consisted of 19 patients where MR volume was assessed by quantitative pulsed Doppler method and instantaneous regurgitation flow rate by proximal flow convergence method. As a result, CRT decreased the regurgitant volume by reducing early-systolic MR. However no significant reduction in late-systolic MR was observed (64). As the sample size is really small, further studies with larger sample size are needed to replicate the findings.

1.4.3.3 Mechanisms of MR Reduction by CRT

CRT has been proven to reduce the severity of functional MR both immediately after device implantation and in the long-term follow up. The acute improvement is related to increase in ventricular closing force, resynchronization of papillary muscle contraction, improvement of annular contraction and correction of diastolic MR; whereas the long-term improvement is mainly attributed to LV reverse remodeling in addition to the above-mentioned factors. Nevertheless, previous publications in CRT patients were based on small sample size with investigation into only one or two factors. The interaction between different parts and their contributions to CRT responses and functional MR improvement warrants further studies.

(1) Increased Ventricular Closing Force

In an acute study of 24 patients with heart failure and LBBB, Breithardt *et al.* evaluated the changes in MR degree using proximal isovelocity surface area (PISA) method during biventricular pacing "on" and "off" modes. When CRT was switched on, a linear correlation between the reduction in degree or duration of MR and the gain in LV + dp/dt was observed. This indicated that the improvement in transmitral pressure gradient (closing force on the mitral leaflets) resulted in an earlier and more effective mitral valve closure in heart failure patients (90).

(2) Resynchronized Papillary Muscle Contraction

The coordination of papillary muscle contraction by CRT may relieve the apical tethering of mitral leaflets by reducing the tethering force. Kanzaki et al. (120) investigated the contraction sequence of papillary muscles by strain rate imaging in 26 patients with LBBB. The reduction in MR severity was significantly correlated with the shortening of time delay between the anterolateral and posteromedial papillary muscles. This finding was also reported in other studies (121).

(3) Improved Mitral Annular Contraction

The improvement in mitral annular contractility observed with CRT may also contribute to the reduction of functional MR. As the annular ring is in continuity with the myocardium at LV basal segments, the increased annular contraction is likely a result of more coordinated contraction of these segments after CRT (168, 169).

(4) Correction of Diastolic MR

Diastolic MR often occurs in a prolonged AV interval when a transmitral pressure gradient in late diastole is developed (53-56). The synchrony between atrial and ventricular contraction could be achieved after CRT by programming an optimal AV delay. This, together with the increased LV closing force which lessens the diastolic leaflet tethering, can reduce or even abolish diastolic MR (57).

(5) LV Reverse Remodeling

The long-term effects of CRT on MR are likely to be contributed by LV reverse remodeling, characterized as a reduction in LV volume and a less spherical LV shape. These favorable changes in LV geometry tend to relocate the papillary muscles, which may reduce the traction force on chordae tendineae and hence the tethering force on mitral leaflets. In patients who received CRT for six months, a significant reduction in functional MR was observed with a less subvalvular traction and LV reverse remodeling (151, 164). Furthermore, the improvement in systolic contraction, global and local LV mechanical dyssynchrony and mitral annular contraction accompanying LV reverse remodeling would help to diminish MR.

1.4.3.4 Predictors of MR Reduction after CRT

Pre-pacing mechanical dyssynchrony has been demonstrated as a predictor of MR improvement after CRT. Patients with significant MR reduction were found to have more mechanical dyssynchrony before device implantation, in particular in the regions underlying the papillary muscle insertion sites, when compared with those with no MR improvement (121, 122, 170). Furthermore, the site of latest activation was related to the occurrence and timing of MR improvement after CRT in a study of 68 patients. In that study, patients were divided into three groups according to the

change of MR after CRT. "Early responders" had at least one grade improvement in MR immediately after CRT implantation; "late responders" showed an improvement of at least one grade MR after six months; and "non-responders" displayed no improvement or even deterioration in MR during follow up. It was found that the LV dyssynchrony involving posterior papillary muscle related to an acute reduction in MR, whereas the LV dyssynchrony in lateral wall resulted in a late response to CRT (122). In addition, preserved systolic strain in the posterior segments could also predict MR reduction after CRT (170, 171).

1.4.3.5 Functional MR and CRT Responses

Although CRT has been confirmed being able to improve heart failure symptoms, functional capacity, cardiac function and prognosis, approximately one-third of patients receiving the therapy are non-responders using composite clinical and/or echocardiographic endpoints (149, 172). In responders to CRT, MR was reduced significantly after CRT and to a greater extent than the non-responders (151, 173). Pre-pacing MR severity has been suggested to be a determinant of CRT response, though the exact mechanisms for lack of response are not fully understood. In a prospective study of 143 patients followed for six months, factors including severe MR at baseline, ischemic heart disease and LV end-diastolic diameter ≥75mm were found to be independent predictors for non-responders who were defined by clinical endpoints as death from heart failure, heart transplantation or increase in six-minute hall-walk distance <10% (174). Another recent study included 20 patients with non-ischemic dilated cardiomyopathy, the presence of significant MR (EROA ≥20 mm^2) before CRT was associated with the lack of LV reverse remodeling at six months as defined by a reduction of LV end-systolic volume <10% (175). On the

other hand, in a prospective study of 102 patients followed up for one year, the lack of CRT responses in terms of no decrease in NYHA functional class or quality of life score was more common in patients with less than the grade 2+ MR at baseline (176). The controversial results suggest that further studies are needed to reconcile the impact of functional MR on CRT response.

1.5 Summary

Functional MR is a common finding in patients with LV systolic dysfunction which is related to a worse prognosis. A graded relationship has been observed between severity of functional MR and mortality when EROA $\geq 20mm^2$. This merits aggressive therapeutic interventions which rely on the understanding of the mechanisms for the development of functional MR. It is a multifactorial process where mitral valve deformation is regarded as the primary mechanism that caused by the apical and outward papillary muscle displacement secondary to LV global and/or local remodeling. Other mechanisms include mitral annular dilation, papillary muscle dysfunction and LV systolic impairment. Recently, LV mechanical dyssynchrony has been suggested as a potential contributor to functional MR. CRT improves functional MR in patients with advanced heart failure, while the MR severity before device implantation and its change seem to be related with CRT responses.

SECTION II

OBJECTIVES AND METHODOLOGY

CHAPTER 2 OBJECTIVES

2.1 Mechanical Dyssynchrony in the Pathogenesis of Functional Mitral Regurgitation (MR)

Multiple factors participate in the pathogenesis of functional MR. Although mitral valve tenting is well known to be the main determinant, recent studies suggest that left ventricular (LV) systolic dyssynchrony may also contribute to functional MR. Therefore, the first objectives of our study were to assess the role of LV systolic dyssynchrony in the pathogenesis of functional MR, and to examine whether LV systolic dyssynchrony had an incremental value to mitral valve tenting in predicting clinically significant MR.

2.2 LV Myocardial Deformation and Functional MR

Functional MR is increasingly recognized as a ventricular disease, in which the primary problem exists in the LV myocardium rather than in the mitral valve itself. Two-dimensional (2D) speckle tracking is a novel echocardiographic technology based on the frame to frame tracking of acoustic signals in gray-scaled 2D image, which allows the assessment of myocardial deformation of different components because of its angle-independent nature. It was aimed to examine in this study whether there was any difference in systolic myocardial deformations, i.e. radial strain, circumferential strain, longitudinal strain and rotation, between patients with significant functional MR and those without.

2.3 Impact of Functional MR on LV Reverse Remodeling after Cardiac Resynchronization Therapy (CRT)

CRT has been confirmed to generate LV reverse remodeling and improve functional MR. However, the relationship between LV reverse remodeling, pre-pacing MR severity and its improvement remains unclear in patients with CRT. Therefore, this study aimed to examine whether the extent of LV reverse remodeling and gain in ejection fraction are affected by the severity of pre-pacing functional MR or its improvement after CRT.

2.4 Mechanisms of Improvement of Early- and Late-systolic Functional MR by CRT

CRT is a device-based therapy for advanced heart failure. The reduction of functional MR is observed with CRT, attributable to LV reverse remodeling, improvement in mechanical dyssynchrony as well as the favorable changes on leaflet tethering. However, the impact of CRT on the biphasic pattern of functional MR has not been well studied. Therefore, this study aimed to examine the change of early- or late-systolic MR in CRT and its mechanisms.

CHAPTER 3 METHODOLOGY

3.1 Study Patients

3.1.1 Patients with Left Ventricular (LV) Systolic Dysfunction

From January 2007 to September 2008, 147 patients who were admitted for clinical signs and symptoms of heart failure at Prince of Wales hospital were enrolled in this study. The clinical and echocardiographic assessments were conducted at three-month or six-month follow up.

Inclusion criteria included:

(1) LV systolic dysfunction with ejection fraction <50%, measured by two-dimensional (2D) echocardiography;

(2) Structurally normal mitral valve apparatus;

(3) Sinus rhythm.

Exclusion criteria included:

(1) History of recent myocardial infarction (less than 16 days);

(2) Clinical or echocardiographic evidence of other cardiac diseases, such as valvular, pericardial, congenital, or infiltrative heart disease;

(3) More than mild aortic regurgitation;

(4) Atrial fibrillation or other kinds of arrhythmia;

(5) Previously implanted cardiac devices;

(6) Suboptimal echocardiographic windows, inadequate for comprehensive assessment.

3.1.2 Patients Receiving Cardiac Resynchronization Therapy (CRT)

Eighty-three patients who received CRT between January 2007 and December 2008 and were followed up for at least three months were enrolled. The clinical and echocardiographic assessments were conducted at baseline and three months after CRT.

The inclusion criteria for CRT were:

(1) Systolic dysfunction with LV ejection fraction $\leq 35\%$;

(2) Symptomatic heart failure with NYHA class III and IV;

(3) On optimal medical therapy;

(4) QRS duration >120ms.

Exclusion criteria were:

(1) Clinical or echocardiographic evidence of other cardiac diseases, such as valvular, pericardial, congenital, or infiltrative heart disease;

(2) Structural abnormalities of the mitral valve apparatus;

(3) More than mild aortic regurgitation;

(4) Atrial fibrillation or other kinds of arrhythmia;

(5) Suboptimal echocardiographic windows, inadequate for comprehensive assessment.

3.1.3 Normal Controls

Forty-five normal subjects from the community were also enrolled in our study. They had:

(1) No history of cardiovascular or systemic disease;

(2) Normal physical examination, including: blood pressure, hemoglucostix and ECG;

(3) No echocardiographic evidence of structural or functional heart disease;

(4) Not on chronic medications.

3.2 Biventricular Pacemaker Implantation and Atrioventricular (AV) Interval Optimization

Biventricular pacemaker (CRT) or pacemaker plus defibrillator (CRT-D) were implanted as previously described (177). The atrial lead was placed in the right atrium (RA), and right ventricular (RV) lead at the RV apex, like in conventional anti-bradycardia pacing. Most importantly, the LV lead was inserted through coronary sinus into the lateral or posterolateral cardiac vein.

At one day after device implantation, the AV interval was optimized for maximal diastolic filling by Ritter's method using Doppler echocardiography. Briefly, the pulse wave Doppler profile of transmitral inflow was obtained at the apical-4 chamber view. Attention was paid to ensure a clear completion of late diastolic atrial wave (A wave). The longest AV interval (AV_{long}) where biventricular pacing maintained was programmed. The duration from the onset of QRS complex to the completion of A wave was measured as QA_{long}. Then the short AV interval of 30 to 50ms (AV_{short}) was programmed when the duration from the onset of QRS complex to the completion of A wave was measured as QA_{short}. The optimal AV interval was calculated using the following formula (178) (Figure 3.1):

$$\text{Optimal AV (ms)} = AV_{short} + [(AV_{long} + QA_{long}) - (AV_{short} + QA_{short})]$$

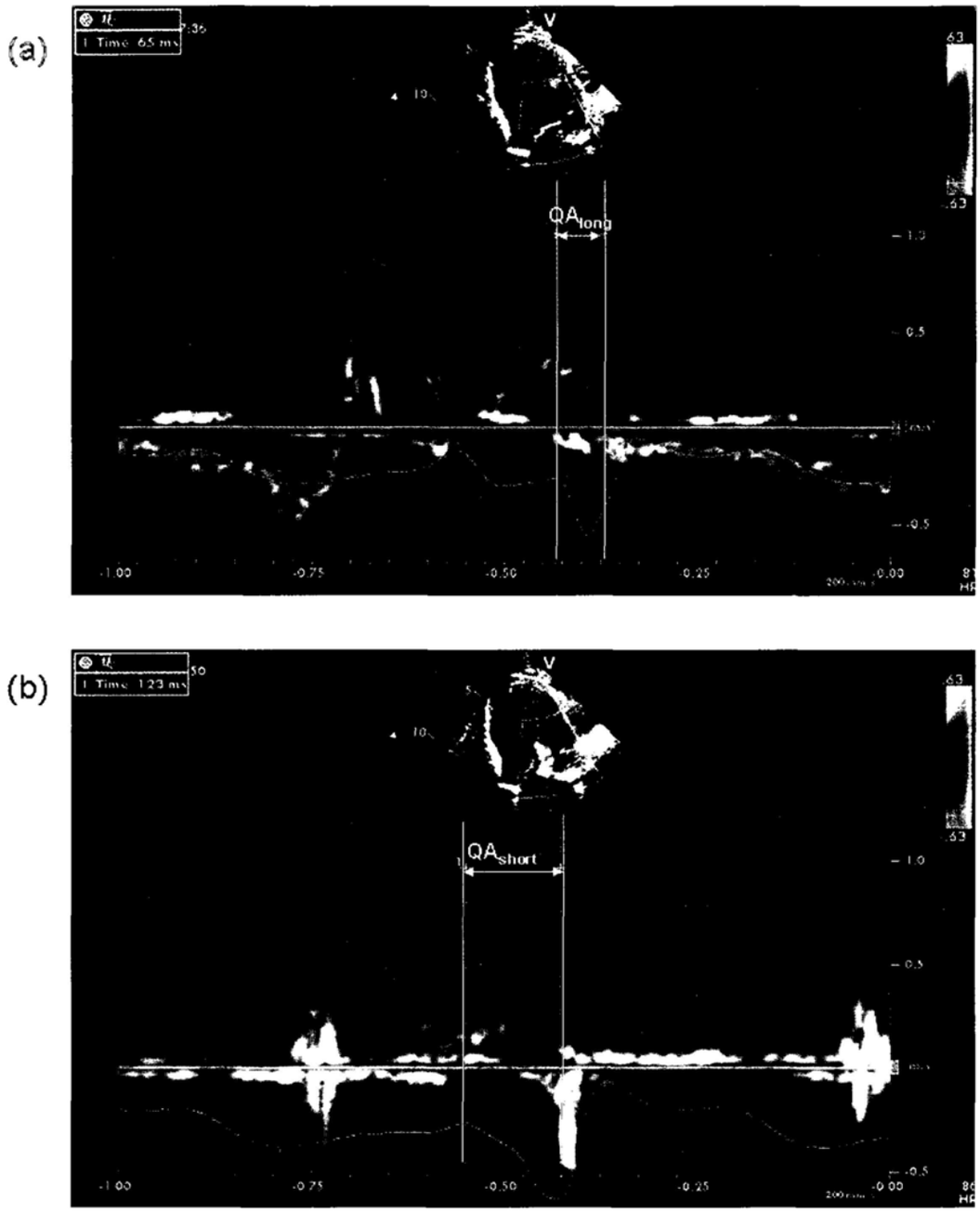

Figure 3.1 Optimization of AV interval by Ritter's method. (a) when long AV interval is programmed at 140ms, QA_{long} is 65ms; (b) when short AV interval is programmed at 50ms, QA_{short} is 123ms. Therefore the optimal AV interval is 82ms based on the formula.

3.3 Clinical Assessment

Clinical assessments were accomplished by observers who were blinded to the results of echocardiography, including:

(1) NYHA functional class;

(2) Minnesota Living with Heart Failure (MLWHF) Quality of life questionnaire score.

3.4 Echocardiographic Assessment

3.4.1 Echocardiography Imaging System

Vivid 7 (Vingmed-General Electric, Horten, Norway)

3.4.2 Software for Offline Analysis

EchoPac 7.0 (Vingmed-General Electric, Horten, Norway)

3.4.3 General Comments on Optimal Image Acquisition

2D echocardiography with tissue Doppler-color imaging (TDI) was performed with a 2.5- or 3.5- m Hz multi-phase-array transducer. Five consecutive beats were stored and the images were digitized and analyzed offline by EchoPac 7.0 (Vingmed-General Electric, Horten, Norway).

3.4.3.1 ECG

ECG was recorded simultaneously with echocardiographic images. Attention was paid to ensure a clear definition of the QRS complex and P wave on ECG signal.

3.4.3.2 2D Echocardiography

At least five consecutive beats were stored during breath hold. Efforts were made to achieve an optimal image with clear visualization of myocardial walls and mitral valve apparatus. In apical images, the maximal LV cavity length was displayed with the same length maintained in all the three apical views. In short-axis images, the LV cavity was attempted looking as round as possible. Frame rate was adjusted to 40-80 fr/s.

3.4.3.3 Spectral Doppler Echocardiography

The continuous wave (CW) or pulse wave (PW) Doppler profile was acquired by the guidance of 2D or color Doppler images, where the alignment between Doppler signal and blood flow was maximized. Five cardiac cycles were saved with the sample volume put in a proper position and 2D or color Doppler images frozen. The size of Doppler spectral velocity tracing was maximized to at least 2/3 of the screen by adjusting the scale and baseline, when the reject, gain and filter were also optimized.

3.4.3.4 Color TDI

Apical 4-, 2- and long-axis views were acquired to assess the long axis motion of LV wall. The alignment between Doppler signal and LV wall was maximized. A possible highest frame rate (usually >100 fr/s) was attempted by adjusting the sector width, depth and pulse repetitive frequency. At least five consecutive cardiac cycles were stored during breath hold.

3.4.4 Parameters Measured by Echocardiography in This Study

3.4.4.1 Quantification of Mitral Regurgitation (MR)

(1) MR Jet Area Ratio

The MR jet area was obtained by tracing the MR color Doppler jet in apical 4-chamber view. The frame with the largest jet area was selected for measurement. The regurgitant jet area was traced including variianced and aliased flow signals as well as contiguous laminar velocities moving in the same direction as MR jet (Figure 3.2). The left atrial (LA) area was obtained by tracing the LA boundary in the same frame.

MR jet area ratio = (MR jet area/ LA area) × 100%, where mild MR is defined as the ratio <20% (179).

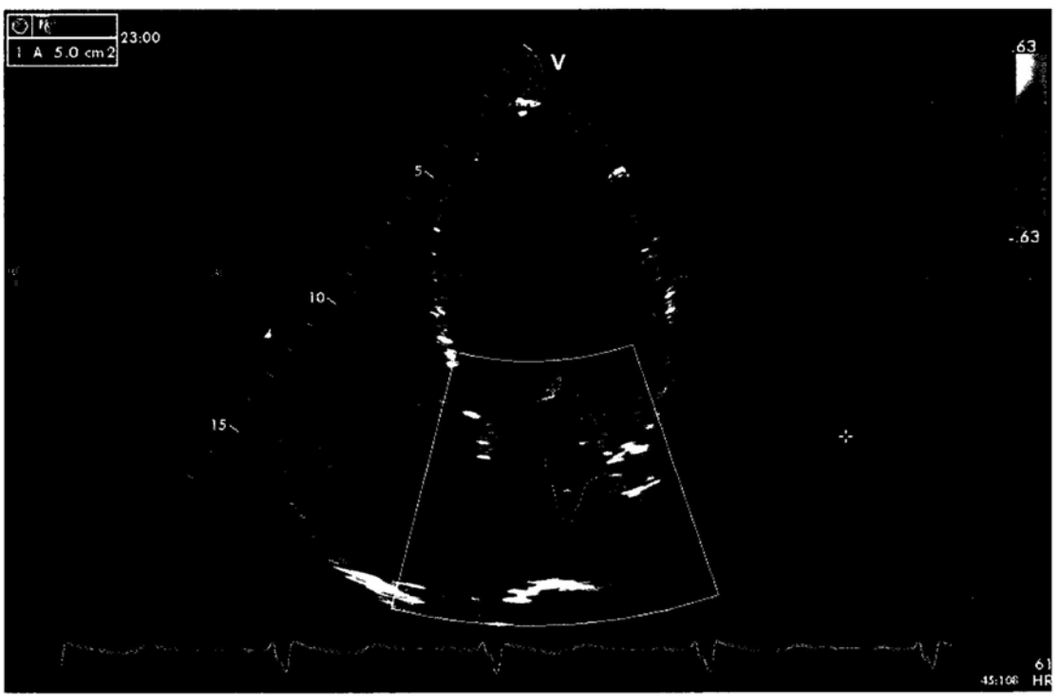

Figure 3.2 Tracing the color Doppler jet of mitral regurgitation in apical 4-chamber view.

(2) MR Volume

MR volume was calculated by the continuity equation, i.e. the mitral inflow stroke

volume minus the LV outflow stroke volume (179). The inner diameter of the mitral annulus (D_{mitral}) was measured at the base of mitral leaflets during early- to mid-diastole, one frame after the leaflet begin to close after its initial opening in apical-4 chamber view. Similarly, the inner left ventricular outflow tract (LVOT) diameter (D_{lvot}) was measured during early systole from the junction of the aortic leaflets with the septal endocardium to the junction of the leaflet with the mitral valve posteriorly in parasternal long-axis view. The pulse wave Doppler time-velocity integral (TVI_{mitral}) of mitral inflow was obtained by placing the sampling volume at the level of mitral annulus. The time-velocity integral (TVI_{lvot}) of LVOT was obtained by placing the sampling volume about 5mm proximal to the aortic valve. The VTI should be measured by tracing the outer edge of the brightest portion of the PW profile (180).

MR volume = $CSA_{mitral} \times TVI_{mitral} - CSA_{lvot} \times TVI_{lvot}$, where CSA presents the cross-sectional area and therefore $CSA_{mitral} = D_{mitral}^2 \times \pi/4$ and $CSA_{lvot} = D_{lvot}^2 \times \pi/4$.

(3) MR Flow Rate and Effective Regurgitant Orifice Area (EROA)

MR flow rate and EROA were calculated using the proximal isovelocity surface area (PISA) method (179). In apical 4-chamber view, shift the baseline on the color bar towards the direction of MR flow to obtain well-defined hemisphere flow convergence. The radius of the hemisphere flow convergence (r) was measured as the maximal distance from first aliasing site to leading edge of the valvular orifice (Figure 3.3). The regurgitant flow rate and EROA were calculated by the following equations:

MR flow rate = $2\pi r^2 V_a$

EROA = $2\pi r^2 V_a / V_{MR}$

Where Va represents the aliasing velocity and V_{MR} represents the peak MR velocity. When multiple jets were present, the regurgitant flow rate and EROA of each jet were calculated and added together where the sum used. The regurgitant flow rate and EROA were considered null in patients with no or trace MR.

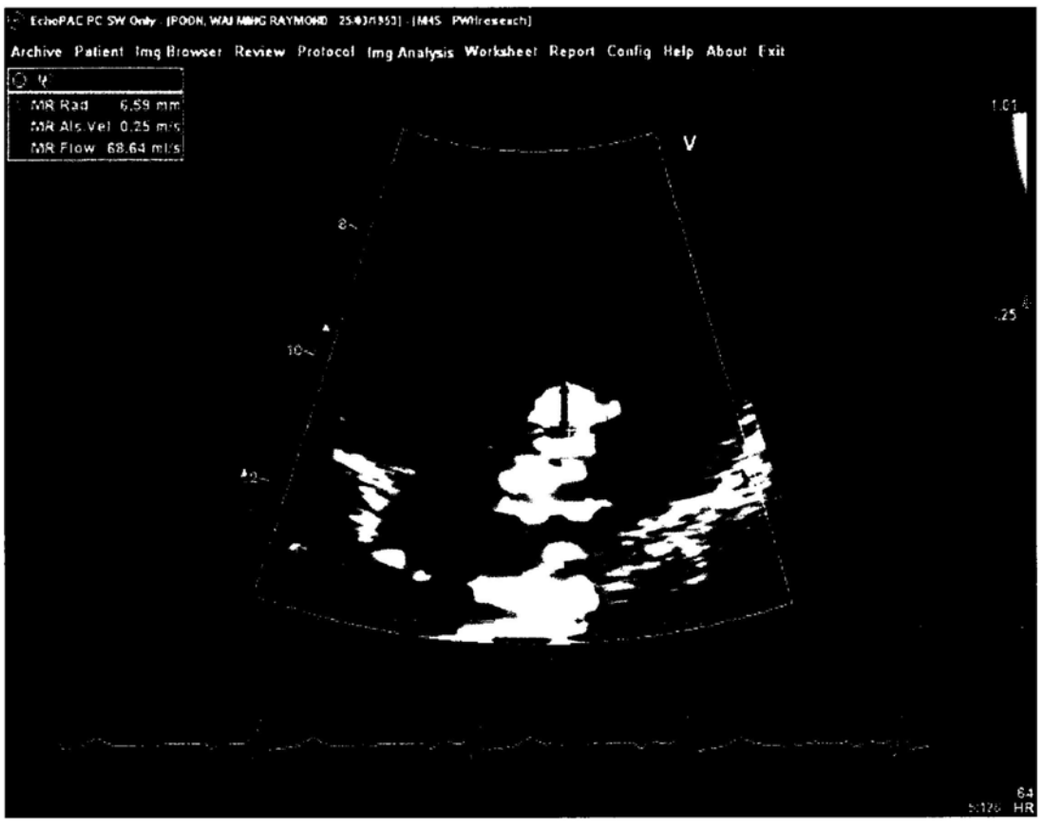

Figure 3.3 Measurement of the radium of the hemisphere flow convergence of mitral regurgitation. The r is indicated by the two-headed arrow.

3.4.4.2 Assessment of LV Global Remodeling

LV end-diastolic volume (LVEDV) and end-systolic volume (LVESV) were calculated from the apical 4- and 2-chamber views, using biplane Simpson's method (181) (Figure 3.4).

LV end-systolic and end-diastolic cavity length and mid-cavity width were measured in the apical 4-chamber view. LV length was obtained from LV apex to mid mitral annular plane, while LV width was obtained at half of the length from the base and perpendicular to it. The LV end-systolic and end-diastolic sphericity indices were calculated for assessment of the change in LV geometry (173) (Figure 3.5):
Sphericity index = LV long-axis dimension / LV short-axis dimension

End-diastole was defined as the frame before or at the initial systolic coaptation of the mitral valve and end-systole was defined as the frame preceding initial early-diastolic mitral valve opening.

(a)

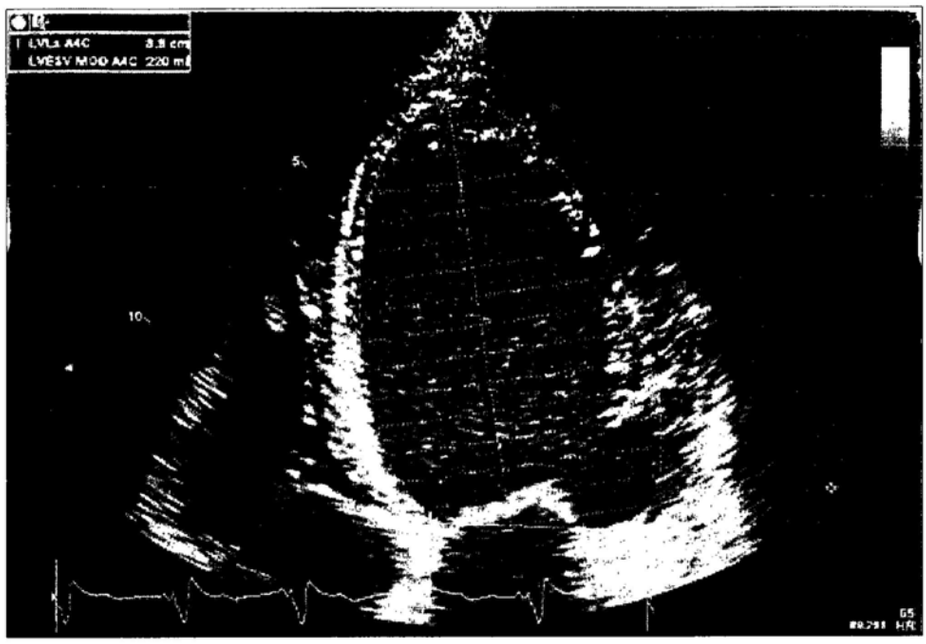

(b)

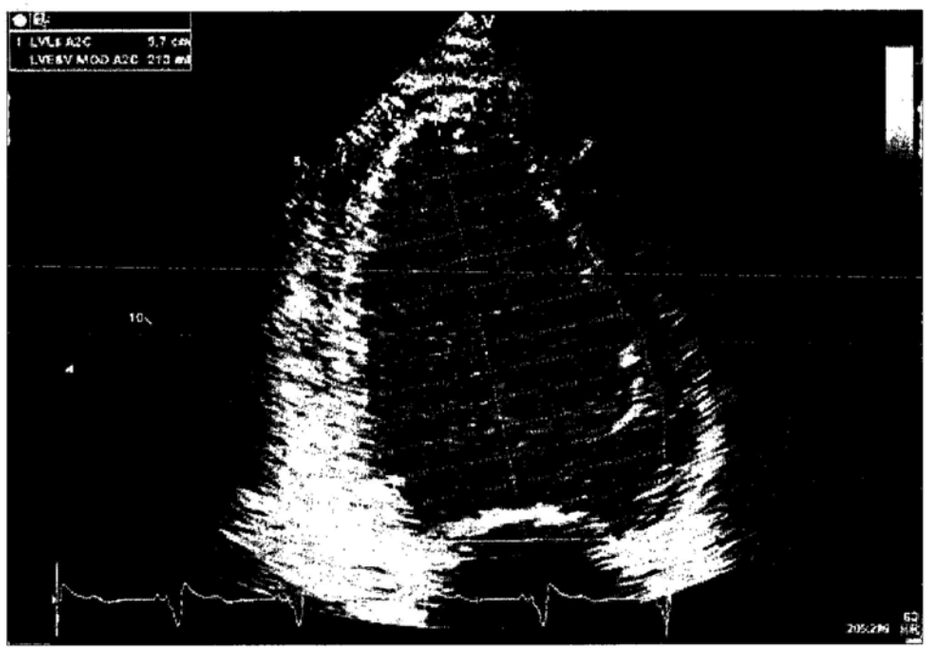

Figure 3.4 Measurement of left ventricular volumes by biplane Simpson's method using apical-4 (a) and apical-2 (b) chamber views.

(a)

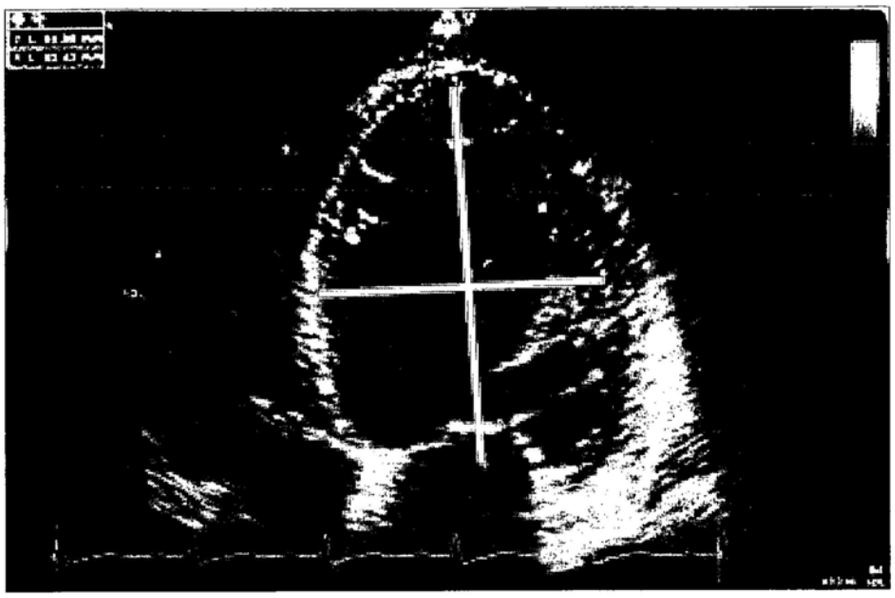

(b)

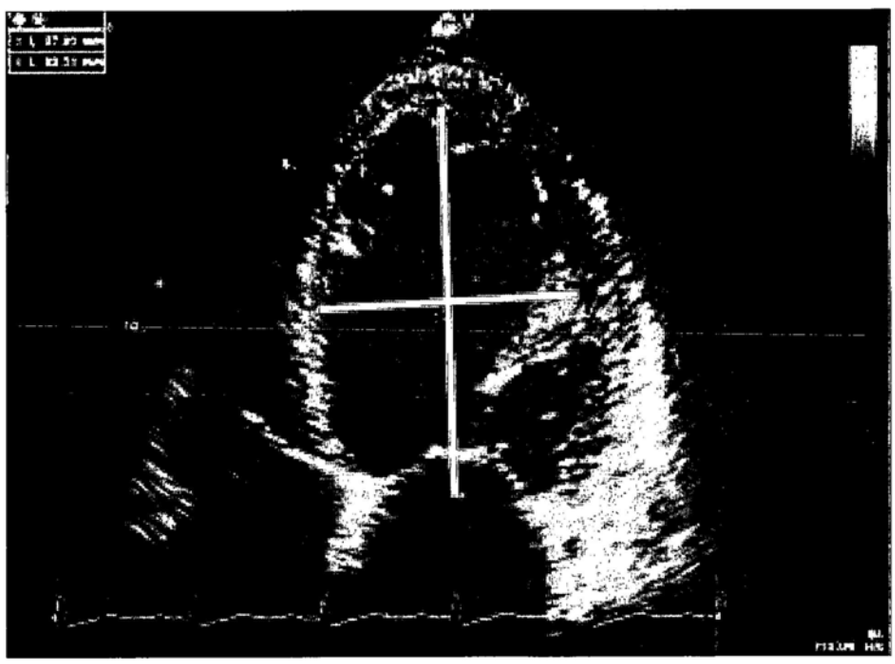

Figure 3.5 Measurement of left ventricular sphericity indices at (a) end-diastole and (b) end-systole in apical-4 chamber view.

3.4.4.3 Assessment of LV Local Remodeling

The papillary-fibrosa distance was measured in the apical long-axis view at mid-systole, from the posteromedial papillary muscle head to the fixed intervalvular fibrosa (83) (Figure 3.6).

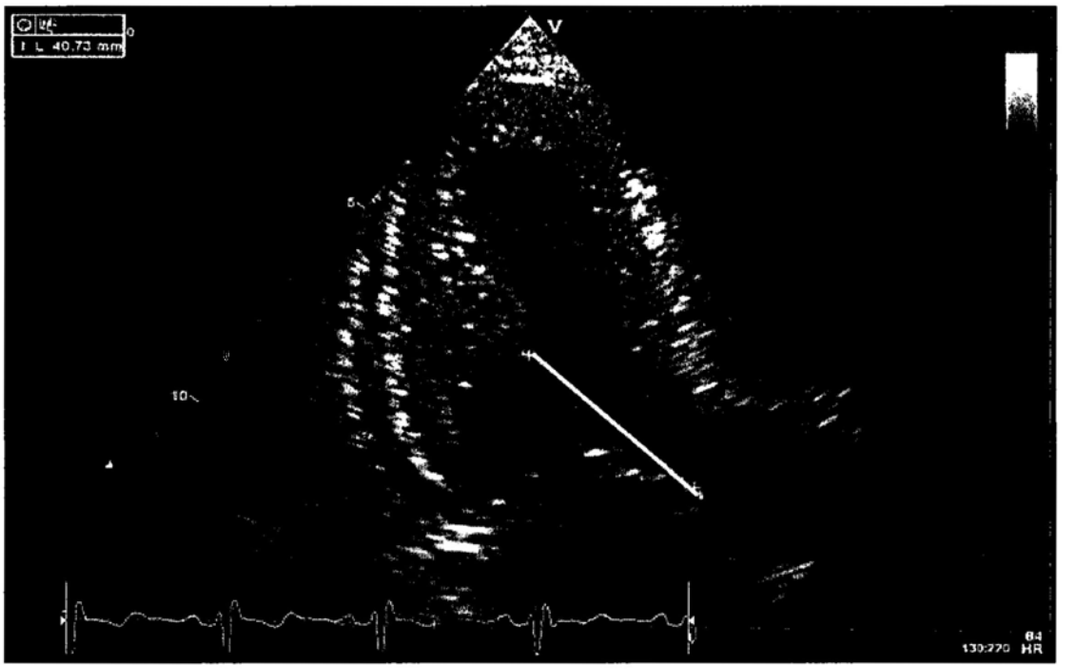

Figure 3.6 Measurement of papillary-fibrosa distance between the posteromedial papillary muscle head and the intervalvular fibrosa in apical long-axis view.

3.4.4.4 Assessment of LV Global Systolic Function

LV ejection fraction was calculated from the apical 4- and 2-chamber views, using biplane Simpson's method (181):

LV ejection fraction = (LVEDV-LVESV) / LVEDV × 100%

The maximal rate of LV pressure rise (+dp/dt) was estimated from the continuous wave Doppler MR velocity curve, the time between velocities 1m/sec and 3 m/sec on the descending slope of the velocity spectrum (Δt) was measured (180) (Figure 3.7).

LV +dp/dt (mmHg/sec) = 32000/Δt

Figure 3.7 Measurement of left ventricular +dp/dt between the 1m/sec and 3m/sec velocities of mitral regurgitation by CW profile.

3.4.4.5 Assessment of Mitral Annular Dilation and Contractility

The mitral annular diameter (D) was measured in apical 4-chamber view at end-diastole for its maximal size and mid-systole for its minimal size respectively (Figure 3.8). The landmark used for identifying inner annular boundaries for measurement was the hinge point where the mitral leaflets attached to the mitral annulus. The mitral annular area (MAA) was calculated based on the formula:

$MAA = D^2 \times \pi/4$

Mitral annular contractility was calculated as the percentage of change in MAA during the cardiac cycle:

$$\text{Mitral annular contractility} = (MAA_{maximal} - MAA_{minimal}) / MAA_{maximal} \times 100\%$$

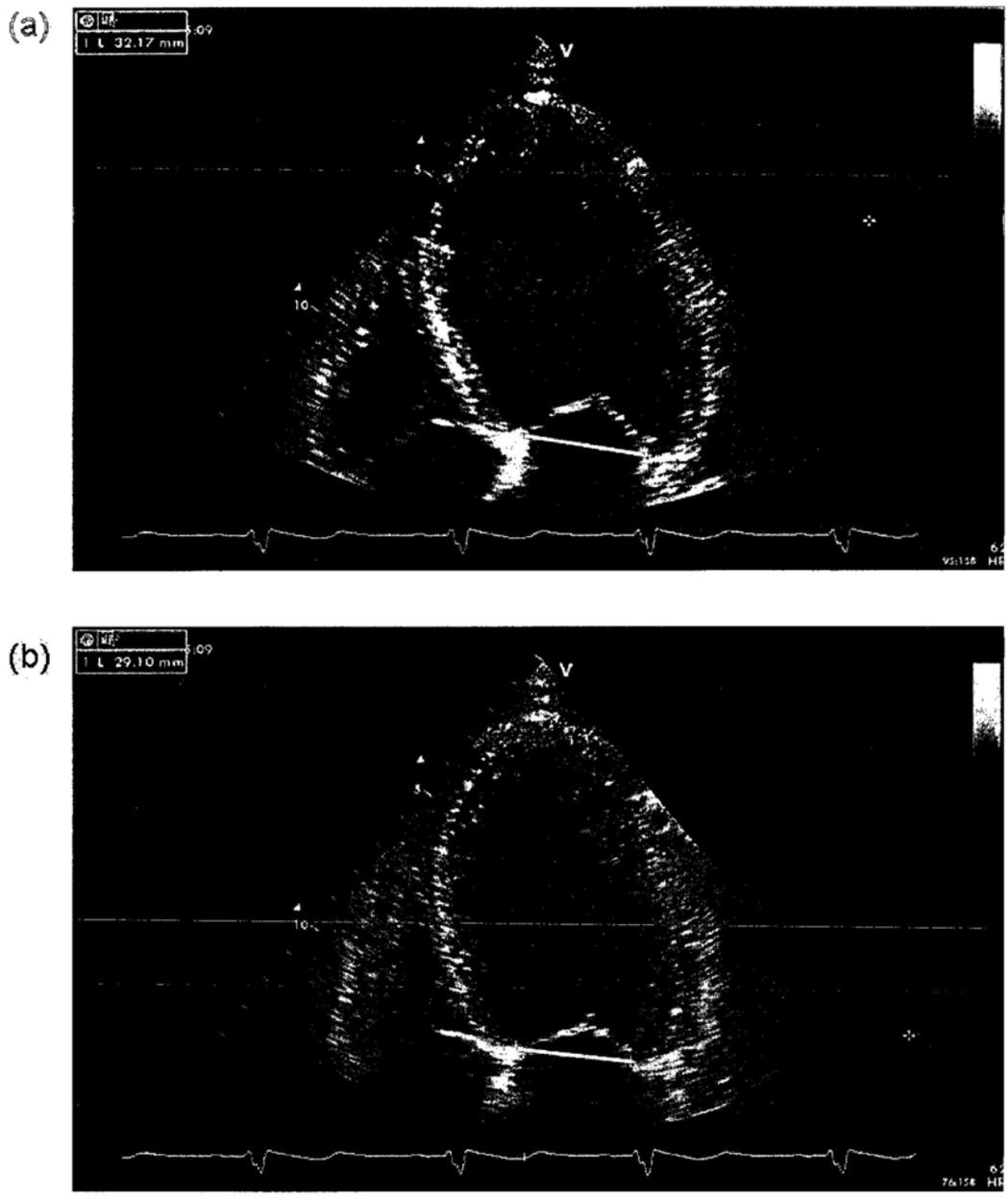

Figure 3.8 Measurement of maximal mitral annular diameter at end-diastole (a) and minimal mitral annular diameter at mid-systole (b) in apical-4 chamber view.

3.4.4.6 Assessment of Mitral Deformation

The mitral valve tenting area was measured as the area enclosed between the annular plane and the atrial surface of the mitral leaflets at mid-systole in the parasternal long-axis view (83). Tenting height was measured as the distance between the coaptation point and the mitral annular plane at mid-systole in the parasternal long-axis view (83) (Figure 3.9).

(a)

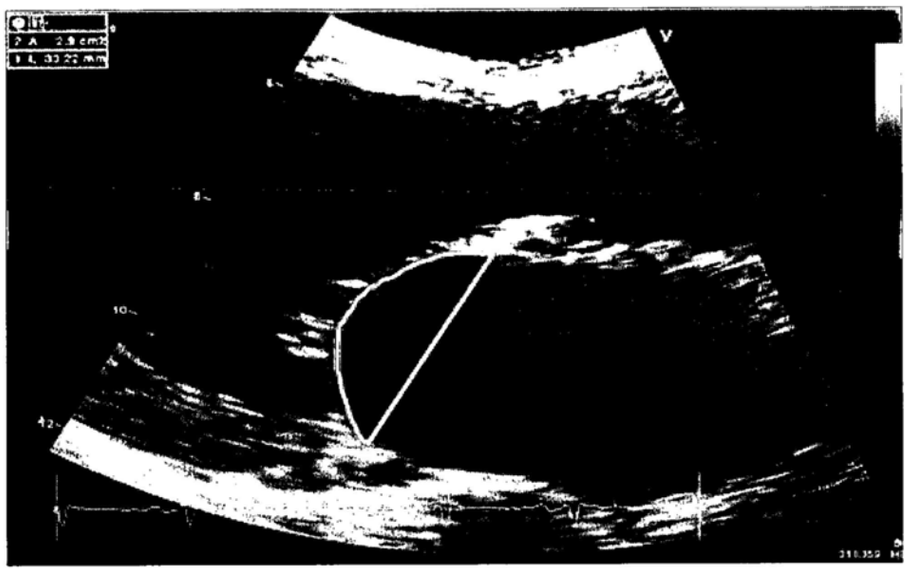

(b)

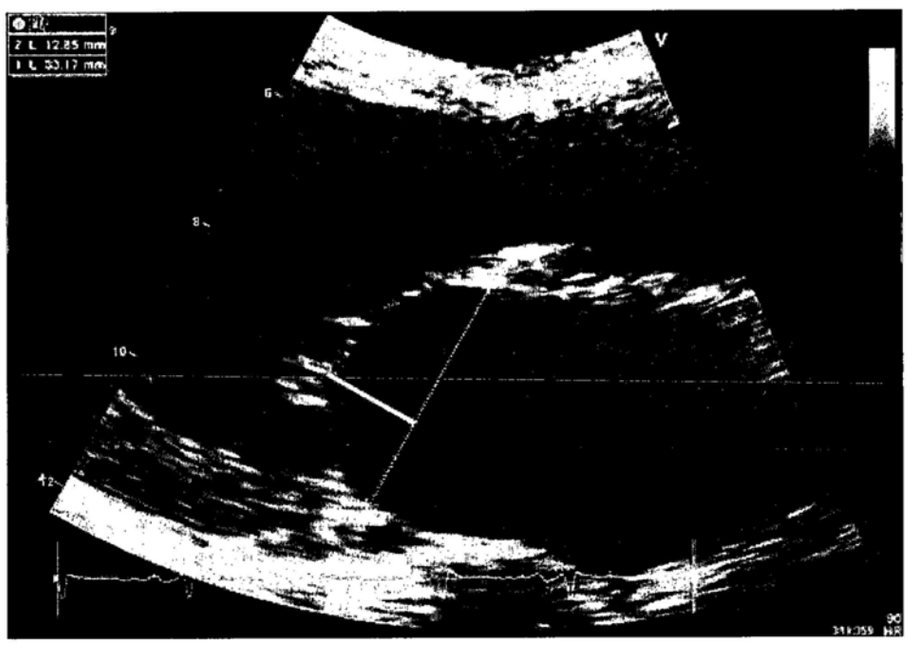

Figure 3.9 Measurement of mitral tenting area (a) and tenting height (b) using zoomed image in parasternal long-axis view.

3.4.4.7 Assessment of Left Ventricular Systolic Mechanical Dyssynchrony

From the apical 2-chamber, apical 4-chamber and apical long-axis views, a 6-basal and 6-mid segmental model was obtained in the LV, namely the septal, lateral, anterior, inferior, anteroseptal, and posterior segments at both basal and mid levels (151, 182, 183) (Figure 3.10).

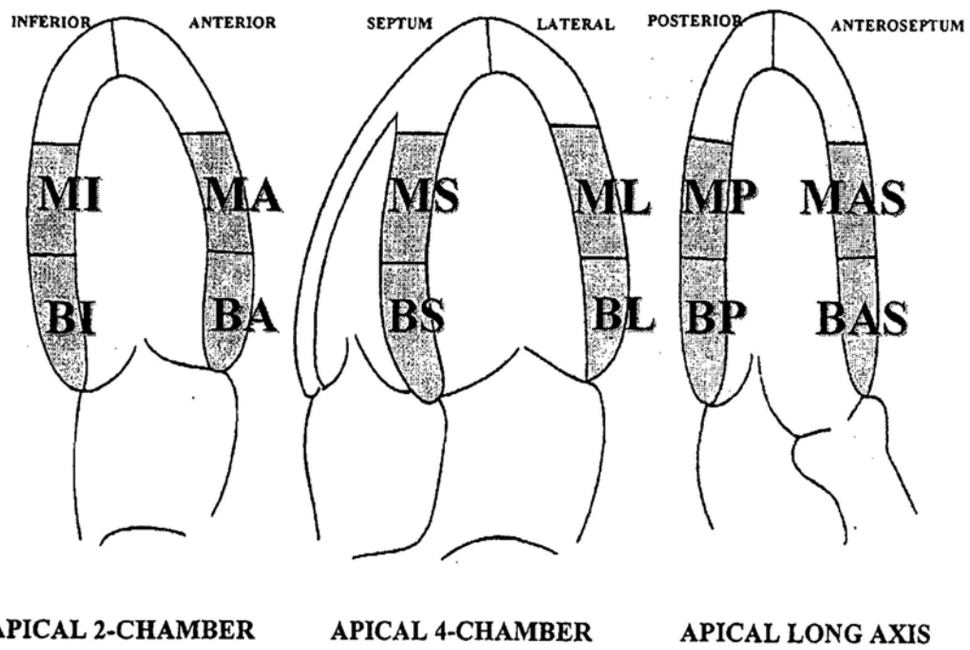

Figure 3.10 The 6-basal and 6-mid segmental model for assessment cardiac function and synchronicity. BS: basal septal segment; MS: mid septal segment; BL: basal lateral segment; ML: mid lateral segment; BA: basal anterior segment; MA: mid anterior segment; BI: basal inferior segment; MI: mid inferior segment; BAS: basal anteroseptal segment; MAS: mid anteroseptal segment; BP: basal posterior segment; MP: mid posterior segment.

LV systolic mechanical dyssynchrony was assessed by 2D color TDI in three apical views (i.e. apical 4-chamber, 2-chamber, and apical long-axis views). Myocardial

velocity curves were reconstituted offline using the 6-basal, 6-mid segmental model in the LV. The positive peak with the highest velocity and longest duration during the ejection phase (between aortic valve opening and aortic valve closure) was identified as the peak systolic velocity. The time to peak systolic velocity during ejection phase (Ts) was measured from the onset of QRS complex in each segment. If the QRS onset was not clear, an uniform point on the ECG was used as the alternative reference for measurement in all the 12 LV segments (184) (Figure 3.11).

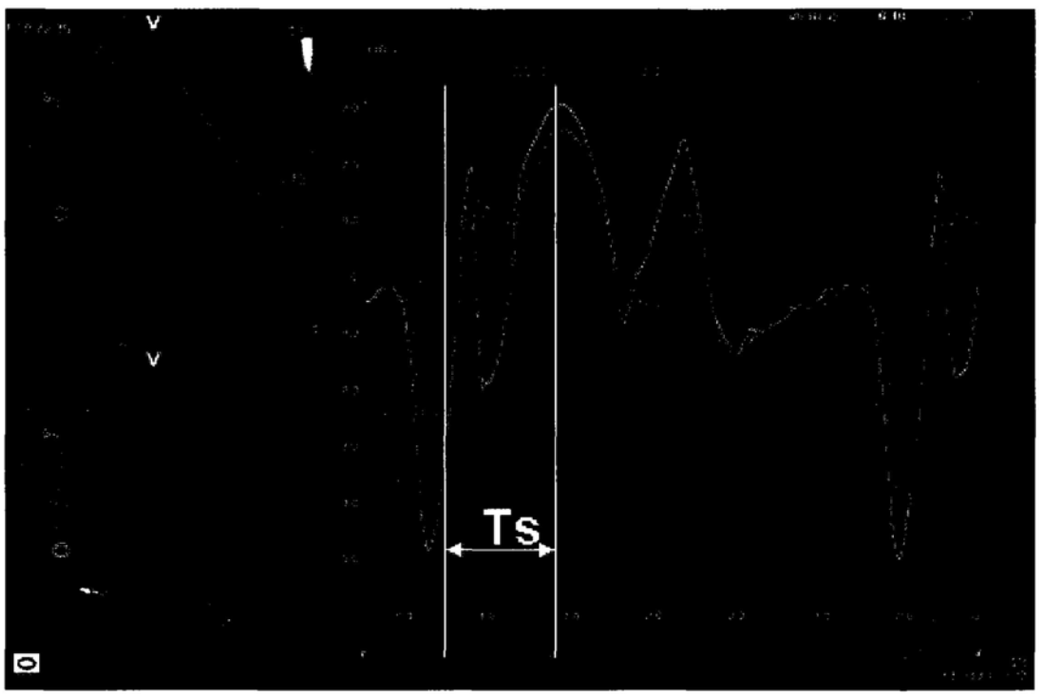

Figure 3.11 Myocardial velocity curve reconstituted in offline analysis of 2D color TDI when the sample volume was placed at the basal and mid septal segment, showing the time from the onset of QRS complex to peak systolic velocity (Ts).

The standard deviation (Ts-SD) and the maximal difference of Ts (Ts-Dif) among the 12 LV segments were calculated as the parameters of global LV systolic mechanical dyssynchrony (173, 185). The absolute difference in Ts between the mid lateral and

mid inferior segments was calculated to reflect regional mechanical dyssynchrony between the anterolateral and posteromedial papillary muscle delay at their attaching sites (APM-PPM delay).

3.4.4.8 Assessment of LV Myocardial Deformation

2D speckle tracking is a novel echocardiographic technology based on the frame to frame tracking of acoustic signals in gray-scaled 2D image, which allows the assessment of myocardial deformation of different components because of its angle-independent nature. LV long- and short-axis deformations as well as LV basal and apical rotation were assessed by 2D speckle tracking imaging. 2D images of basal, mid and apical short-axis views, as well as apical-4 chamber, apical-2 chamber and apical long-axis views were acquired with frame rate of 40-80 fr/s. Offline analysis was performed using customized software (EchoPac-PC SW-only, Version 7.0.0, Vingmed-GE, Horten, Norway).

Firstly, a cardiac cycle with good image quality was selected. Then the endocardial border was traced manually at end-systole. A region of interest for speckle tracking was generated automatically between the endocardial and epicardial borders. Manual adjustment was allowed to optimize the inclusion of the LV wall. The data was processed automatically by the system for individual segments, and the tracking quality was automatically evaluated for each segment. Once the tracking quality had been satisfactory in all segments, the data was accepted by the system and myocardial strain curves would then be generated. An 18 segment modeling was preset in the speckle tracking modality by the software, i.e. there were six evenly divided segments in each of the three long-axis or short-axis views. The peak systolic

strain (ε) for each segment was recorded for further calculation. The longitudinal systolic strain (ε-long) was measured from apical-4, apical-2 and apical long-axis views, which represents the shortening and elongation of the heart on the long-axis and turns out a negative peak at end-systole (Figure 3.12). The circumferential systolic strain (ε-circum) and radial systolic strain (ε-radial) were measured from the basal, mid and apical parasternal short-axis views. The former represents the compression and expansion of myocardial deformation which is a negative peak (Figure 3.13), and the latter refers to the thickening and thinning of the myocardium which turns out a positive peak (Figure 3.14). Measurement of rotation was only performed in parasternal short-axis views at basal and apical levels. When viewed from the apex, the basal rotation is clockwise with a negative tracing (Figure 3.15) while the apical rotation is counterclockwise with a positive tracing (Figure 3.16). LV torsion (Tor) was calculated as the net difference of rotation between the basal and apical segments. The following parameters were calculated in the study.

Global ε-long: Mean longitudinal peak systolic strain of the 18 LV segments

Basal ε-long: Mean longitudinal peak systolic strain of the 6-basal LV segments

Mid ε-long: Mean longitudinal peak systolic strain of the 6-mid LV segments

Apical ε-long: Mean longitudinal peak systolic strain of the 6-apical LV segments

Global ε-radial: Mean radial peak systolic strain of the 18 LV segments

Basal ε-radial: Mean radial peak systolic strain of the 6-basal LV segments

Mid ε-radial: Mean radial peak systolic strain of the 6-mid LV segments

Apical ε- radial: Mean radial peak systolic strain of the 6-apical LV segments

Global ε-circum: Mean circumferential peak systolic strain of the 18 LV segments

Basal ε-circum: Mean circumferential peak systolic strain of the 6-basal LV segments

Mid ε-circum: Mean circumferential peak systolic strain of the 6-mid LV segments

Apical ε-circum: Mean circumferential peak systolic strain of the 6-apical LV segments

Basal rot: Mean rot of the 6-basal LV segments

Apical rot: Mean rot of the 6-apical LV segments

Tor: Net-difference between basal and apical mean rot

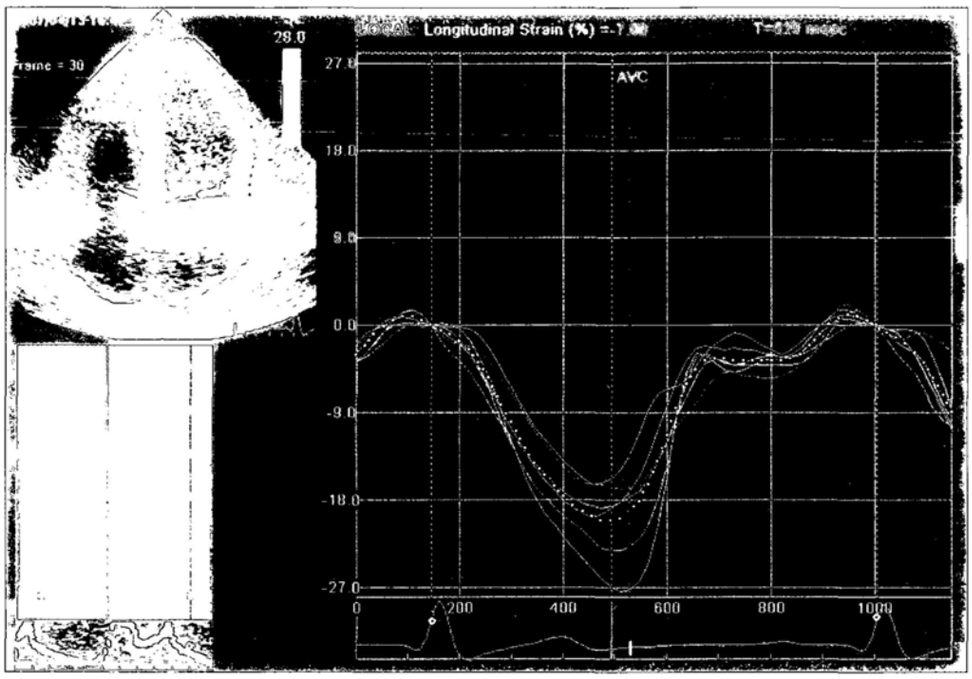

Figure 3.12 2D speckle tracking derived myocardial longitudinal strain curves in apical-4 chamber view, which showed a negative tracking.

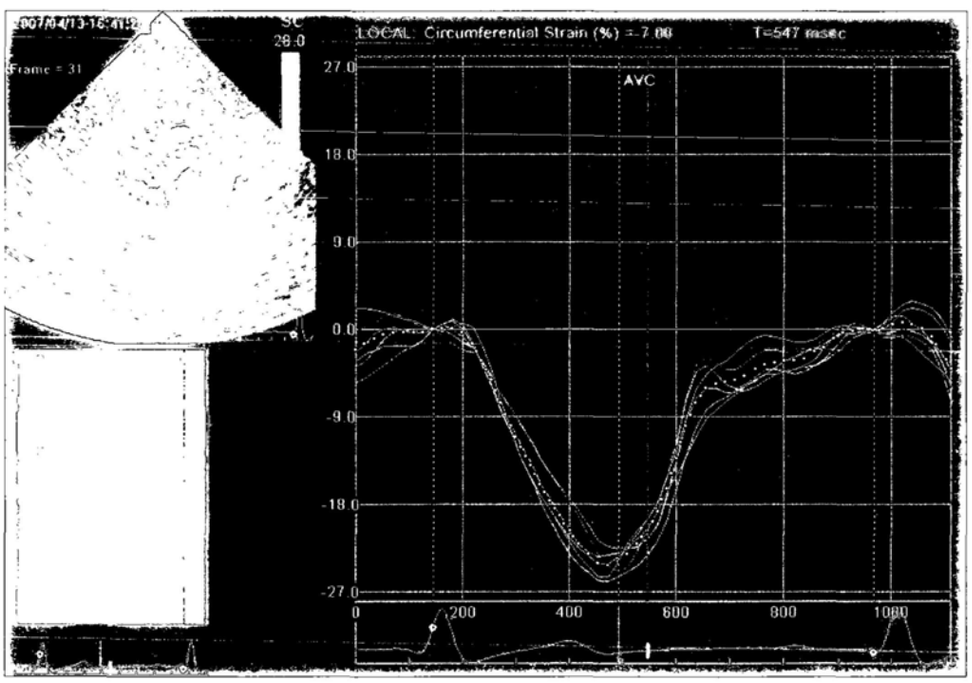

Figure 3.13 2D speckle tracking derived myocardial circumferential strain curves in parasternal short-axis view at apical level, which showed a negative tracking.

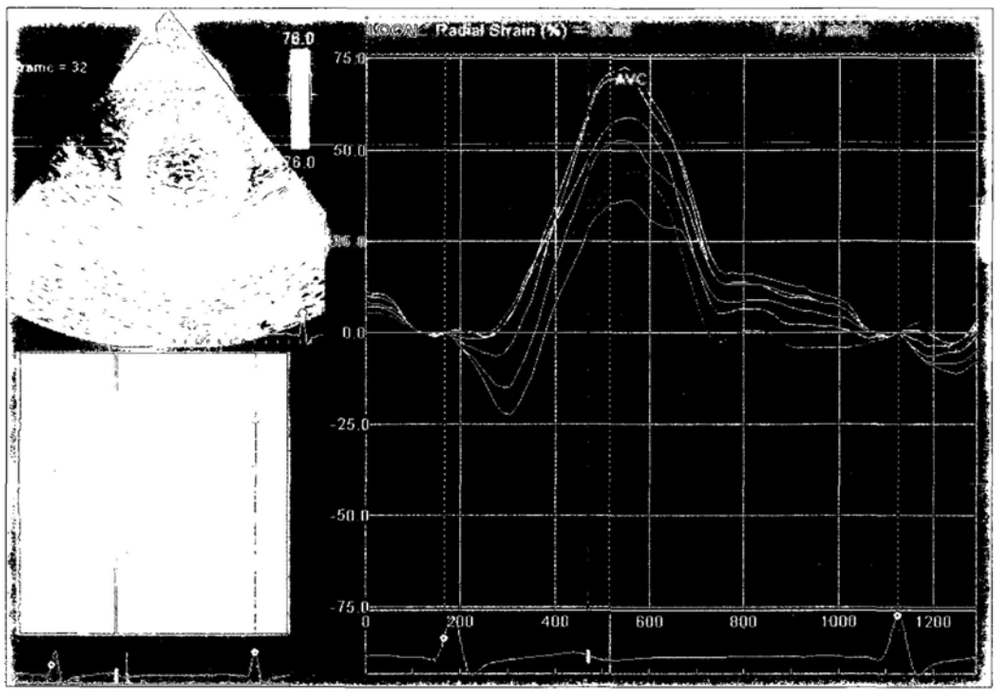

Figure 3.14 2D speckle tracking derived myocardial radial strain curves in parasternal short-axis view at apical level, which showed a positive tracking.

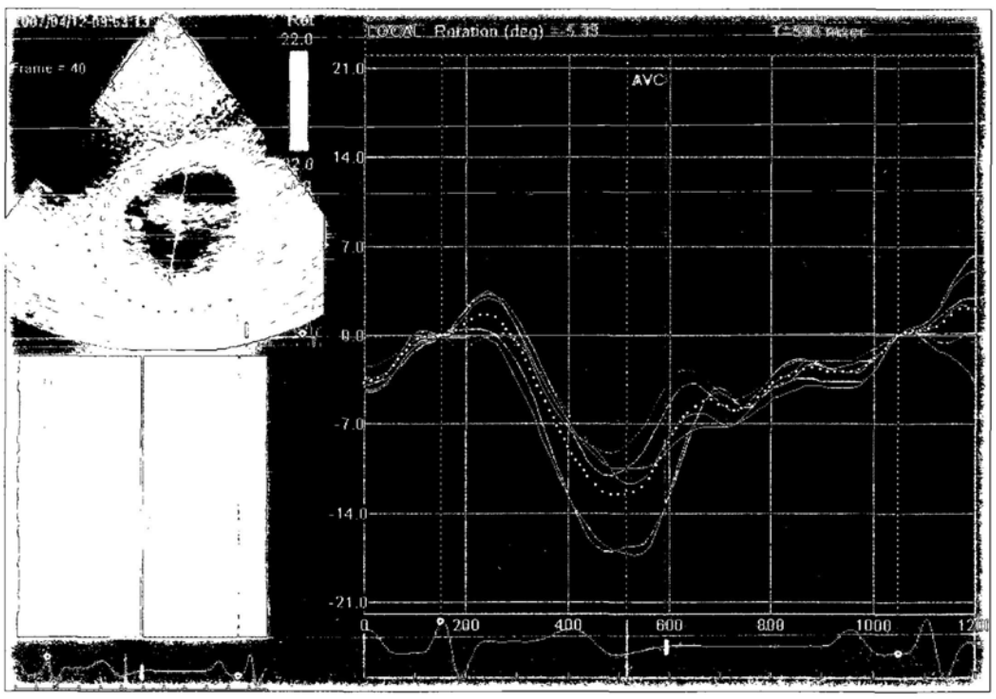

Figure 3.15 2D speckle tracking derived myocardial rotational strain curves in parasternal short-axis view at basal segments, which showed a negative tracking.

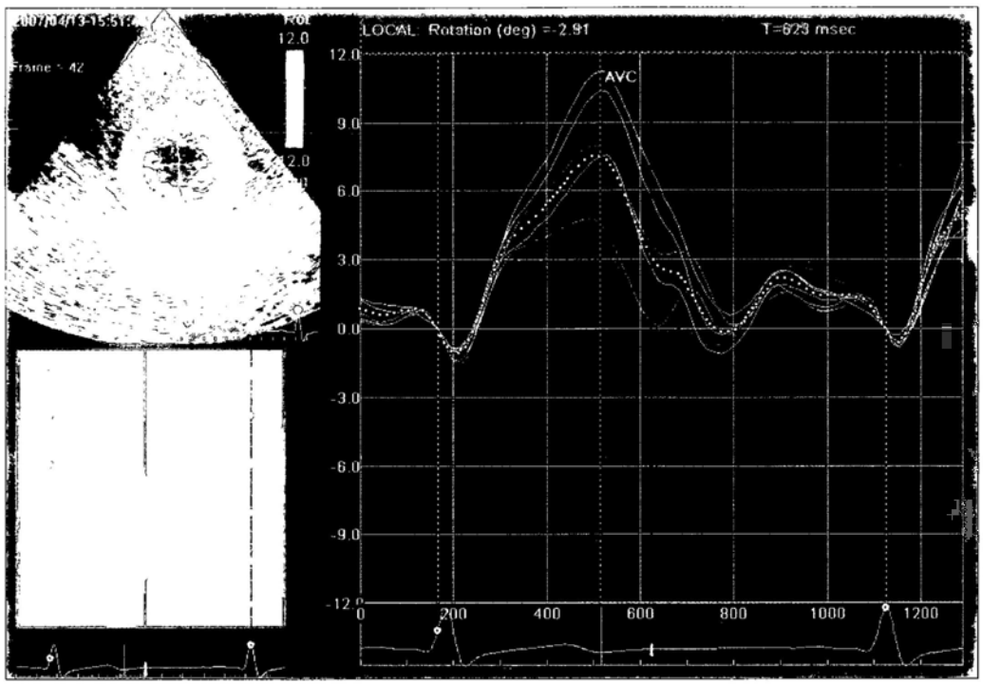

Figure 3.16 2D speckle tracking derived myocardial rotational strain curves in parasternal short-axis view at apical segments, which showed a positive tracking.

3.5 Statistical Analysis

Data were analyzed using a statistical software program (SPSS for windows, version 13.0, SPSS Inc, Chicago, Illinois, USA). Continuous variables were expressed as mean±SD. Categorical data were summarized as frequencies and percentages. Continuous data between two groups were compared by unpaired t-test. Continuous data between more than two groups were compared by one way analysis of variance with the Scheffe correction for significance. Analysis of covariance was used to examine the effects of age and gender on dependent variables when necessary. Categorical data between two or more groups were compared by Pearson chi-square test. Paired t-test or Wilcoxon signed ranks test was used when appropriate to compare paired parameters before and after treatment. Pearson correlation analysis was employed to examine the relationship between continuous variables. Receiver-operating characteristics (ROC) curve was used to define the cutoff point values. Linear or Logistic regression analysis was performed to investigate the association between continuous data or binominal data when appropriate. Forward stepwise multivariate Logistic regression analysis was performed to assess potential independent covariates. A probability value of $p < 0.05$ was considered statistically significant.

SECTION III

RESULTS

CHAPTER 4 LEFT VENTRICULAR MECHANICAL DYSSYNCHRONY AS A DETERMINANT IN THE PATHOGENESIS OF FUNCTIONAL MITRAL REGURGITATION

4.1 Background

Functional mitral regurgitation (MR) is frequently observed in patients with congestive heart failure, which conveys adverse prognosis (33, 34). The pathogenesis of functional MR involves multiple factors, whereas the basic mechanism is believed to be the increased mitral leaflet tethering due to the outward displacement of papillary muscles caused by global and regional left ventricular (LV) remodeling (83, 85-87). Other factors such as degree of LV remodeling and cavity dilatation have also been described (91, 92, 94).

LV mechanical dyssynchrony, which illustrates discoordinated contraction of the LV segments, has been suggested to occur in heart failure with a high prevalence and implies a poor prognosis (143, 145, 186). Recent studies showed that the immediate reduction of functional MR by cardiac resynchronization therapy (CRT) was associated with reduction in LV regional mechanical dyssynchrony involving LV segments bearing the two papillary muscles (120, 121). Further studies suggested that LV regional mechanical dyssynchrony could be a potential contributor to the severity of functional MR (84, 125). However, the contribution of LV global mechanical dyssynchrony has not been evaluated. Therefore, we undertook this quantitative study of patients with LV systolic dysfunction to assess the contribution of LV systolic dyssynchrony to functional MR, and to examine whether LV global or

regional systolic dyssynchrony will have an incremental value to other potential predictors of significant functional MR.

4.2 Methods

4.2.1 Patients

The study population consisted of 147 patients with impaired LV systolic dysfunction (defined as LV ejection fraction<50% measured by two-dimensional echocardiography). All patients were in sinus rhythm. The structures of the mitral valve apparatus were normal by echocardiographic examination in all patients. Patients with organic mitral valve diseases, more than trace aortic regurgitation, clinical or echocardiographic evidence of other cardiac diseases, previous implantation of any type of pacemaker or defibrillator, history of recent myocardial infarction (<16 days), as well as atrial fibrillation or other arrhythmia were excluded from the study.

4.2.2 Echocardiography

Standard transthoracic echocardiography, including tissue Doppler imaging (TDI) was performed in all patients (Vivid 7, Vingmed-General Electric, Horton, Norway). The assessments of MR severity, LV global and local remodeling, LV systolic function, mitral valve deformation and LV mechanical dyssynchrony were performed by offline analysis (EchoPac PC 7.0.0, Vingmed-General Electric, Horton, Norway).

The degree of functional MR was assessed by using the proximal isovelocity surface area (PISA) method and the quantitative Doppler method simultaneously (179). The effective regurgitant orifice area (EROA) was calculated using the PISA method. The

regurgitant volume and regurgitant fraction were calculated by the continuity equation. In patients with no or trivial MR by color Doppler echocardiography, EROA was assumed as zero.

For the assessment of LV global remodeling, LV end-systolic (LVESV) and end-diastolic (LVEDV) volumes were measured by Biplane Simpson's method (181). LV end-systolic and end-diastolic cavity length and mid cavity width were measured and sphericity indices at end-systole and end-diastole were calculated to assess the geometry of the LV (173). LV ejection fraction (181) and LV +dp/dt (180) were measured to evaluate LV systolic function.

LV local remodeling was assessed by papillary-fibrosa distance, which was measured from the posteromedial papillary muscle head to intervalvular fibrosa in apical long-axis view (83).

Mitral valve deformation was assessed by tenting area and tenting height measured from the parasternal long-axis view at mid-systole (83). The maximal and minimal mitral annular dimensions were measured and the maximal and minimal mitral annular areas (MAA) were calculated. Mitral annular contractility was calculated as the percentage of changes in MAA during the cardiac cycle.

LV systolic mechanical dyssynchrony was assessed by two-dimensional color-coded TDI in three apical views (i.e. apical 4-chamber, 2-chamber, and apical long-axis views). Myocardial velocity curves were reconstituted offline using the 6-basal, 6-mid segmental model in the LV as previously described. The time to the peak

systolic velocity during ejection phase (Ts) were measured in each segment (151, 182, 183). Both LV global and regional systolic dyssynchrony were assessed, whereas the former was assessed by the maximal difference of Ts among the 12 LV segments (Ts-dif) (185), while the latter was assessed using the absolute difference in Ts between the mid lateral and mid inferior segments, which reflect the delay between the anterolateral and posteromedial papillary muscle attaching sites (APM-PPM delay).

4.2.3 Statistical Analysis

Continuous variables are expressed as mean±SD. Categorical data are summarized as frequencies and percentages. Unpaired t-test or Pearson chi-square test was used when appropriate in comparisons between patient with and without significant functional MR. Pearson correlation analysis was employed to examine the relationship between EROA and the other clinical and echocardiographic parameters. Receiver-operating characteristics (ROC) curve was constructed to evaluate the contributions of valvular tenting and dyssynchrony to the degree of MR and to define the cutoff value for predicting significant functional MR. Determinants of significant functional MR was identified by univariate logistic regression followed by forward stepwise multivariate logistic regression. A p value <0.05 was considered statistically significant.

4.3 Results

4.3.1 Patient Baseline Characteristics

The mean age of patients was 65±13 years and there were 109 males. All had systolic dysfunction with ejection fraction of 30±9% (ranged from 13% to 48%). The

etiology of heart failure was identified as ischemic by documented history of myocardial infarction and/or positive coronary angiography in 76 (55%) patients while non-ischemic in the other 71 (45%) patients by negative coronary angiography. In patients with non-ischemic etiologies, 2 were hypertensive, 5 were alcoholic and 59 were suffering from idiopathic dilated cardiomyopathy. The mean QRS duration was 109ms and 44 (30%) patients had a prolonged QRS complex of >120ms. Medications included angiotensin-converting enzyme inhibitors (ACEi) or angiotensin receptor blockers (ARB) in 116 (79%), β-blockers in 105 (71.4%), diuretics in 92 (62.6%), nitrates in 45 (30.6%), spironolactone in 24 (16.3%) and digoxin in 14 (9.5%) patients.

4.3.2 Severity of Functional MR and Its Determinants

There were 11 (7.5%) patients with no or trace MR that could not be assessed by PISA method and hence recorded as zero, whereas the other 136 patients had measurable MR. Among the whole study population, the mean EROA was 17±13mm^2 (ranged from 0 to 61 mm^2), the regurgitant volume was 32±20ml (ranged from 0 to 76 ml), and the regurgitant fraction was 25±18% (ranged from 0 to 89%). By using EROA ≥20mm^2 as the cutoff value for clinically significant MR as previously validated (83), 47 (32%) patients had significant MR.

Comparisons were performed between patients with significant functional MR (Group 1, n=47) and those without (Group 2, n=100). The mean EROA was obviously larger in Group 1 than Group 2 (33±10 vs. 10±7mm^2, $p<0.001$), as well as the regurgitant volume (46±12 vs. 15±10ml, $p<0.001$) and regurgitant fraction (54±14 vs. 22±14%, $p<0.001$). Table 4.1 shows that no significant difference was

found in baseline demographics between the two groups except a borderline lower systolic blood pressure ($p=0.048$) in Group1. With respect to echocardiographic parameters, Group 1 and Group 2 were different in the extent of LV remodeling, LV contractility, mitral valve deformation as well as LV global and regional systolic dyssynchrony. As shown in Table 4.2, Group 1 had a larger LVEDV ($p=0.018$) and LVESV ($p=0.021$), greater end-systolic and end-diastolic LV short-axis dimension (both $p<0.05$), greater papillary-fibrosa distance ($p<0.001$), lower LV +dp/dt ($p<0.001$), larger tenting area ($p<0.001$) and tenting height ($p<0.001$) as well as more severe LV global ($p<0.001$) and regional ($p=0.001$) systolic dyssynchrony. In addition, it was observed that the size of EROA correlated with LV remodeling, LV contractility, mitral valvular and annular deformation, as well as LV global and regional systolic dyssynchrony (Table 4.2). Of note, the correlation between EROA and LV global systolic dyssynchrony (Ts-Dif) was closer than that of EROA and regional dyssynchrony (APM-PPM delay).

Table 4.1 Clinical characteristics of patients with and without significant mitral regurgitation

	EROA ≥ 20mm^2 (n=47)	**EROA < 20mm^2 (n=100)**	**P value**
Age, years	66±14	65±12	0.393
Gender, % patients			0.952
Male	74.5	74	
Female	25.5	26	
Etiology of heart failure, % patients			0.416
Ischemic	46.8	54	
Non-ischemic	53.2	46	
Body surface area, m^2	1.6±0.2	1.6±0.2	0.106
Systolic blood pressure, mmHg	118±18	127±21	0.048
QRS duration, ms	112±26	107±28	0.299

EROA, effective regurgitant orifice area.

Table 4.2 Echocardiographic characteristics of patients with and without significant mitral regurgitation

	Comparison between groups			Correlation with EROA	
	EROA≥20mm^2 (n=47)	**EROA<20mm^2 (n=100)**	**P value**	**Correlation coefficient**	**P value**
Global LV remodeling					
LV end-diastolic volume, ml	185±67	160±52	0.018	0.317	<0.001
LV end-systolic volume, ml	135±60	112±44	0.021	0.357	<0.001
End-systolic LV cavity length, cm	8.1±1.0	7.9±0.9	0.201	0.178	0.031
End-systolic LV cavity width, cm	4.6±0.80	5.0±1.0	0.010	0.317	<0.001
End-systolic LV sphericity index	1.67±0.27	1.76±0.28	0.063	-0.235	0.002
End-diastolic LV cavity length, cm	8.9±0.9	8.6±0.8	0.448	0.105	0.204
End-diastolic LV cavity width, cm	5.3±0.7	5.6±0.8	0.012	0.277	0.001
End-diastolic LV sphericity index	1.57±0.19	1.64±0.18	0.022	-0.244	0.003
Local LV remodeling					

Papillary-fibrosa distance, cm	3.8±0.4	3.4±0.4	<0.001	0.481	<0.001
LV contractility					
LV +dp/dt, mmHg/s	674±153	789±207	0.001	-0.347	<0.001
LV ejection fraction, %	28±9	31±9	0.051	-0.303	<0.001
Mitral valvular deformation					
Tenting area, cm^2	3.1±0.6	2.2±0.6	<0.001	0.655	<0.001
Tenting height, cm	1.4±0.2	1.1±0.2	<0.001	0.516	<0.001
Annular factors					
Diastolic mitral annular area, cm^2	7.0±1.3	6.8±1.1	0.420	0.194	0.018
Systolic mitral annular area, cm^2	6.4±1.4	6.1±1.1	0.176	0.244	0.003
Mitral annular contractility, %	9±5	11±6	0.055	-0.217	0.008
LV systolic dyssynchrony					
Ts-Dif, ms	108±52	67±40	<0.001	0.375	<0.001
APM-PPM delay, ms	71±47	46±38	0.001	0.274	0.001

APM-PPM delay, the absolute difference in time to peak systolic velocity between the mid lateral and mid inferior left ventricular segments; EROA, effective regurgitant orifice area; LV, left ventricle; Ts-Dif, the maximal difference in time to peak systolic velocity among the 12 LV segments.

To examine for predictors of clinically meaningful MR, the clinical and echocardiographic parameters in group comparison and correlation analysis were tested using univariate analysis, and the significant covariates were further testified by multivariate logistic regression analysis. It was shown that mitral valve tenting area (OR: 1.020, 95%CI: 1.012, 1.029, $p<0.001$) and Ts-Dif (OR: 1.011, 95%CI: 1.001, 1.021, $p=0.032$) were the only two independent predictors of significant MR (Table 4.3). Although tenting area was the most powerful factor ($\chi^2=50.30$, $p<0.001$), Ts-Dif ($\chi^2=4.89$, $p<0.001$) showed an incremental value for predicting the occurrence of severe functional MR ($\chi^2=55.20$ vs. 50.30, $p=0.027$) (Figure 4.1).

Table 4.3 Univariate and multivariate logistic regression analysis for predictors of significant mitral regurgitation

	Univariate analysis			Multivariate analysis		
	β	**CI**	**P value**	**β**	**CI**	**P value**
Systolic blood pressure, mmHg	0.982	0.965, 1.000	0.051	-	-	NS
Heart failure etiology, ischemic	1.334	0.666, 2.673	0.416	-	-	-
LV end-systolic volume, ml	1.009	1.002, 1.016	0.014	-	-	NS
LV +dp/dt, mmHg/s	0.997	0.995, 0.999	0.002	-	-	NS
Tenting area, mm^2	1.024	1.016, 1.032	<0.001	1.020	1.012, 1.029	<0.001
Papillary-fibrosa distance, mm	1.267	1.145, 1.403	<0.001	-	-	NS
Systolic mitral annular area, mm^2	1.002	0.999, 1.005	0.182	-	-	-
Ts-Dif, ms	1.020	1.011, 1.029	<0.001	1.011	1.001, 1.021	0.030
APM-PPM delay, ms	1.014	1.005, 1.023	0.002	-	-	NS

Abbreviations as in table 4.2.

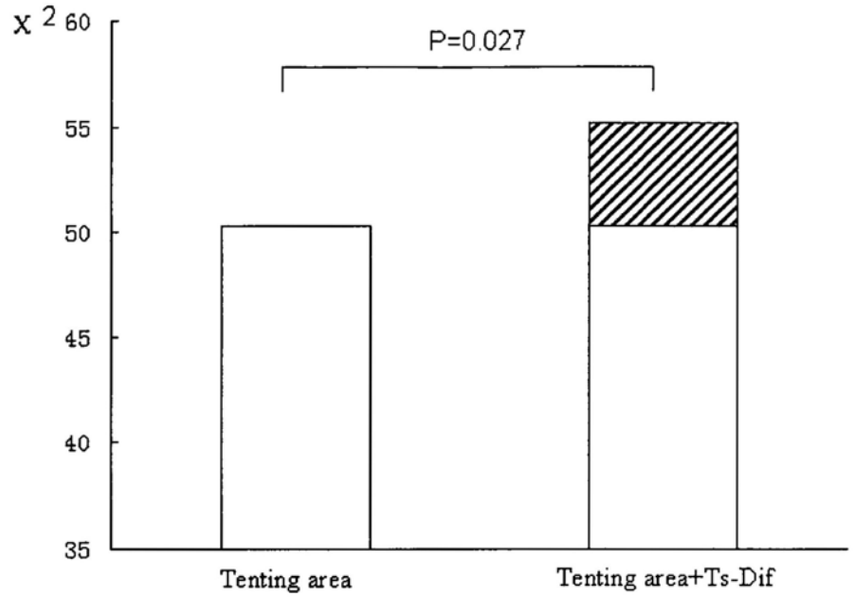

Figure 4.1 Incremental value of left ventricular global dyssynchrony over mitral valve tenting in predicting significant functional mitral regurgitation.

4.3.3 Mitral Valve Tenting, LV Dyssynchrony and Functional MR

From the shoulder of the ROC curve (Figure 4.2), a tenting area of 2.65cm^2 was associated with significant functional MR with a sensitivity of 83% and a specificity of 83% (AUC 0.87, $p<0.001$). The corresponding sensitivity and specificity were 66% and 72% for a Ts-Dif of 85ms (AUC 0.74, $p<0.001$). The prevalence of significant functional MR was the highest in patients who had both tenting area$\geq$2.65cm^2 and Ts-Dif $\geq$85ms (76.5%), the lowest in those with neither factors (4.5%), and was intermediate in those with only one factor (38.3%) (χ^2=54.64, $p<0.001$) (Figure 4.3). Figure 4.4 illustrated an example of patient who had neither significant functional MR nor significant LV global systolic dyssynchrony, whereas figure 4.5 illustrated an example of patients with significant functional MR and significant LV global systolic dyssynchrony.

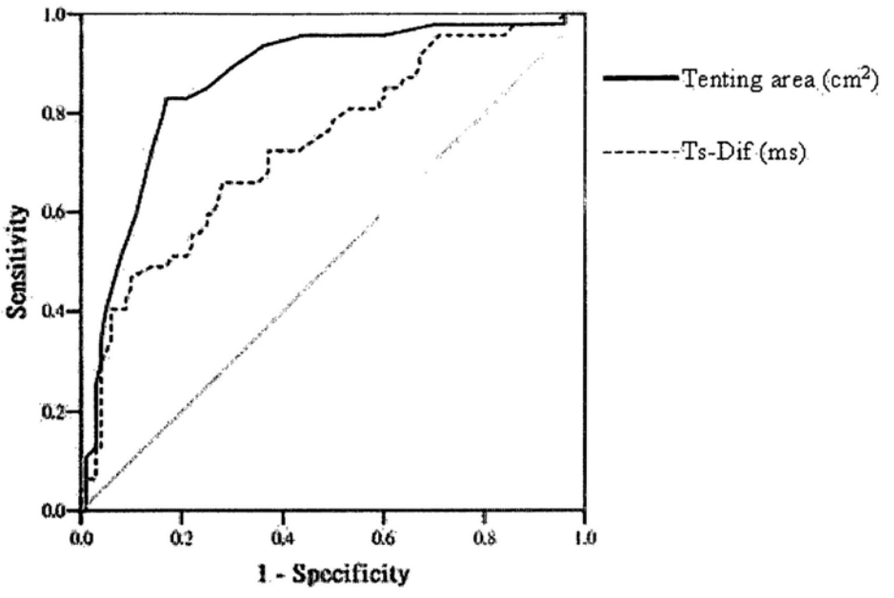

Figure 4.2 Mitral valve tenting area and left ventricular (LV) global dyssynchrony (Ts-Dif) predict the presence of significant functional mitral regurgitation. Receiver-operating characteristics curves showing the performance of mitral valve tenting area (solid line) as well as the maximal difference in time to peak systolic velocity among the 12 LV segments (Ts-Dif) (dotted line) in predicting the presence of significant functional mitral regurgitation.

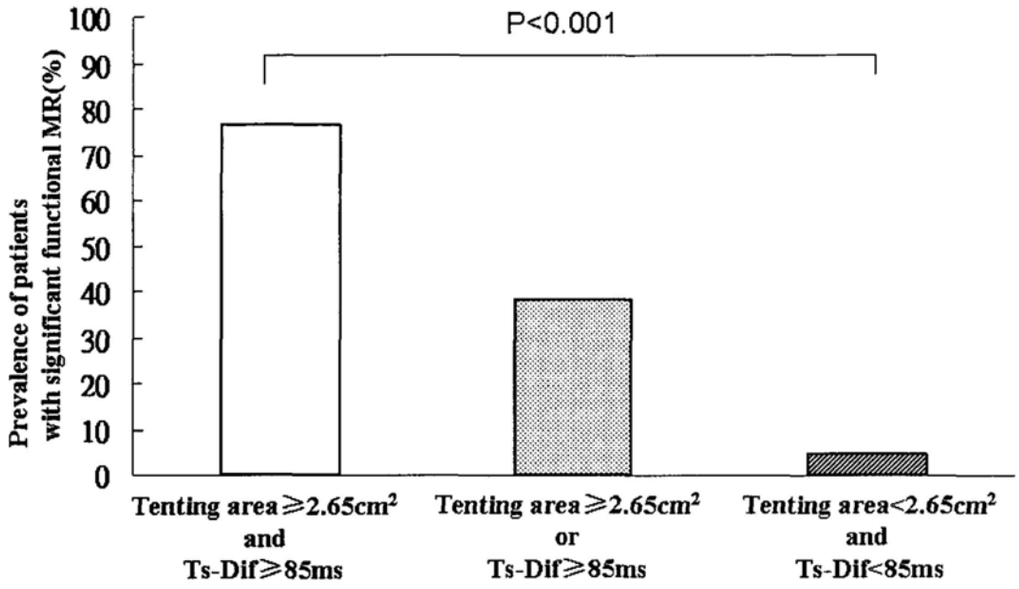

Figure 4.3 Impact of mitral valve tenting and left ventricular global dyssynchrony on the presence of significant functional mitral regurgitation (MR).

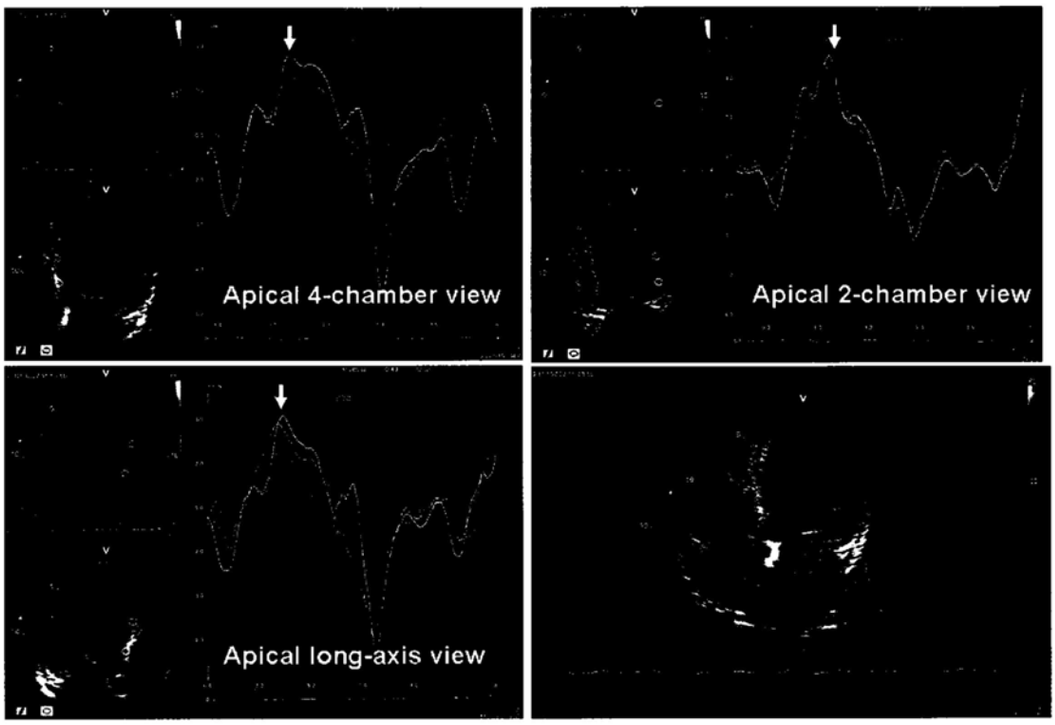

Figure 4.4 An example of patient without significant functional mitral regurgitation (EROA 9mm^2), and no excessive left ventricular global systolic dyssynchrony (Ts-Dif 32ms). The mitral valve tenting area was 2.80cm^2. Arrows are indicating the peak systolic velocity.

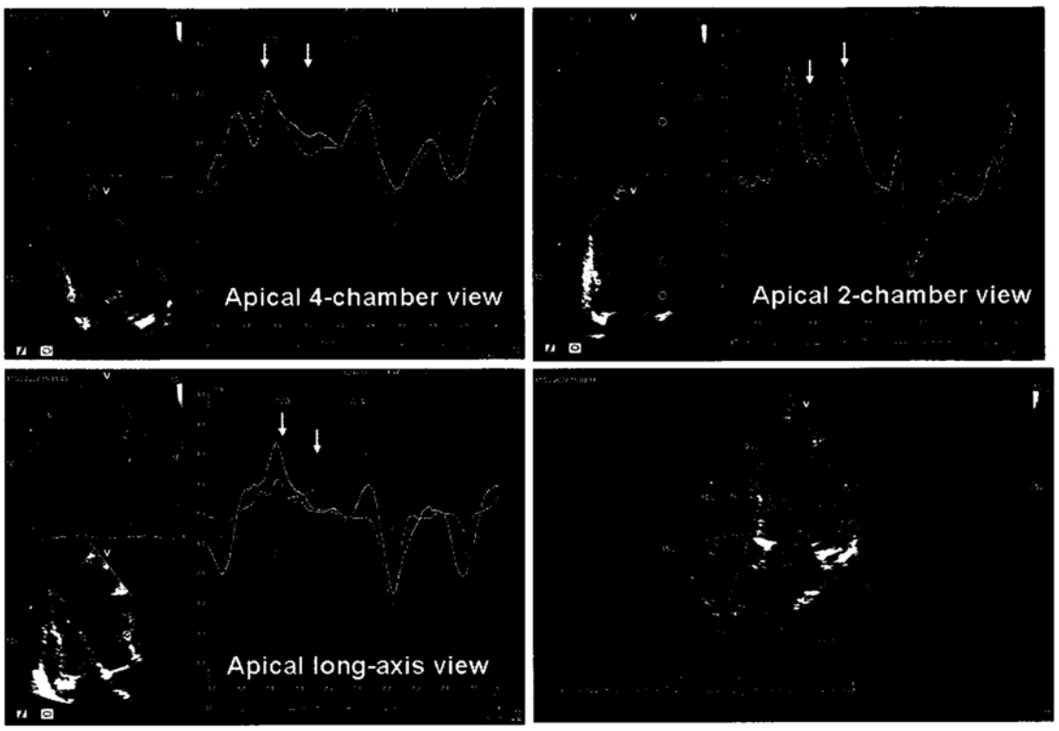

Figure 4.5 An example of patient with significant functional mitral regurgitation (EROA 34mm^2), and significant left ventricular global systolic dyssynchrony (Ts-Dif 112ms). The mitral valve tenting area was 3.60cm^2. Arrows are indicating the peak systolic velocity.

4.4 Discussion

In the present study, we demonstrated that in patients with LV systolic dysfunction, mitral valve tenting area was the most powerful predictor for the presence of significant functional MR. The other independent predictor was global LV systolic dyssynchrony, which had incremental value to mitral valve tenting area.

4.4.1 Mitral Valve Deformation as the Major Determinant of Functional MR

Several geometric and hemodynamic factors are interrelated and serve to determine the presence and degree of functional MR. Among them, mitral valve deformation caused by subvalvular tethering is considered to be the main determinant of MR severity (83, 84, 87). In prior studies, multiple parameters had been proposed for the assessment of mitral valve deformation, such as tenting area (83), tenting height (83), tenting volume by three-dimensional echocardiography (187), as well as leaflets concavity (101). In these studies, the degree of functional MR was found closely related to the extent of mitral valve deformation. In the present study, we also observed significant correlation between EROA and mitral valve deformation. Among multiple echocardiographic parameters assessed, mitral valve tenting area had the highest correlation coefficient of 0.655 with EROA. In fact, mitral valve tenting area is the strongest predictor for significant functional MR among the only parameters related to mitral valve deformation.

4.4.2 Contribution of LV Systolic Dyssynchrony to Functional MR

LV intraventricular systolic dyssynchrony is a subject of growing attention, in particular when patients with systolic dysfunction were assessed (143, 145, 186). Apart from its prognostic importance (186), its implication in cardiac

resynchronization (151, 173, 182, 184, 185, 188, 189), LV dyssynchrony may also play a role in the pathophysiologic mechanism of functional MR in patients with LV systolic dysfunction or heart failure. In early studies, the relationship between functional MR and dyssynchrony was demonstrated indirectly through the surrogate measurement of QRS duration, where higher degree of functional MR was associated with longer QRS duration (123, 173, 182, 184, 185, 188, 189). With the development of TDI, it provides another non-invasive tool to quantify regional motion and the severity of LV mechanical dyssynchrony. By using TDI derived velocity, a recent study has suggested that in patients with systolic dysfunction, systolic dyssynchrony was shown not to be an independent determinant of functional MR in the whole study patients that consisted of 39 ischemic and 35 non-ischemic subjects (84). Only in the subgroup analysis that the authors concluded LV systolic dyssynchrony was an independent determinant of functional MR in non-ischemic patients, but not ischemic ones. By applying TDI strain measurement between the two papillary muscles in 32 patients with non-ischemic dilated cardiomyopathy, another study concluded that regional dyssynchrony and LV chamber sphericity were independent determinant of functional MR, though surprisingly neither mitral valve tenting area nor coaptation distance were significant (125).

In the current study with a large sample size, we examined the potential predictive value of LV systolic dyssynchrony in patients with systolic dysfunction. In particular, we had performed a detailed analysis that included parameters of representing both global (Ts-Dif) and regional (APM-PPM delay) LV systolic dyssynchrony into multivariate analysis model. This will differentiate whether global or inter-papillary dyssynchrony will play an independent role. It was shown that Ts-Dif not only had a

larger correlation coefficient with EROA than APM-PPM delay, but in fact APM-PPM delay was no more an independent predictor of functional MR when Ts-Dif was also included into the statistical model. Interestingly QRS duration was not different between the two groups with and without significant functional MR. Therefore, it appears that the development of functional MR is not only determined by the uncoordinated motion generated from the two papillary muscles, but rather different LV segments with dyssynchronous motion in concerto contribute to the development of functional MR. The previous study by Agricola et al (84) was not able to different whether global or regional dyssynchrony would play a more important role as they measure eight segments adjacent to papillary muscles which would have included contribution of both factors.

LV systolic mechanical dyssynchrony may contribute to the severity of functional MR by several pathways. Firstly, the presence of LV global systolic mechanical dyssynchrony may decrease the efficiency of LV contraction during systole, thus decrease LV closing force acting on the mitral leaflets (90). Secondly, dyssynchronous contraction of the papillary muscle insertion site of the LV free wall may induce geometric distortion of the mitral valve apparatus (121, 122). Lastly, dyssynchronous contraction of the LV basal segments may render a non-simultaneous contraction of papillary muscles and adjacent LV walls, resulting in uneven timing of leaflet coaptation (128).

From our study, we have found out that a cutoff value of Ts-Dif of 85ms predicted the development of functional MR in our cohort that consisted of both ischemic and non-ischemic patients. This value indicated only moderate level of intraventricular

dyssynchrony, when compared with previously published value of 100ms which might favorable response after cardiac resynchronization therapy for heart failure patients (185). Of note, this cutoff value provides an incremental predictive value over MV tenting area of ≥ 2.65 cm^2 in predicting functional MR.

In conclusion, our study showed in patients with LV systolic dysfunction, significant functional MR is a relatively common condition. Significant functional MR was predicted not only predominately by the mitral valve tenting area, but also the degree of global LV systolic dyssynchrony. Furthermore, a cutoff value of Ts-Dif $\geq$85ms and mitral valve tenting area $\geq 2.7 cm^2$ was determined. The predictive values of these parameters need to be further assessed by large sample size studies.

CHAPTER 5 DIFFERENTIAL CHANGES IN LEFT VENTRICULAR MYOCARDIAL DEFORMATION IN PATIENTS WITH AND WITHOUT FUNCTIONAL MITRAL REGURGITATION

5.1 Background

Functional mitral regurgitation (MR) is increasingly recognized as a ventricular disease, in which the primary problem exists in the left ventricular (LV) myocardium rather than in the mitral valve itself. During the development of congestive heart failure, the LV undergoes complex change in geometry and function, accompanied by alterations of individual myocardial deformational components (190, 191). The presence of functional MR may further burden the failing LV with additional volume overload. However, it is unknown whether there is any difference in myocardial deformation between heart failure patients with and without functional MR. The recently introduced and validated modality of two-dimensional speckle tracking echocardiography (2DSTE) enables angle independent assessments of myocardial deformation in different directions. Therefore, the objectives of this study were to examine by 2DSTE whether the individual myocardial deformational component (radial, circumferential, longitudinal strain and rotation) and the basal to apical segmental myocardial deformation were different between heart failure patients with and without significant MR.

5.2 Methods

5.2.1 Patients

This study consisted of 45 patients with LV systolic dysfunction (defined as LV ejection fraction<50%) and significant functional MR [effective regurgitant orifice

area (EROA) ≥20 mm^2] (51, 52), 90 patients with matched ejection fraction but no significant functional MR (EROA<20 mm^2), and 45 normal controls who came from the community. One hundred and forty-seven patients with LV systolic dysfunction were recruited consecutively in the heart failure registry in the Prince of Wales hospital of Hong Kong for clinical signs and symptoms of heart failure from January 2007 to September 2008. Among them, 47 patients had significant functional MR (EROA≥20 mm^2), 2 of whom were excluded from this study because of the inadequate image quality for 2DSTE analysis. They were matched for LV ejection fraction with 90 patients with LV systolic dysfunction and insignificant functional MR (EROA<20 mm^2) who came from the other 100 patients with LV systolic dysfunction.

5.2.2 Echocardiography

Echocardiographic evaluation (Vivid 7 and EchoPac PC 7.0.0, Vingmed-General Electric, Horton, Norway) included quantification of MR, evaluation of LV systolic function and LV global remodeling, examination of LV mechanical dyssynchrony, and assessment of individual myocardial deformational component.

The severity of MR was evaluated by effective regurgitant orifice area EROA which was calculated using the proximal isovelocity surface area (PISA) method, as well as regurgitant volume and regurgitant fraction which were calculated by the continuity equation (179). In patients with no or trivial MR by color Doppler echocardiography, the EROA was assumed as zero.

LV end-systolic (LVESV) and end-diastolic (LVEDV) volumes and LV ejection fraction were measured using the biplane Simpson's method (181). LV cavity length and mid cavity width were measured at end-systole and end-diastole using apical-4 chamber view. The end-systolic and end-diastolic sphericity indices were calculated to evaluate the geometric change of the LV (173).

LV mechanical dyssynchrony was assessed by two-dimensional color tissue Dopper imaging (TDI) in three apical views (i.e. apical 4-chamber, 2-chamber, and long-axis views). The standard deviation of time to peak systolic velocity (Ts) among the 12 LV segments (Ts-SD) was calculated as the parameter for LV systolic mechanical dyssynchrony (151, 182-184).

Myocardial deformation measurements were performed by 2DSTE in the three apical views and parasternal short-axis views at basal, mid and apical levels. The data was accepted when the tracking quality satisfied the automatic evaluation of the system in all the six segments in the view. Then the longitudinal, circumferential and radial strain curves were obtained for each segment in the 18-segmental LV model. And the rotation curves were obtained in each segment of the basal and apical parasternal short-axis views. The peak systolic longitudinal (ε-long), circumferential (ε- circum) and radial (ε-radial) strains were measured in each segment while the peak rotation (Rot) was only assessed in the segments of basal and apical level. The following parameters were calculated for assessing global and segmental multidirectional myocardial deformation.

Global ε-long: Mean longitudinal peak systolic strain of the 18 LV segments

Basal ε-long: Mean longitudinal peak systolic strain of the 6-basal LV segments

Mid ε-long: Mean longitudinal peak systolic strain of the 6-mid LV segments

Apical ε-long: Mean longitudinal peak systolic strain of the 6-apical LV segments

Global ε-radial: Mean radial peak systolic strain of the 18 LV segments

Basal ε-radial: Mean radial peak systolic strain of the 6-basal LV segments

Mid ε-radial: Mean radial peak systolic strain of the 6-mid LV segments

Apical ε- radial: Mean radial peak systolic strain of the 6-apical LV segments

Global ε-circum: Mean circumferential peak systolic strain of the 18 LV segments

Basal ε-circum: Mean circumferential peak systolic strain of the 6-basal LV segments

Mid ε-circum: Mean circumferential peak systolic strain of the 6-mid LV segments

Apical ε-circum: Mean circumferential peak systolic strain of the 6-apical LV segments

Basal Rot: Mean rot of the 6-basal LV segments

Apical Rot: Mean rot of the 6-apical LV segments

Tor: Net-difference between basal and apical mean Rot

5.2.3 Statistical Analysis

Categorical data are summarized as frequencies and percentages. Continuous data between two groups were compared by unpaired t-test. Categorical data were compared by Chi square test. Relationship between deformational parameters and LV geometry was identified by Pearson's correlation. A probability value of $p<0.05$ was considered as statistically significant.

5.3 Results

5.3.1 Reduction of LV Myocardial Deformation in Patients with LV Systolic Dysfunction

The comparison on myocardial deformation between normal controls and patients with LV systolic dysfunction is shown in Table 5.1. As the patients were older (66±13 vs. 51±9, $p<0.001$) and predominantly male (73.3% vs. 53.3%, $\chi^2=6.24$, $p=0.012$), the p values presented in the table were adjusted for age and gender. Compared with the normal controls, patients with LV systolic dysfunction showed remarkable reduction in all the measured components of myocardial deformation, including global ε-long, global ε-circum, global ε-radial and Tor (all $p<0.001$). The findings were similar when the corresponding individual LV plane (basal, mid, apical) was compared between the two groups (all $p<0.001$).

When the mean-2SD from the normal controls was used to derive the cutoff values for different myocardial components, it was -16.3% for global ε-long, -20.4% for global ε-circum, 24.5% for global ε-radial and 11.1 degree for torsion. As a result, the impairment of global ε-long was found in 96.3%, global ε-circum in 100%, global ε-radial in 78.4% and LV torsion in 72.7% of the patients with LV systolic dysfunction.

Table5.1 Comparisons between normal controls and patients with LV systolic dysfunction

	Normal controls N=45	**Patients with LV systolic dysfunction N=135**	**P value**
Global ε-long, %	-21.3±2.5	-10.1±3.1	<0.001*
Basal ε-long, %	-21.0±2.9	-10.9±3.6	<0.001*
Mid ε-long, %	-21.1±2.4	-9.6±3.7	<0.001*
Apical ε-long, %	-21.9±4.6	-9.9±4.6	<0.001*
Global ε-circum, %	-27.0±3.3	-9.8±3.0	<0.001*
Basal ε-circum, %	-21.7±3.7	-11.3±3.9	<0.001*
Mid ε-circum, %	-25.8±4.5	-9.5±3.6	<0.001*
Apical ε-circum, %	-33.6±4.9	-8.7±4.5	<0.001*
Global ε-radial, %	45.1±10.3	18.5±9.7	<0.001*
Basal ε-radial, %	47.5±13.1	21.9±13.7	<0.001*
Mid ε-radial, %	53.6±15.4	21.4±13.6	<0.001*
Apical ε-radial, %	33.9±18.3	12.2±11.1	<0.001*
Torsion, degree	21.7±5.3	8.1±5.5	<0.001*
Basal rotation, degree	-7.5±3.7	-5.1±3.5	<0.001*
Apical rotation, degree	14.1±5.1	3.0±4.7	<0.001*

*P value adjusted for age and gender.

LV, left ventricle; ε-circum, circumferential peak systolic strain; ε-long, longitudinal peak systolic strain; ε-radial, peak radial systolic strain.

5.3.2 Differences in Individual Components of Myocardial Deformation and LV Geometry between Patients with and without Significant Functional MR

The patients with and without significant functional MR were comparable in age, gender, ejection fraction, etiology of hear failure and medications, except that MR was more severe in the former group measured by the EROA, regurgitant volume and regurgitant fraction (all $p<0.001$).

Comparisons on the individual component of myocardial deformation between patients with and without significant functional MR showed differential changes (Table 5.2). The global ε-radial ($p=0.011$) and global ε-circum ($p=0.023$) were significantly decreased in patients with significant MR, whereas no difference was found in the global ε-long between the two groups ($p=0.486$) (Figure 5.1a). At the same time, the degree of Tor was similar in patients with and without MR ($p=0.309$) (Figure 5.1b).

The patients with significant functional MR also had higher degree of LV remodeling compared to patients without significant functional MR, as reflected by a larger LVEDV ($p=0.042$) and LVESV ($p=0.047$), as well as increased end-systolic ($p=0.024$) and end-diastolic ($p=0.022$) LV cavity width and end-diastolic sphericity index ($p=0.018$) (Table 5.3 and Figure 5.2). In addition, significant correlations were found between end-systolic LV cavity width and global ε-circum ($r=0.484$, $p<0.001$) and global ε-radial ($r=-0.471$, $p<0.001$) (Figure 5.3). A larger Ts-SD was also observed with the MR patient group ($p<0.001$) (Table 5.3).

Table 5.2 Comparison of individual components of myocardial deformation between patients with and without significant functional MR

	Patients with significant functional MR N=90	**Patients without significant functional MR N=45**	**P value**
Global ε-long, %	-10.3±2.9	-9.9±3.6	0.486
Global ε-circum, %	-10.2±3.1	-9.0±2.8	0.023
Global ε-radial, %	20.0±9.0	15.6±10.2	0.011
Torsion, degree	8.4±5.7	7.4±5.1	0.309

MR, mitral regurgitation; Other abbreviaitons as in Table 5.1

Table 5.3 Differences in left ventricular volumes and geometry between patients with and without significant functional MR

	Patients with significant functional MR N=90	**Patients without significant functional MR N=45**	**P value**
LV end-diastolic volume, ml	163±53	184±67	0.042
LV end-systolic volume, ml	114±44	135±61	0.047
LV ejection fraction, %	31±8	28±9	0.141
End-systolic LV cavity length, cm	8.0±0.9	8.1±1.0	0.335
End-systolic LV cavity width, cm	4.6±0.7	5.0±1.0	0.024
End-systolic LV sphericity index	1.75±0.26	1.67±0.25	0.079
End-diastolic LV cavity length, cm	8.7±0.8	8.7±1.0	0.612
End-diastolic LV cavity width, cm	5.3±0.7	5.6±0.8	0.022
End-diastolic LV sphericity index	1.64±0.18	1.56±0.18	0.018
Ts-SD, ms	28.0±18.2	44.5±21.3	<0.001

Ts-SD, standard deviation in time to peak systolic velocity among 12 LV segments; Other abbreviations as in Table 5.1 and 5.2.

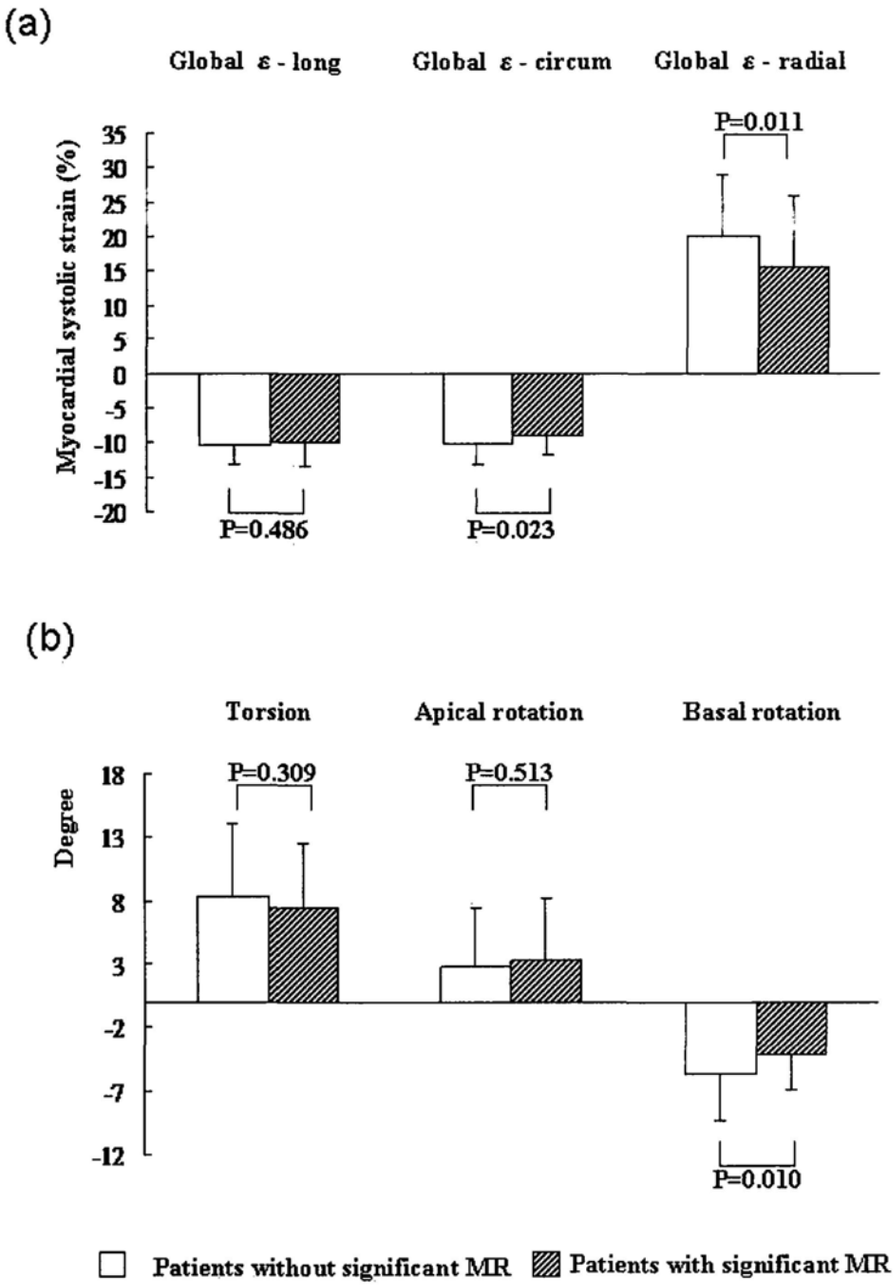

Figure 5.1 Bar charts showing the differences in mean longitudinal (global ε-long), circumferential (global ε-circum) and radial (global ε-radial) peak systolic strain of the 18 left ventricular segments (a) and left ventricular torsion and rotation (b) between patients with and without significant functional mitral regurgitation (MR).

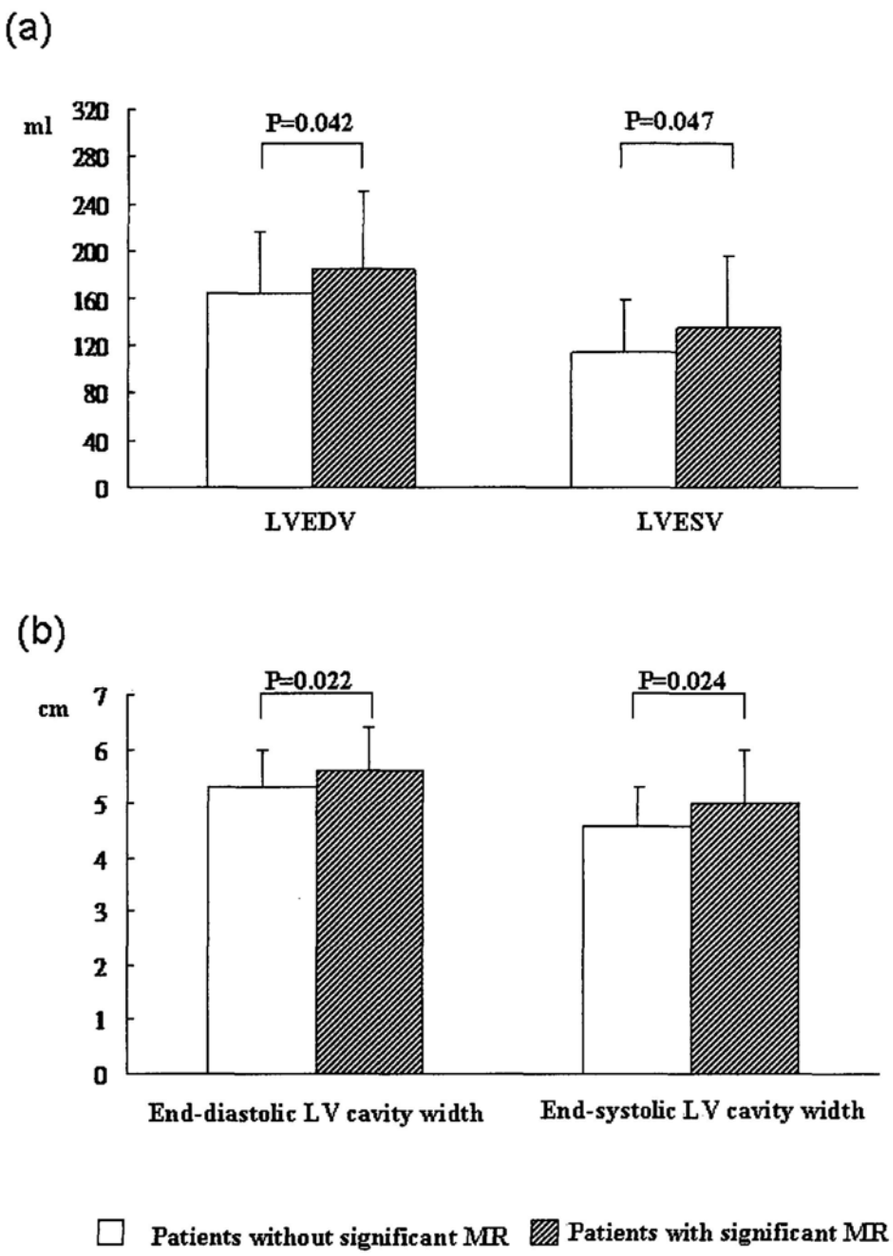

Figure 5.2 Bar charts comparing left ventricular (LV) end-diastolic volume (LVEDV) and end-systolic volume (LVESV) (a), as well as end-diastolic and end-systolic LV cavity width (b) between patients with and without significant functional mitral regurgitation (MR).

(a)

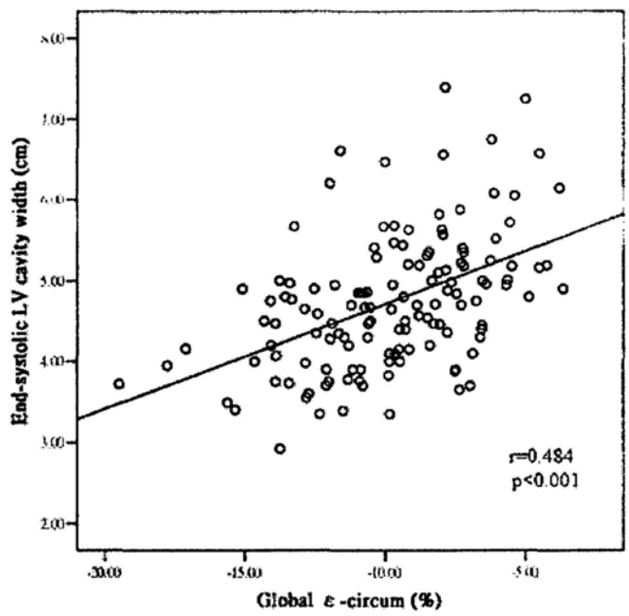

(b)

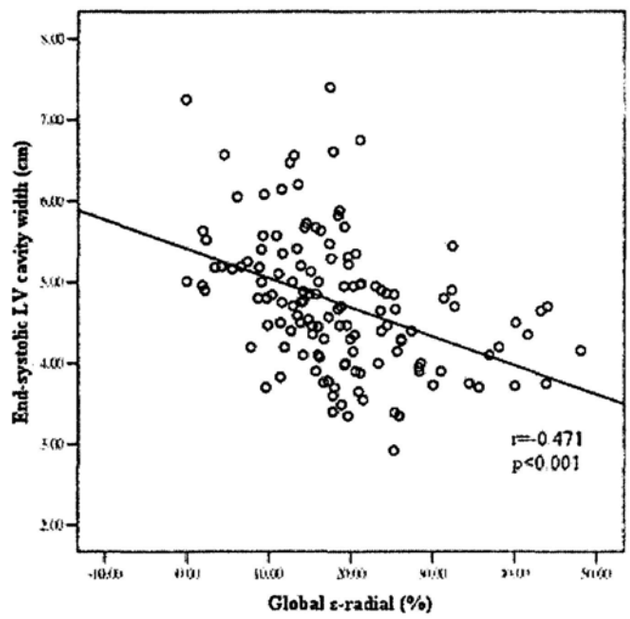

Figure 5.3 Scatter plots showing the correlation between end-systolic left ventricular (LV) cavity width and mean circumferential peak systolic strain of the 18 LV segments (global ε-circum) (a); and the correlation between end-systolic LV cavity width and mean radial peak systolic strain of the 18 LV segments (global ε-radial) (b) in patients with LV systolic dysfunction.

5.3.3 Differences in Segmental Myocardial Deformation between Patients with and without Significant Functional MR

When the segmental ε-long, ε-circum and ε-radial from basal to apical planes were compared between the two patient groups, a similar differential change was observed as that for the global deformation. As shown in Table 5.4, no difference occurred in the segmental ε-long of all the three levels. On the other hand, patients with significant functional MR had decreased values in basal ε-radial ($p=0.012$), mid ε-radial ($p=0.010$) and mid-circum ($p=0.014$) while the basal ε-circum also showed a trend of lower value in patients with MR ($p=0.093$). Although Tor was identical between patients with and without significant MR, the degree of basal Rot was smaller in the former group ($p=0.01$) (Figure 5.1b). Interestingly, there was no difference found in apical segments for all the deformation components between the two patient groups (Table 5.4).

Table 5.4 Comparison of segmental myocardial deformation between patients with and without significant functional mitral regurgitation

	Patients with significant functional MR N=90	**Patients without significant functional MR N=45**	**P value**
Basal ε-long, %	-11.3±3.7	-10.2±3.5	0.096
Mid ε-long, %	-9.9±3.7	-9.0±3.5	0.209
Apical ε-long, %	-9.7±4.2	-10.4±5.4	0.384
Basal ε-circum, %	-11.7±4.2	-10.5±3.2	0.093
Mid ε-circum, %	-9.9±3.9	-8.5±2.8	0.014
Apical ε-circum, %	-9.0±4.4	-7.9±4.8	0.176
Basal ε-radial, %	24.1±13.6	17.8±13.0	0.012
Mid ε-radial, %	23.5±13.4	17.2±13.0	0.010
Apical ε-radial, %	12.5±10.2	11.8±12.9	0.743
Basal rotation, degree	-5.7±3.6	-4.1±2.8	0.010
Apical rotation, degree	2.8±4.6	3.3±4.9	0.513

Abbreviations as in Table 5.1 and 5.2.

5.4 Discussion

In the present study, we demonstrated that all the myocardial deformational parameters were depressed in patients with LV systolic dysfunction compared with normal controls, including the longitudinal, circumferential and radial strains, as well as LV torsion. The circumferential and radial strains were further decreased in patients with significant functional MR, which was only significant in basal and mid LV segments but not in apical segments. The degree of LV basal rotation was also lower in the MR patient group. Furthermore, the decrease in myocardial deformation was associated with greater extent of LV remodeling as reflected by the LV cavity dilatation.

LV myocardial architecture has been described in previous studies as a transmural continuum between two helical fiber geometries, where longitudinal fiber with a right-handed helical geometry in the subendocardial layer transitions into a circumferential direction in the mid wall and becomes longitudinal again in a left-handed helical geometry in the subepicardial layer (192). Due to the complex alignment of the myocardial fibers, LV deformation during systole can be expressed in three ventricular coordinates: a longitudinal shortening, a circumferential shortening and a radial thickening. In addition, rotational movements around the long axis of the LV are produced as a result of the helical orientation of the subendocardial and subepicardial myocardial fibers.

The reduction in individual myocardial deformational components in patients with LV systolic dysfunction has been reported, though the extent of impairment may not be the same in each component (190, 191). The longitudinal myocardial fibers

aligned at the subendocardial and subepicardial layers are responsible for the majority of LV systolic function (193) and more susceptible to pathological conditions. Therefore, the impairment of long-axis myocardial deformation can be observed earlier than the short-axis deformation, even before the onset of heart failure symptoms and the occurrence of LV dysfunction (194, 195). On the other hand, in patients with LV systolic dysfunction where the longitudinal myocardial fibers are severely impaired, LV contraction is likely to be more determined by the short-axis myocardial fibers. Despite identical ejection fraction and ε-long in the present study, the differential changes in ε-circum and ε-radial between patients with and without significant MR suggests that higher degree of functional MR is associated with more severe ventricular disease which cannot be identified by ejection fraction. This is also supported by previous findings that greater extent of functional MR is associated with increased mortality, independent of the degree of LV systolic dysfunction measured by ejection fraction (51).

The progression of heart failure is characterized by progressive LV remodeling, where the dilation of LV mid cavity dimension resulting in a more spherical LV represents a major geometric change. This spherical shape of LV may further increase the workload of the heart and cause worsening of cardiac function. The increase in LV cavity width is accompanied by the reduction in short-axis function which are important in maintaining the normal shape of the LV. This will in turn give rise to further deterioration in LV geometry. In the current study, though all the parameters of myocardial deformation decreased in patients with LV systolic dysfunction compared with normal controls, the radial and circumferential strain was further reduced in patients with significant functional MR, which was associated

with a greater LV remodeling, in particular LV mid cavity dimension. In addition, the differential change was found in basal and mid but not apical segments. This implies that LV remodeling not only causes apical and outward displacement of the papillary muscles which leads to incompetence of mitral leaflets, but also relates to functional MR through the change in myocardial deformation, LV geometry, mitral annular contraction and mechanical dyssynchrony as well.

CHAPTER 6 IMPACT OF REDUCTION IN FUNCTIONAL MITRAL REGURGITATION ON REVERSE REMODELING RESPONSE AFTER CARDIAC RESYNCHRONIZATION THERAPY

6.1 Background

Cardiac resynchronization therapy (CRT) is an established therapy for patients with advanced chronic heart failure with prolonged QRS duration (146). Clinical data have suggested the beneficial role of CRT on symptoms, functional capacity (148-150), cardiac function (151, 152) and prognosis (153-155). On cardiac functional assessment, apart from evidence of improvement in systolic function leading to left ventricular (LV) reverse remodeling, improvement of functional mitral regurgitation (MR) has been described in previous studies (90, 120-122, 166). In fact, improvement of functional MR could be an important component underlying the favorable hemodynamic changes and gain in systolic function due to volume unloading effect in the LV and pressure offload in the left atrium (LA) (196, 197). However, it has not been explored whether the presence of pre-pacing functional MR and its improvement might have impact on the improvement of LV systolic function and reverse remodeling. Therefore, the present study was aimed to examine the impact of baseline MR and MR improvement on the extent of changes in LV volume and ejection fraction after CRT.

6.2 Methods

6.2.1 Patients

The study population consisted of 83 patients with advanced congestive heart failure who had received CRT implantation for three months. The inclusion criteria for

receiving CRT were compatible with the current guideline, i.e. evidence of LV systolic dysfunction with LV ejection fraction ≤35% despite optimal medical therapy, NYHA class III and IV as well as QRS duration on surface ECG >120ms (146). All patients were in sinus rhythm before device implantation. Patients with clinical or echocardiographic evidence of other cardiac disease, structural abnormalities of the mitral valve apparatus or more than mild aortic regurgitation were excluded from this study. The atrioventricular interval was optimized using Ritter's method on day one after the implantation (178). Clinical and echocardiographic assessments were performed before and three months after CRT. The study protocol was approved by the Ethics Committee of the institution and written informed consents were obtained from all the patients.

6.2.2 Echocardiography

Transthoracic echocardiography was performed (Vivid 7, Vingmed-General Electric, Horton, Norway) before and three months after CRT implantation. LV end-diastolic volume (LVEDV), end-systolic volume (LVESV) and ejection fraction were calculated using biplane Simpson's method (181). In the apical 4-chamber view, the LV end-systolic and end-diastolic cavity length and mid-cavity width were measured. The end-systolic and end-diastolic sphericity indices were estimated for assessment of the change in LV geometry (173). At three months after CRT, patients with a reduction in LVESV of ≥15% were defined as responders of LV reverse remodeling (173).

MR was quantified semi-quantitatively from color flow Doppler images in the apical 4-chamber view by the ratio of MR jet area to LA area (JA/LAA). The severity of

MR was graded on a three-point scale: no or mild (JA/LAA<20%), moderate (JA/LAA 20-40%), severe (JA/LAA≥40%). At three months after CRT, a reduction of at least one grade in MR was considered a significant improvement in MR (179).

LV mechanical dyssynchrony was assessed by two-dimensional color tissue Doppler imaging (TDI) using the 6-basal and 6-mid segmental model. The standard deviation (Ts-SD) in the time to peak systolic velocity among the 12 LV segments was calculated as the parameter for global LV systolic dyssynchrony (151, 182-184).

6.2.3 Clinical Assessment

Assessment of clinical status included New York Heart Association (NYHA) functional class and Minnesota Living with Heart Failure (MLWHF) quality of life score.

6.2.4 Statistical Analysis

Continuous variables were expressed as mean±SD. Categorical data were summarized as frequencies and percentages. Paired t-test or Wilcoxon signed ranks test was used when appropriate to compare between baseline and after CRT. Unpaired t-test was used to compare between responders and nonresponders. One-way ANOVA or Pearson chi-square test was used when appropriate to compare among the three patient groups. Determinants of LV reverse remodeling were identified by univariate logistic regression followed by backward stepwise multivariate logistic regression. A p value <0.05 was considered statistically significant.

6.3 Results

6.3.1 LV Reverse Remodeling and Improvement in MR after CRT

The demographic and clinical characteristics of the patients are shown in Table 6.1. At 3 months after CRT implantation, LV reverse remodeling was achieved by the reduction in LVEDV and LVESV, as well as gain in ejection fraction (all $p<0.001$) (Table 6.2). Forty-five out of 83 patients (54%) were found to be the responders with the reduction of LVESV $\geq$15% while the other 38 (46%) were nonresponders. Improvement of LV geometry was achieved by a greater extent of decrease in the LV width ($p<0.001$) than the length ($p<0.05$) which resulted in a higher sphericity index ($p<0.05$), i.e. a less globular shape of LV.

When compared between baseline and three month, functional MR was significantly improved after CRT in terms of the JA/LAA ratio and the grade of MR severity (both $p<0.05$) (Table 6.2). In the 35 patients with no or mild MR before device implantation, the MR JA/LAA showed minimal changes (from 8±7% to 5±7%, $p=0.006$) and none of the patients had any change in MR grade after CRT. On the other hand, in the 48 patients who had more than mild pre-pacing MR, it was reduced significantly after CRT as reflected by a decrease in the JAA/LAA (38±15% vs. 29±15 %, $p<0.001$) and the MR grade (moderate: 30, severe: 18 vs. no or mild: 17, moderate: 20, severe: 11, $p<0.001$). Among the 48 patients, 22 (45.8%) had at least one grade of MR reduction after CRT while the other 26 (54.2%) patients did not have such improvement, including 1 with one grade of worsening and 25 without any change of grade in MR. Both the patients with more than mild MR (n=48) and those with no or mild MR (n=35) before implantation showed significant LV reverse remodeling response after CRT (all $p<0.001$), however there were no differences in the degrees of reduction in LVEDV (-7.7±12.8 vs. -10.0±13.8%) and LVESV

(-17.1±16.0 vs. -18.6±16.6%) as well as gain in ejection fraction (7.2±7.1 vs. 7.0±6.8%) (all p=NS). Similarly, no significant difference was found in responder rate between the two groups (54.3% vs. 54.2%, χ^2=0, p=1.0).

In addition, LV mechanical dyssynchrony was improved after CRT, as reflected by a significant reduction in Ts-SD ($p<0.05$). The clinical status was also significantly improved, which included a lower NYHA class ($p<0.001$) and MLWHF quality of life score after CRT ($p<0.005$) (Table 6.2).

Table 6.1 Baseline demographic and clinical characteristics of the study population

Parameters	**Patients (n=83)**
Age, years	65±13
Gender, % male	62 (74.7%)
Etiology of heart failure, % ischemic	39 (47.0%)
NYHA class, % patients	
III	81 (97.6%)
IV	2 (2.4%)
MLWHF Quality of life score	27±20
Medications:	
Diuretic	77%
ACEi or ARB	85%
β-Blocker	79%
Spironolactone	28%
Nitrate	28%
Digoxin	14%

ACEi, angiotensin-converting enzyme inhibitor; ARB, angiotensin receptor blocker; MLWHF, Minnesota Living with Heart Failure; NYHA, New York Heart Association.

Table 6.2 Comparison of echocardiographic and clinical parameters at baseline and three months after cardiac resynchronization therapy

Parameters	**Baseline**	**3-Month**	**P value**
LV end-diastolic volume, ml	168±56	154±61	<0.001
LV end-systolic volume, ml	123±48	102±50ml	<0.001
LV ejection fraction, %	28±6	36±8	<0.001
End-systolic LV cavity length, cm	8.1±0.9	7.9±0.9	0.032
End-systolic LV cavity width, cm	4.7±0.8	4.4±0.9	<0.001
End-systolic LV sphericity index	1.7±0.3	1.9±0.3	<0.001
End-diastolic LV cavity length, cm	8.7±0.9	8.6±0.9	0.028
End-diastolic LV cavity width, cm	5.5±0.9	5.2±0.9	<0.001
End-diastolic LV sphericity index	1.6±0.2	1.7±0.3	0.011
Ts-SD, ms	39±15	34±17	0.010
JA/LAA, %	25±20	19±17	<0.001
Grade of MR, %			<0.001
No or mild	42	61	
Moderate	36	25	
Severe	22	13	
MLWHF Quality of life score	27±20	21±19	0.003
NYHA class, % patients			<0.001
I	0	8	
II	0	75	
III	98	17	
IV	2	0	

LV, left ventricle; JA/LAA, ratio of the mitral regurgitant jet area to left atrial area;

MR, mitral regurgitation; Ts-SD, the standard deviation in time to peak systolic velocity among the 12 LV segments. Other abbreviations as in Table 6.1.

6.3.2 MR Improvement in Responders and Nonresponders

Table 6.3 displays the baseline and change in LV volumes and functional MR between the responders and nonresponders of reverse remodeling. Before the device implantation, no difference was observed in MR severity no matter the JA/LAA ($p=0.928$) or the grade of MR ($p=0.904$) was used. Although responders had slightly smaller LVEDV at baseline ($p=0.043$), the LV ejection fraction was comparable between the 2 groups of patients. At 3 months after CRT, the reduction of MR JA/LAA was significantly greater in responders than nonresponders ($p<0.001$). Meanwhile, despite the identical grade of MR at baseline, the grade of MR at 3-month follow up was markedly lower in responders ($p<0.001$). Not surprisingly, the reduction in LV volumes and gain in ejection fraction were more obvious in responders than nonresponders (all $p<0.001$).

Table 6.3 Comparison of mitral regurgitation and left ventricular remodeling between responders and nonresponders

Parameters	**Responder (n=45)**	**Nonresponder (n=38)**	**P value**
Baseline JA/LAA, %	25±17	25±22	0.928
Grade of MR at baseline, %			0.904
Mild	42.2	42.1	
Moderate	37.8	34.2	
Severe	20.0	23.7	
Baseline LV end-diastolic volume, ml	157±44	182±67	0.043
Baseline LV end-systolic volume, ml	114±37	133±58	0.075
Baseline LV ejection fraction, %	28±5	28±7	0.954
Absolute change in JA/LAA, %	-11±11	-2±10	<0.001
Grade of MR at 3-month, %			0.004
Mild	77.8	42.1	
Moderate	15.6	36.8	
Severe	6.7	21.1	
Change in LV end-diastolic volume, %	-16±12	0±9	<0.001
Change in LV end-systolic volume, %	-30±11	-3±7	<0.001
Absolute change in LV ejection fraction, %	11±6	2±5	<0.001

Abbreviations as in Table 6.2.

6.3.3 The Relationship between Functional MR and Degree of LV Reverse Remodeling

In the 48 patients who had more than mild MR at baseline, significant correlation was observed between the percentage change in LVESV and the change in MR JA/LAA after CRT ($r=0.583$, $p<0.001$) (Figure 6.1). When the improvement of MR JA/LAA was included in a multivariate logistic regression model with other baseline parameters such as pre-pacing MR JA/LAA, LV ejection fraction, LV cavity width at end-systole and Ts-SD, the Ts-SD before implantation ($\beta=1.074$, $p=0.014$) and improvement of MR JA/LAA ($\beta=0.885$, $p=0.002$) were the independent determinants of LV reverse remodeling.

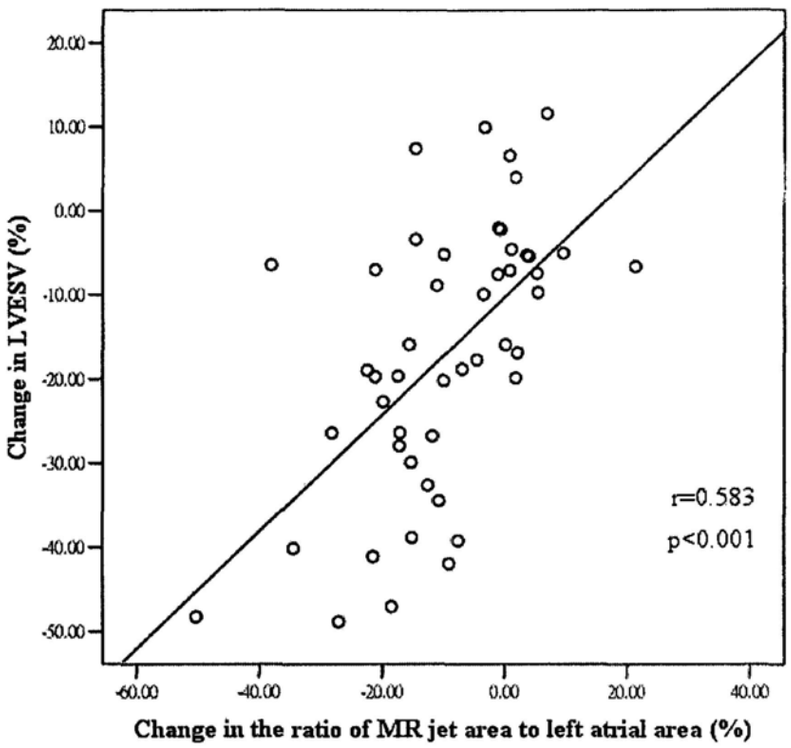

Figure 6.1 Scatter plots showing the correlation between the change in left ventricular end-systolic volume (LVESV) and the change in the ratio of mitral regurgitant (MR) jet area to left atrial area after cardiac resynchronization therapy.

Furthermore, the 48 patients were divided into two groups, i.e. the patients with a significant MR improvement identified by at least one grade reduction after CRT (Group 1, n=22) and those without (Group 2, n=26). The 35 patients with no or mild functional MR at baseline were classified into Group 3.

Although the LV volumes at baseline were relatively larger in Group 1 and Group 2, the LV ejection fraction was comparable among the three groups. At 3-month after CRT, all the three groups showed improvement in LVESV and ejection fraction while the reduction in LVEDV was not observed in Group 2 (Table 6.4). Furthermore, the magnitude of LV reverse remodeling was different among the three groups when assessed by absolute and percentage changes in LVESV after CRT. Interestingly, the greatest reduction in LVESV was found in Group 1 (-36±18ml or -29.1±13.6%), the least in Group 2 (-9±14ml or -7.0±9.6%), and intermediate in Group 3 (-19±19ml or -18.6±16.6%) (all $p<0.05$) (Figure 6.2a). Similarly, Group 1 showed the greatest gain in LV ejection fraction (12.2±5.5%), which was followed by Group 3 (7.0±6.8%), and was the least in the Group 2 (3.0±5.5%) (all $p<0.05$) (Figure 6.2b). Accordingly, the responder rate was the highest in Group 1 (86.4%), intermediate in the Group 3 (54.3%), and was the lowest in Group 2 (26.9%) ($\chi^2=16.96$, $p<0.001$). Figure 6.3 to 6.5 showed examples of the extent of changes in LVESV among the three groups. With respect to the changes in LV geometry, both end-systolic and end-diastolic sphericity indices were increased in Group 1, while only end-systolic sphericity index was increased in Group 3, but were neither of them in Group 2 after CRT (Table 6.4).

For baseline clinical status, the NYHA class and quality of life score were similar

among the three groups. At 3-month after CRT, NYHA class was significantly improved in all the three groups, though improvement of quality of life score was only observed in Group1 and Group 3, but not in Group 2 (Table 6.4).

Table 6.4 Comparisons between patients with MR improvement, patients without MR improvement and patients with no or mild MR at baseline

Parameters	**Patients with MR improvement (n=22)**			**Patients without MR improvement (n=26)**			**Patients with no or mild MR at baseline (n=35)**		
	Baseline	***3-Month***	***P value***	***Baseline***	***3-Month***	***P value***	***Baseline***	***3-Month***	***P value***
LV end-diastolic volume, ml	171±44	149±51	<0.001	190±68	186±73	0.349	150±48†	134±47	<0.001
LV end-systolic volume, ml	128±43	92±44	<0.001	141±57	132±57	0.003	106±40†	87±40	<0.001
LV ejection fraction, %	27±6	39±8	<0.001	27±6	30±7	0.011	30±6	37±8	<0.001
End-systolic LV cavity length, cm	8.1±0.7	7.8±0.9	0.033	8.2±1.2	8.1±1.0	0.675	7.9±0.8	7.8±0.7	0.089
End-systolic LV cavity width, cm	5.0±0.6	4.4±0.8	<0.001	5.1±0.8	4.9±0.8	0.068	4.2±0.7*†	4.0±0.9	0.011
End-systolic LV sphericity index	1.62±0.24	1.81±0.28	<0.001	1.63±0.20	1.68±0.20	0.283	1.9±0.3*†	2.0±0.4	0.046
End-diastolic LV cavity length, cm	8.7±0.6	8.5±0.8	0.080	8.9±1.0	8.7±1.1	0.105	8.6±0.9	8.5±0.8	0.573
End-diastolic LV cavity width, cm	5.7±0.6	5.2±0.7	<0.001	5.9±0.9	5.6±0.90	0.094	4.9±0.7*†	4.7±0.7	0.168
End-diastolic LV sphericity index	1.56±0.19	1.65±0.21	<0.001	1.52±0.17	1.57±0.18	0.360	1.8±0.2*†	1.8±0.3	0.224

MLWHF Quality of life score	26±17	14±12	0.004	28±20	30±23	0.667	26±21	18±18	0.003
NYHA class, % patients			<0.001			<0.001			<0.001
I	0	18		0	11		0	0	
II	0	77		0	62		0	83	
III	100	5		100	27		94	17	
IV	0	0		0	0		6	0	

*p<0.05 compared to patients with MR improvement; †p<0.05 compared to patients without MR improvement.

Abbreviations as in Table 6.1 and 6.2.

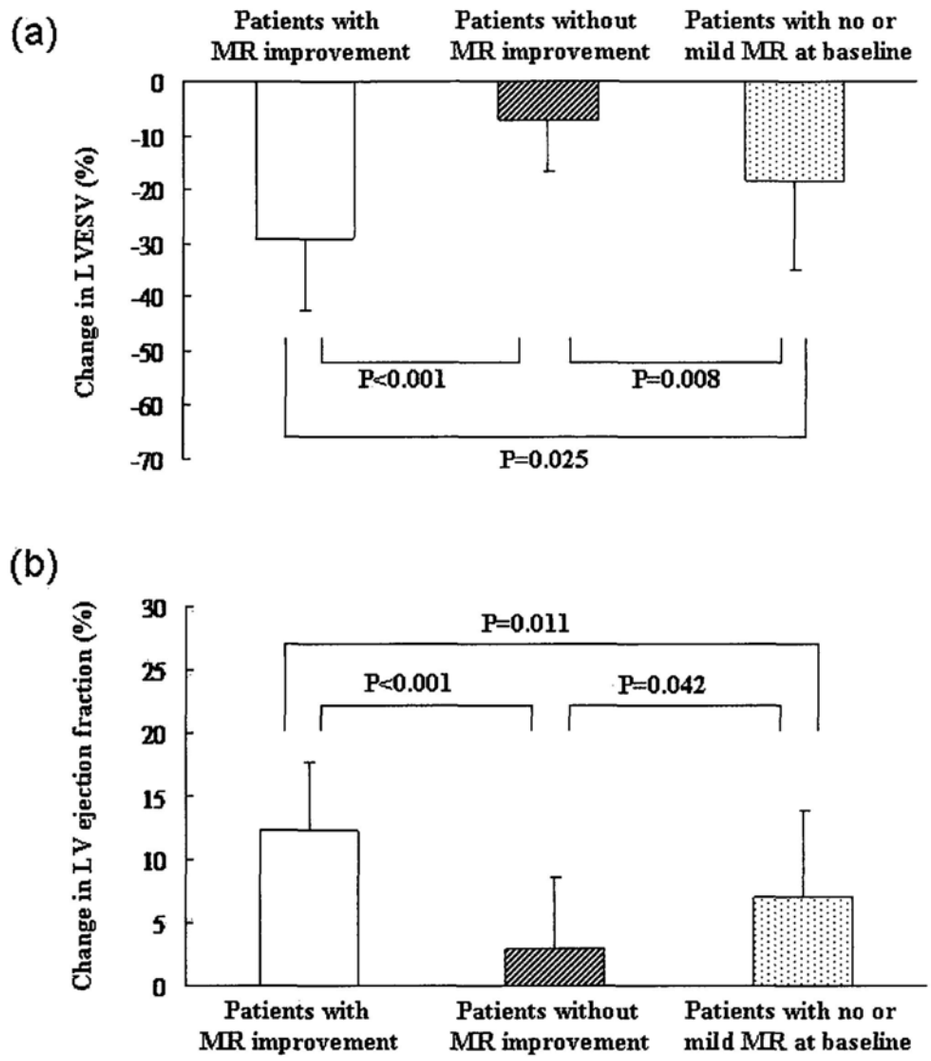

Figure 6.2 Bar charts comparing the extent of reduction in left ventricular end-systolic volume (LVESV) (a) and gain in left ventricular ejection fraction (b) among the three groups, namely patients with mitral regurgitation (MR) improvement, patients without MR improvement and patients with no or mild MR at baseline.

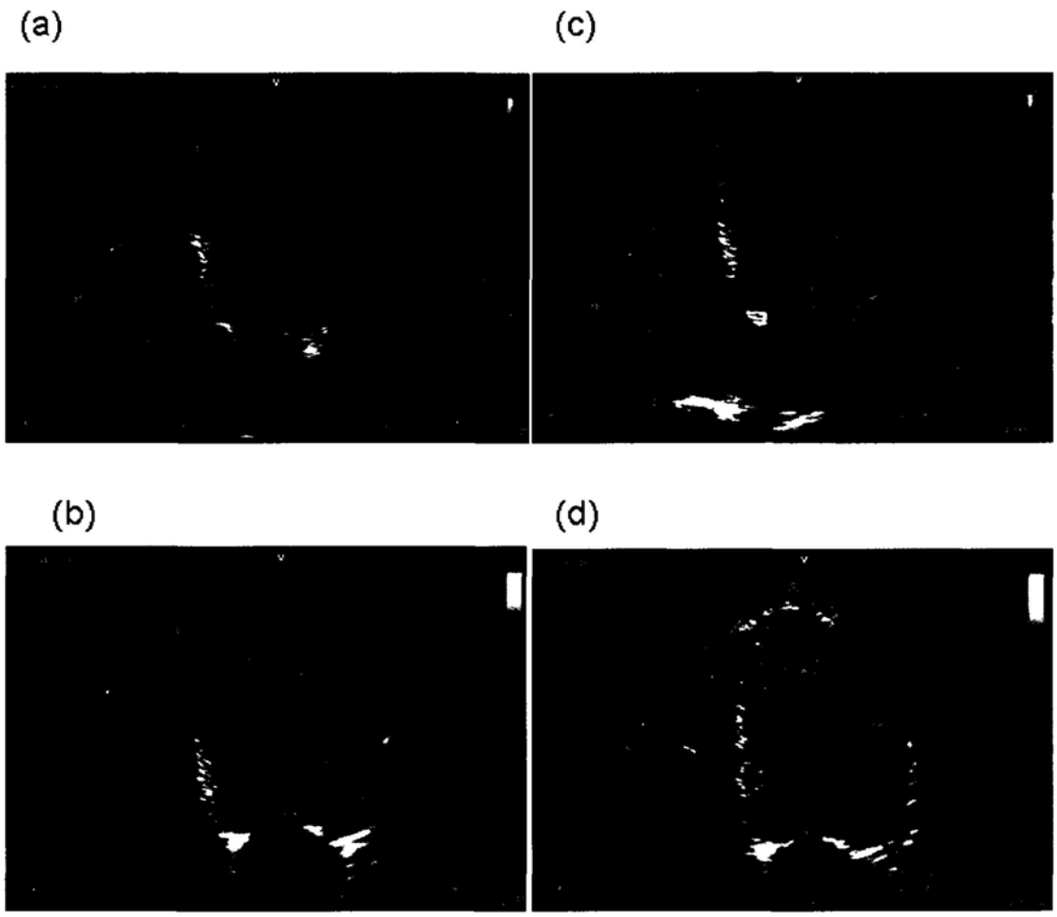

Figure 6.3 A patient from Group 1 before (a&b) and after (c&d) cardiac resynchronization therapy. The ratio of mitral regurgitant jet area to left atrial area decreased from 27% to 4% (a&c). And there was 48.9% reduction in left ventricular end-systolic volume (b&d).

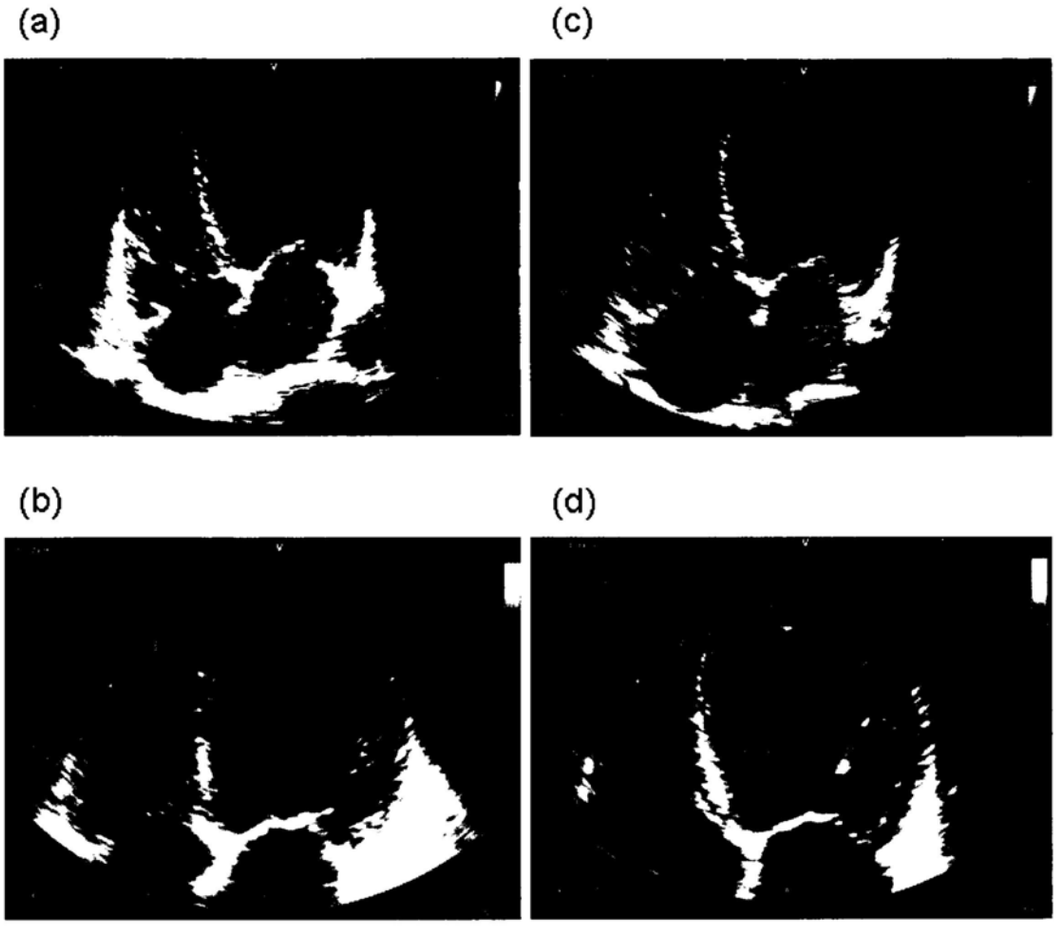

Figure 6.4 A patient from Group 2 before (a&b) and after (c&d) cardiac resynchronization therapy. The ratio of mitral regurgitant jet area to left atrial area increased from 47% to 52% (a&c). And there was 9.9% increase in left ventricular end-systolic volume (b&d).

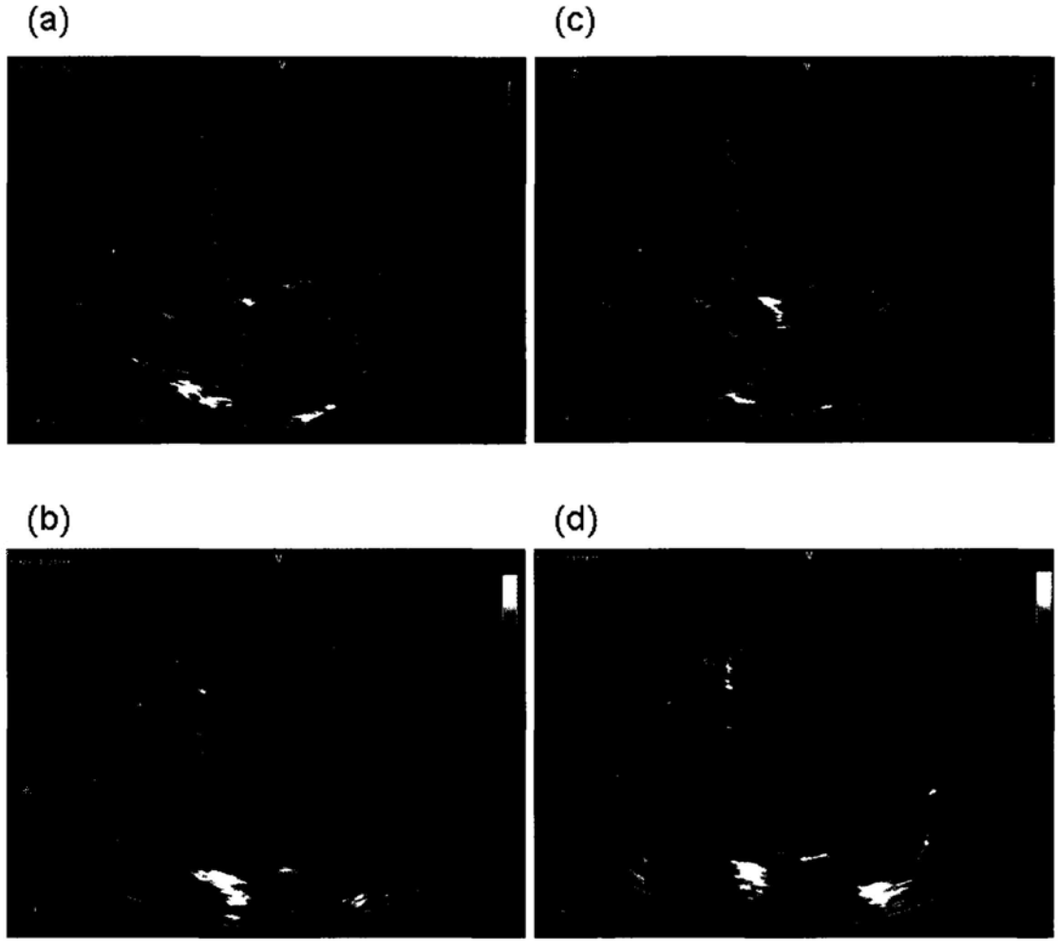

Figure 6.5 A patient from Group 3 before (a&b) and after (c&d) cardiac resynchronization therapy. The mitral regurgitation at baseline and 3 months are trivial (a&c) with 37.8% reduction in left ventricular end-systolic volume (b&d).

6.4 Discussion

The present study demonstrated that the improvement of MR was related to LV reverse remodeling (i.e. LV end-systolic volume reduction≥15%) after CRT. The extent of LV reverse remodeling was greatest in patients with MR improvement (-29.1±13.6%), followed by those with "no or mild" MR at baseline (-18.6±16.6%), and was least in those without MR improvement (-7.0±9.6%).

Although improvement of functional MR after CRT has been described in previous studies (90, 120-122, 166), its impact on LV reverse remodeling has not been explored. The present study illustrated that improvement of functional MR, but not the degree of pre-pacing functional MR, was an important determinant of LV reverse remodeling. The extent of LV reverse remodeling (measured by reduction of LVESV) showed no difference between patients with more than mild pre-pacing MR and those with "no or mild" pre-pacing MR. At the same time, the comparison between responders and nonresponders showed no difference in pre-pacing MR. However, the extent of LV reverse remodeling (measured by reduction of LVESV) was more than 4-fold different in patients with and without significant improvement of MR (-29.1 vs. -7.0%). Consequently, the prevalence of volumetric responders was more than 3-fold different between the two groups (86.4% vs. 26.9%). Interestingly, patients without significant pre-pacing MR showed intermediate response for the extent of reduction in LVESV and prevalence of volumetric responders. Therefore, it appears that the status of functional MR plays a pivotal role in determining CRT response.

In heart failure patients, functional MR could have been caused by a few major factors, namely failure of mitral leaflet coaptation due to mid cavity dilatation,

regional displacement of papillary apparatus resulting in incomplete coaptation and LV dysfunction resulting in poor coaptation force (83, 85-87, 94). In the presence of wide QRS complexes, MR could have been worsened by the dyssynchrony of LV or papillary muscle attaching sites that dissipates contractile force and distorts mitral apparatus geometry by uncoordinated regional contraction (84, 120, 121, 125). Of note, the presence of functional MR *per se* could have worsened LV volumetric overload and exacerbate left atrial pressure and volume overload, which will set up a vicious cycle that accelerates LV remodeling and deterioration of systolic function. Therefore, when patients responded to CRT and developed a more synchronous timing of LV contraction, the LV would show initial response by improving the forward systolic force and increasing ejection fraction. In the subset who also have co-existing functional MR, the beneficial effect will be augmented through additional reduction of MR by increased mitral valve coaptation force and improved synchronicity of the papillary muscles and the nearby LV wall (90, 120, 122). When initial LV reverse remodeling is achieved, the favorable improvement of LV geometry with decrease in LV mid-cavity dilatation will further alleviate the amount of restrictive mitral leaflet movement during systole. As a result, a positive feedback mechanism will be established which contributes to further LV reverse remodeling and reduction of functional MR.

CHAPTER 7 IMPROVEMENT OF EARLY- AND LATE-SYSTOLIC FUNCTIONAL MITRAL REGURGITATION AND IMPROVEMENT OF MITRAL DEFORMATION AFTER CARDIAC RESYNCHRONIZATION THERAPY

7.1 Backgrounds

Treatment of functional mitral regurgitation (MR) is of clinical importance, since the presence of functional MR in heart failure patients is associated with reduced survival (33, 34, 40, 51). Several studies have suggested that cardiac resynchronization therapy (CRT) results in improvement of functional MR in refractory heart failure that may be related to the increase in mitral valve coaptation force(90), reduction of papillary muscle dyssynchrony (120-122) and LV reverse remodeling (151, 164). However, the pattern of functional MR is more complex and not homogenous that systolic MR has been observed to occur in two distinctive periods, namely early-systolic MR which starts from the isovolumic period and late-systolic MR (61-64). In order to understand the effect of CRT on functional MR and its mechanisms, it would be interesting to investigate the changes in the biphasic pattern in addition to the total MR after CRT. Therefore, the objectives of the present study were to examine whether CRT would improve early- or late-systolic MR, or both; and to explore the determinants of MR improvement at different phases.

7.2 Methods

7.2.1 Patients

This study consisted of 48 patients who had at least mild functional MR at baseline and received CRT. Patients with clinical or echocardiographic evidence of other

cardiac disease or greater than mild aortic regurgitation were excluded. Before the device implantation, the patients were all in symptomatic heart failure [i.e. New York Heart Association (NYHA) functional class III: 100%] despite optimal medical therapy, who had evidence of LV systolic dysfunction (ejection fraction ≤35%) and wide QRS complex (≥120ms) on surface ECG. All patients were in sinus rhythm before device implantation. The atrioventricular interval was optimized using Ritter's method on day one after the implantation (178). Clinical and echocardiographic assessments were performed before and three months after CRT. The study protocol was approved by the Ethics Committee of the institution and written informed consents were obtained from all the patients.

7.2.2 Echocardiography

Echocardiographic evaluation (Vivid 7 and EchoPac PC 7.0.0, Vingmed-General Electric, Horton, Norway) included quantification of MR, LV systolic function and LV global remodeling, assessment of mitral valvular deformation, and examination of LV global and regional dyssynchrony.

For the assessment of MR severity, both the overall severity of MR and its early- and late-systolic components were evaluated. The total MR volume was calculated by the continuity equation as previously described (179). Early- and late-systolic MR were estimated by the instantaneous MR flow rate at early and late-systole which was calculated by using the proximal isovelocity surface area (PISA) method (179). The dynamic change in the severity of MR was calculated by frame-by-frame analysis throughout the period from mitral valve closure to mitral valve opening. Then images at the timing of the maximum proximal flow convergence area at early- and

late-systole were separately selected for assessing the instantaneous MR flow rate (64). At three months after CRT, a reduction of ≥10% in MR volume was considered a significant improvement in MR. Similarly, a 10% reduction or greater in early- and late-systolic MR flow rate was regarded as an improvement in early- and late-systolic MR, respectively.

For the assessment of LV global remodeling and systolic function, LV end-diastolic volume (LVEDV), end-systolic volume (LVESV) and ejection fraction were calculated using biplane Simpson's method (181). LV cavity length and width were measured at end-systole and end-diastole. LV sphericity index was calculated to assess LV geometry (173). The maximal rate of LV pressure rise (+dp/dt) was estimated on the MR continuous-wave Doppler spectrum (180).

For mitral valvular deformation, systolic mitral valve tenting area and tenting height were measured (83).

LV mechanical dyssynchrony was assessed by two-dimensional color tissue Dopper imaging (TDI) in three apical views (i.e. apical 4-chamber, 2-chamber, and long-axis views). The maximal difference of time to peak systolic velocity (Ts) among the 12 LV segments (Ts-dif) was calculated as the parameter for global systolic dyssynchrony (151, 182-185), while the absolute difference in Ts between the mid lateral and mid inferior segments was taken to reflect regional dyssynchrony between the anterolateral and posteromedial papillary muscle at their attaching sites (APM-PPM delay).

7.2.3 Clinical Assessment

Clinical assessments included New York Heart Association (NYHA) functional class and Minnesota Living with Heart Failure (MLWHF) quality of life score.

7.2.4 Statistical analysis

Continuous variables are expressed as mean±SD. Categorical data are summarized as frequencies and percentages. Paired t-test or Wilcoxon signed ranks test was used when appropriate in comparison between baseline and after CRT. Unpaired t-test or chi-square test was used when appropriate in comparisons between patients with and without significant improvement in total MR after CRT. Determinants of improvement in total, early-systolic and late-systolic MR were identified by univariate logistic regression followed by backward stepwise multivariate logistic regression. A p value <0.05 was considered statistically significant.

7.3 Results

7.3.1 Improvement in Total Functional MR and Its Early- and Late-systolic Components after CRT

The demographic and clinical characteristics of the patients are shown in Table 7.1. At three months after CRT, significant reductions in the total MR volume (38±20 vs. 33±21ml, $p<0.01$), as well as the early- (71±52 vs. 60±51ml/s, $p<0.01$) and late-systolic (49±46 vs. 42±46ml/s, $p<0.05$) components of MR were observed (Table 7.2). The mean reduction in total MR volume was -5±11ml (-14.3±32.7%), while that in early- and late-systolic MR were -11±22ml/s (-17.5±29.4%) and -7±21ml/s (-16.7±40%) respectively. Interestingly, both the baseline (71±52 vs. 49±46ml/s, $p<0.001$) and improvement (-11±22 vs. -7±21ml/s, $p<0.01$) in functional

MR is greater in early- than late-systolic MR. By using the cutoff value of ≥10% reduction, a significant improvement in total MR was found in 24 (50%) patients. Similarly, a significant improvement in early- and late-systolic MR was identified in 24 (50%) and 20 (42%) patients, respectively. As a result, improvement of both early- and late-systolic MR was observed in 14 (29%) patients, improvement of only early-systolic MR in 10 (21%), improvement of only late-systolic MR in 6 (12%) while lack of improvement in either phase in 18 (38%) patients.

As shown in Table 7.2, LV reverse remodeling was evident at three months with the reduction of LV volumes and gain in ejection fraction (all $p<0.001$). Improvement of LV geometry was achieved by a greater extent of decrease in the LV width than the length which resulted in higher values of sphericity index, i.e. a less globular shape (all $p<0.05$). Improvement of mitral valvular deformation was observed, as reflected by reduction in tenting area and tenting height (both $p<0.01$). In addition, LV global dyssynchrony was decreased after CRT, whereas no change of LV regional dyssynchrony was observed (Table 7.2).

Table 7.1 Baseline demographic and clinical characteristics of the study population

Parameters	**Patients (n=48)**
Age, years	67±13
Gender, % male	32 (66.7%)
Etiology of heart failure, % ischemic	22 (45.8%)
NYHA class, % patients	
III	48 (100%)
IV	0 (0%)
MLWHF Quality of life score	27±19
Medications:	
Diuretic	77%
ACE inhibitor or angiotensin receptor blocker	89%
β-Blocker	77%
Spironolactone	34%
Nitrate	32%
Digoxin	19%

ACE, angiotensin-converting enzyme; MLWHF, Minnesota Living with Heart Failure; NYHA, New York Heart Association.

Table 7.2 Changes in mitral regurgitation and other echocardiographic parameters at three months after cardiac resynchronization therapy

	Baseline	**3-Month**	**P value**
MR volume, ml	38±20	33±21	0.002
Early-systolic MR flow rate, ml/s	71±52	60±51	0.001
Late-systolic MR flow rate, ml/s	49±46	42±46	0.032
LV end-diastolic volume, ml	181±59	169±66	<0.001
LV end-systolic volume, ml	135±51	114±55	<0.001
LV ejection fraction, %	27±6	34±8	<0.001
LV +dp/dt, mmHg/s	729±265	837±312	0.011
End-systolic LV cavity length, cm	8.1±1.0	8.0±1.0	0.140
End-systolic LV cavity width, cm	5.1±0.7	4.6±0.8	<0.001
End-systolic LV sphericity index	1.63±0.22	1.74±0.25	0.002
End-diastolic LV cavity length, cm	8.8±0.9	8.6±1.0	0.016
End-diastolic LV cavity width, cm	5.8±0.8	5.4±0.8	0.001
End-diastolic LV sphericity index	1.54±0.18	1.60±0.19	0.017
Tenting area, cm^2	2.2±0.7	2.0±0.7	<0.001
Tenting height, cm	1.1±0.3	1.0±0.3	0.001
Ts-dif, ms	108±36	93±40	0.023
APM-PPM delay, ms	65±35	66±36	0.880

APM-PPM delay, the absolute difference in time to peak systolic velocity between the mid lateral and mid inferior left ventricular segments; LV, left ventricle; MR, mitral regurgitation; Ts-Dif, the maximal difference in time to peak systolic velocity among the 12 LV segments.

7.3.2 Comparisons between Patients with and without Significant Improvement in MR after CRT

According to the percentage reduction in total MR volume after CRT, the 48 patients were divided into two groups, i.e. patients with improvement in total MR defined by a reduction of ≥10% (Group 1, n=24) and those without (Group 2, n=24). Table 7.3 shows the comparisons between the two groups before and after the CRT. Despite no differences in baseline total MR volume, early- and late-systolic MR flow rate, Group 1 showed a reduction of all the three MR parameters by 33% ($p<0.001$), 37% ($p<0.001$) and 40% ($p=0.004$) respectively. However, Group 2 showed a significant increase in total MR volume by 5% ($p=0.045$) and late-systolic MR flow rate by 7% ($p=0.014$) with no change in early-systolic MR flow rate (p=NS) (Table 7.3) (Figure 7.1). In Group 1, improvement of both early- and late-systolic MR was observed in 14 (58%), improvement of only early-systolic MR in 7 (29%) and improvement of only late-systolic MR in 3 (13%) patients, while none of the patients showed absence of improvement in both components. On the contrary, these figures were 0, 3 (12.5%), 3 (12.5%) and 18 (75%) patients respectively in the Group 2 (Group 1 vs. Group 2, $\chi^2=33.60$, $p<0.001$).

The baseline echocardiographic parameters of LV volume, geometry, contractility and mitral valvular deformation were comparable between the two groups (Table 7.3). At 3-month follow up, the Group 1 showed evidence of LV reverse remodeling with significant decrease in both LVESV and LVEDV (both $p<0.001$) and a dramatic increase in ejection fraction by 11% (absolute value) ($p<0.001$). In contrast, there was no reduction in LVEDV and only a mild reduction in LVESV ($p=0.014$), while ejection fraction increased slightly by 3% in the Group 2. Most of the other

echocardiographic parameters assessed were only improved in the Group 1, which included the favorable decrease in LV cavity length (both $p<0.01$), increase in sphericity index (both $p<0.01$), increase in +dp/dt ($p=0.004$), as well as decrease in tenting area ($p<0.001$) and tenting height ($p=0.004$) (Table 7.3). For dyssynchrony assessment, parameters for global systolic dyssynchrony of Ts-dif ($p<0.05$) and regional dyssynchrony of APM-PPM delay ($p<0.05$) at baseline were significantly greater in the Group 1 than Group 2. Interestingly, both Ts-dif ($p<0.001$) and APM-PPM delay ($p=0.016$) were shortened significantly after CRT in the Group 1 indicating an improvement of systolic dyssynchrony. On the other hand, the APM-PPM delay was further prolonged after CRT ($p=0.015$) in the Group 2, while Ts-dif showed no significant change after CRT.

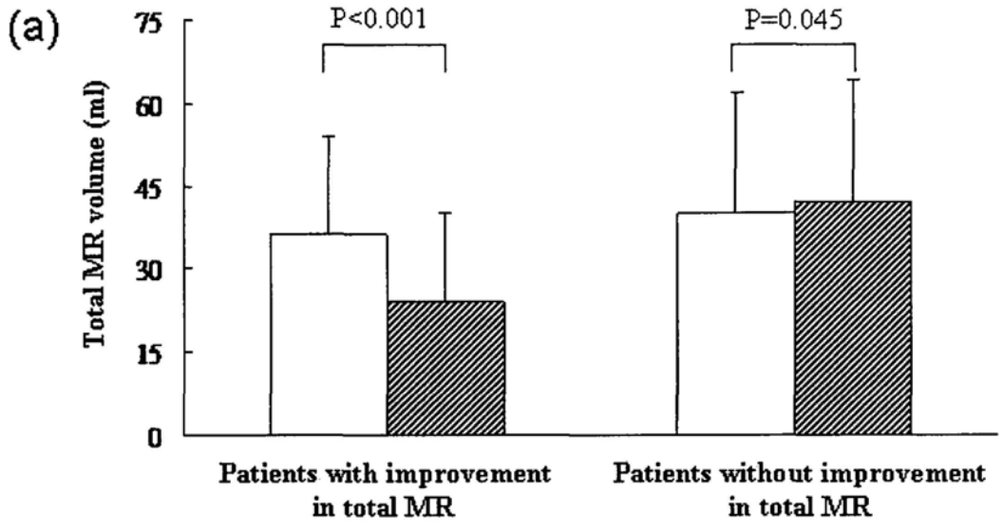
(a)
Total MR volume (ml)
75
60
45
30
15
0
P<0.001
P=0.045
Patients with improvement in total MR
Patients without improvement in total MR

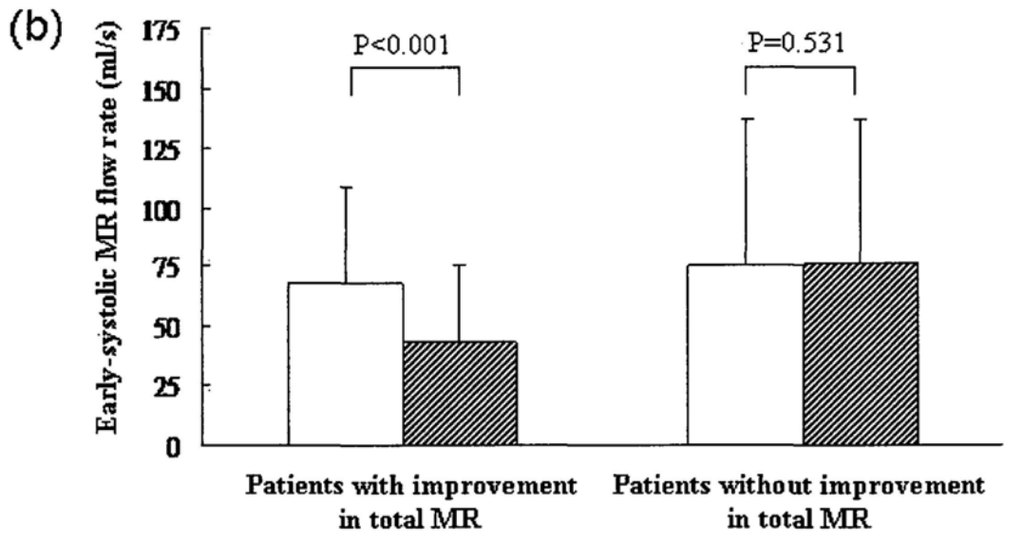
(b)
Early-systolic MR flow rate (ml/s)
175
150
125
100
75
50
25
0
P<0.001
P=0.531
Patients with improvement in total MR
Patients without improvement in total MR

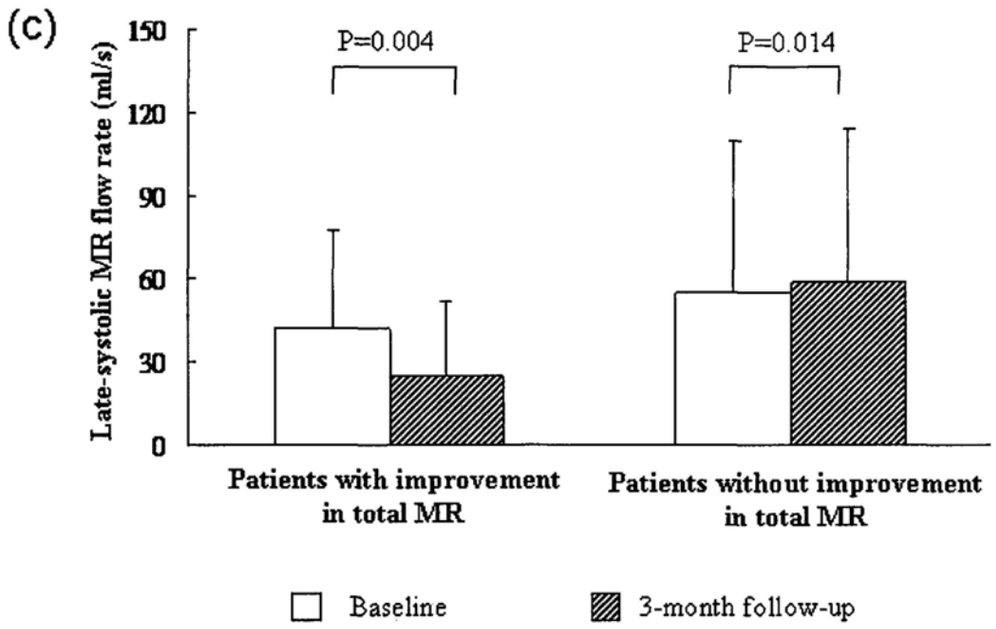

Figure 7.1 Changes in different components of mitral regurgitation (MR) after cardiac resynchronization therapy.

Comparison of severity of total MR volume (a); early-systolic MR flow rate (b) and late-systolic MR flow rate (c) at baseline and three months after cardiac resynchronization therapy. Patients were segregated into those with improvement of total MR with and those without.

Table 7.3 Comparison of MR and other echocardiographic parameters in patients with and without total MR improvement

Parameters	**Patients with improvement in total MR (n=24)**			**Patients without improvement in total MR (n=24)**		
	Baseline	***3-Month***	***P***	***Baseline***	***3-Month***	***P***
MR volume, ml	36±18	24±16	<0.001	40±22	42±22	0.045
Early-systolic MR flow rate, ml/s	68±40	43±32	<0.001	75±62	76±61	0.531
Late-systolic MR flow rate, ml/s	42±35	25±27	0.004	55±55	59±55	0.014
LV end-diastolic volume, ml	166±42	142±47	<0.001	197±69	195±72	0.740
LV end-systolic volume, ml	124±41	89±41	<0.001	146±58	138±56	0.014
LV ejection fraction, %	27±6	39±8	<0.001	27±6	30±7	0.010
LV +dp/dt, mmHg/s	715±274	931±361	0.004	742±261	752±236	0.815
End-systolic LV cavity length, cm	8.1±0.7	7.7±0.9	0.008	8.2±1.2	8.2±1.0	0.965
End-systolic LV cavity width, cm	4.9±0.6	4.3±0.7	<0.001	5.2±0.8	5.0±0.8	0.042
End-systolic LV sphericity index	1.65±0.23	1.81±0.27	0.006	1.59±0.20	1.67±0.20	0.119
End-diastolic LV cavity length, cm	8.7±0.7	8.4±0.8	0.021	8.9±1.0	8.8±1.1	0.320

End-diastolic LV cavity width, cm	5.6±0.6	5.1±0.7	<0.001	6.0±0.9	5.7±0.90	0.173
End-diastolic LV sphericity index	1.57±0.19	1.65±0.20	0.001	1.51±0.17	1.56±0.18	0.359
Tenting area, cm^2	2.2±0.5	1.8±0.5	<0.001	2.2±0.9	2.2±0.8	1.000
Tenting height, cm	1.0±0.2	0.9±0.2	0.004	1.1±0.3	1.1±0.3	0.075
APM-PPM delay, ms	76±27	54±33	0.016	53±39*	78±36	0.015
Ts-dif, ms	119±31	78±32	<0.001	98±39*	108±43	0.166

*$p<0.05$ compared with patients with improvement in total MR.

Abbreviations as in Table 7.2.

7.3.3 Determinants of Improvement in Total, Early and Late-systolic MR after CRT

Determinants of improvement in total MR (i.e. ≥10% reduction) at 3-month after CRT were examined in which changes in LV volume, geometry, +dp/dt, mitral valvular deformation as well as global and regional measures of LV systolic dyssynchrony were examined (Table 7.4). In the univariate model, the changes in LVESV, LV cavity width, ejection fraction, tenting area, tenting height, Ts-dif and APM-PPM delay correlated with the improvement in total MR. However, in multivariate analysis, only the reductions of LVESV (β=0.596, p=0.044) and tenting area (β=0.721, p=0.047) were confirmed to be independent determinants of improvement in total MR (Table 7.4).

Table 7.4 Univariate and multivariate regression analysis for determinants of improvement in total MR

Parameters	**Univariate model**			**Multivariate model**		
	ß	***95% CI***	***P value***	***ß***	***95% CI***	***P value***
ΔLV end-systolic volume, %	0.810	0.720, 0.911	<0.001	0.596	0.360, 0.986	0.044
ΔEnd-systolic sphericity index, %	1.017	0.980, 1.056	0.372	-	-	-
ΔLV +dp/dt, mmHg/s	1.004	1.001, 1.007	0.018			NS
ΔEnd-systolic LV cavity length, %	0.952	0.885, 1.024	0.184	-	-	-
ΔEnd-systolic LV cavity width, %	0.941	0.889, 0.995	0.033			NS
ΔTenting Area, %	0.872	0.805, 0.946	0.001	0.721	0.522, 0.995	0.047
ΔTenting height, %	0.959	0.919, 1.001	0.057	-	-	-
ΔTs-dif, ms	0.964	0.943, 0.986	0.001			NS
ΔAPM-PPM delay, ms	0.973	0.956, 0.992	0.004			NS
ΔLV ejection fraction, %	1.374	1.139, 1.658	0.001			NS

Δ, changes between 3-month and baseline. Other abbreviations as in Table 7.2.

Further analysis were performed to determine independent predictors of improvement in early- and late-systolic MR. The results of multivariate regression model analysis are shown in Tables 7.5 and 7.6. It was observed that independent determinants of improvement in early-systolic MR included reductions of LVESV (β=0.723, p=0.014) as well as Ts-dif (β=0.926, p=0.039). In contrast, independent determinants of improvement in late-systolic MR were reductions of mitral valve tenting area (β=0.889, p=0.004) and Ts-dif (β=0.977, p=0.024). Figure 7.2 showed an example of patient with reductions in both early- and late-systolic MR, as well as LV reverse remodeling and improvement in LV global dyssynchrony.

Table 7.5 Univariate and multivariate regression analysis for determinants of improvement in early-systolic MR

Parameters	**Univariate model**			**Multivariate model**		
	ß	***95% CI***	***P value***	***ß***	***95% CI***	***P value***
ΔLV end-systolic volume, %	0.813	0.725, 0.913	<0.001	0.723	0.558, 0.936	0.014
ΔEnd-systolic sphericity index, %	1.022	0.983, 1.062	0.280	-	-	-
ΔLV +dp/dt, mmHg/s	1.004	1.001, 1.007	0.012			NS
ΔEnd-systolic LV cavity length, %	0.933	0.860, 1.012	0.095	-	-	-
ΔEnd-systolic LV cavity width, %	0.923	0.867, 0.983	0.012			NS
ΔTenting Area, %	0.926	0.878, 0.977	0.005			NS
ΔTenting height, %	0.951	0.909, 0.996	0.032			NS
ΔTs-dif, ms	0.966	0.946, 0.986	0.001	0.926	0.860, 0.996	0.039
ΔAPM-PPM delay, ms	0.985	0.972, 0.999	0.036			NS
ΔLV ejection fraction, %	1.336	1.123, 1.589	0.001			NS

Abbreviations as in Table 7.2 and 7.4.

Table 7.6 Univariate and multivariate regression analysis for determinants of improvement in late-systolic MR

Parameters	**Univariate model**			**Multivariate model**		
	ß	***95% CI***	***P value***	***ß***	***95% CI***	***P value***
ΔLV end-systolic volume,%	0.940	0.899, 0.983	0.006			NS
ΔEnd-systolic sphericity index, %	1.011	0.976, 1.048	0.527	-	-	-
ΔLV +dp/dt, mmHg/s	1.002	0.999, 1.004	0.134	-	-	-
ΔEnd-systolic LV cavity length, %	0.944	0.872, 1.021	0.149	-	-	-
ΔEnd-systolic LV cavity width, %	0.953	0.903, 1.005	0.075	-	-	-
ΔTenting Area, %	0.892	0.833, 0.955	0.001	0.889	0.821, 0.962	0.004
ΔTenting height, %	0.972	0.933, 1.012	0.164	-	-	-
ΔTs-dif, ms	0.976	0.960, 0.993	0.006	0.977	0.958, 0.997	0.024
ΔAPM-PPM delay, ms	0.978	0.961, 0.995	0.010			NS
ΔLV ejection fraction, %	1.115	1.010, 1.231	0.031			NS

Abbreviations as in Table 7.2 and 7.4.

(a) (d)

(b) (e)

(c) (f)

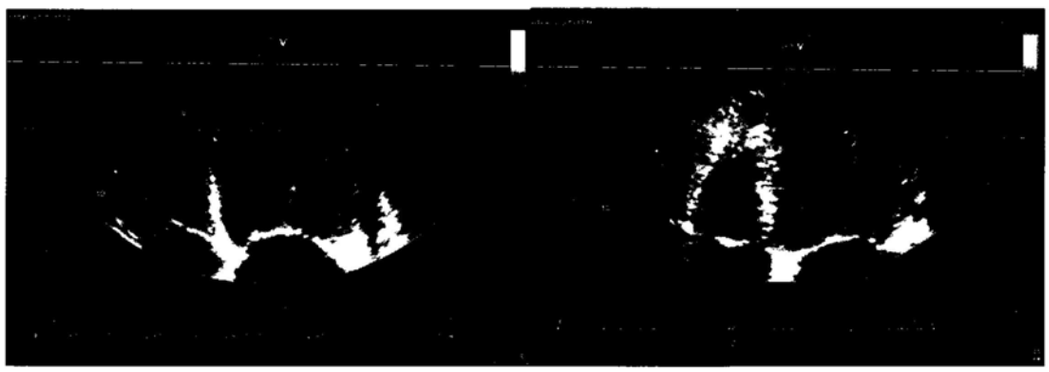

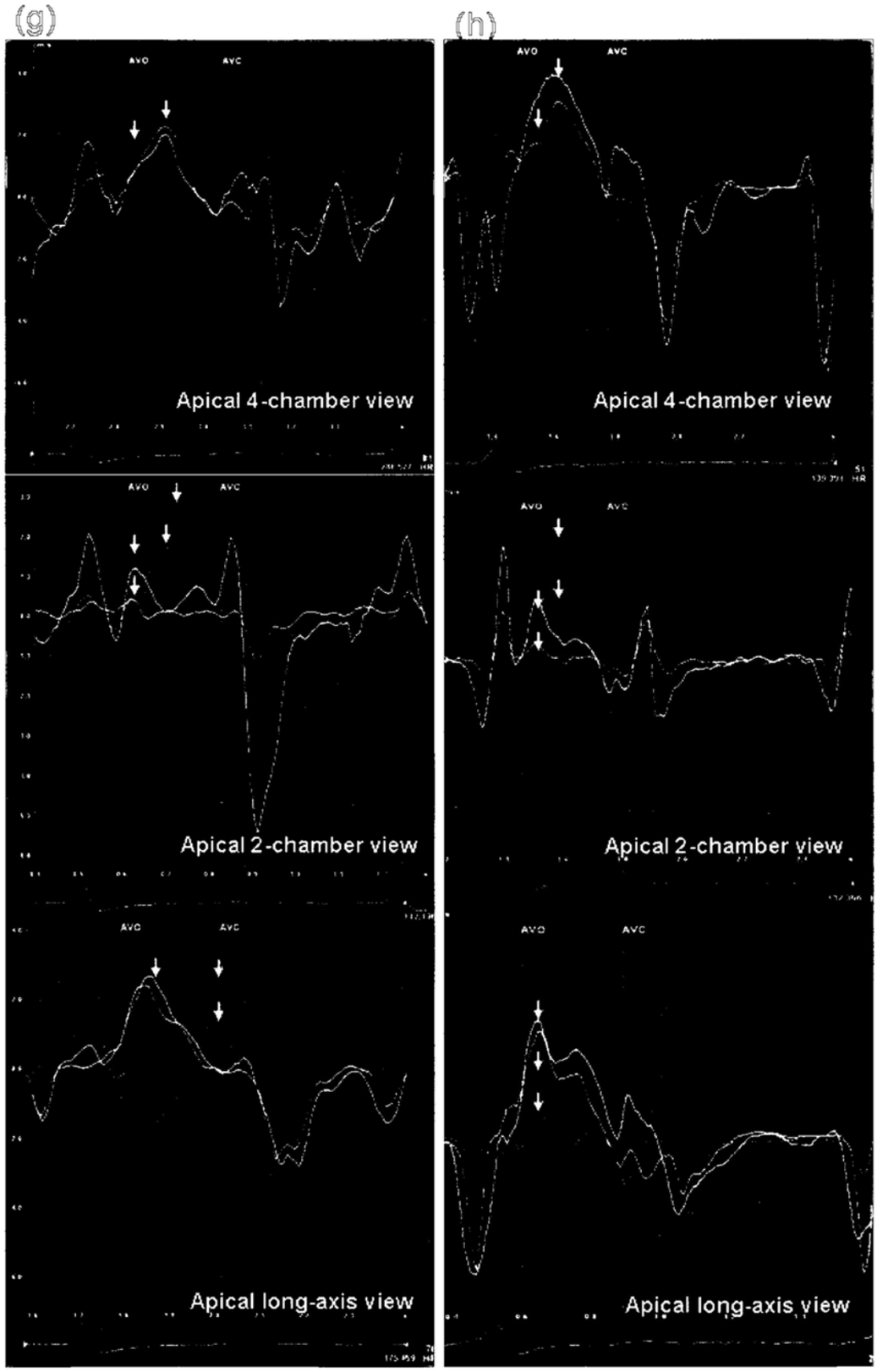

Figure 7.2 An example of patient with reduction in both the early- and late-systolic mitral regurgitation (MR). This patient also demonstrated significant left ventricular

(LV) systolic dyssynchrony at baseline which was improved after cardiac resynchronization therapy (CRT) as well as LV reverse remodeling at 3-month. **a**, early-systolic MR before CRT; **b**, late-systolic MR before CRT; **c**, LV end-systolic volume was 189ml before CRT; **d**, early-systolic MR after CRT; **e**, late-systolic MR after CRT; **f**, LV end-systolic volume was 153ml after CRT; **g**, Color-coded tissue Doppler imaging with myocardial velocity curves generated from the 12 LV segments before CRT (the dyssynchrony parameter, Ts-dif, was 162ms); **h**, Myocardial velocity curves of the 12 LV segments after CRT (Ts-dif was 76ms). Arrows are indicating peak systolic velocity.

7.4 Discussion

This study documented the effectiveness of CRT in reducing functional MR in patients with advanced heart failure with specific emphasis on different phases of MR. CRT decreased total MR by reducing both the early- and late-systolic functional MR. And the reduction in early-systolic MR was significantly greater than the reduction in late-systolic MR. The determinants of improvement of functional MR in different systolic phase appeared to be different. While improvement of early-systolic MR was determined by the degree of LV reverse remodeling as well as global dyssynchrony, improvement of late-systolic MR was determined by reduction of mitral valve tenting area and global dyssynchrony.

7.4.1 Effect of CRT on Early- and Late-systolic Components of Functional MR

Many studies have described the improvement of functional MR after CRT (90, 120-122, 151, 164, 166), but few of them take functional MR as a dynamic lesion which varies in severity over the whole regurgitant period, though this is important for understanding the mechanism of reducing MR by CRT. Former study with a smaller population (n=19) reported that CRT only reduce early-systolic MR (64). However, our study with a larger population of patients with functional MR received CRT (n=48) observed a reduction of both early- and late-systolic MR, which is in contrast to the earlier study. Moreover, compared with patients who only had improvement in either early- or late-systolic MR, patients with both improvements in early- and late- systolic MR appears to be more likely to have improvement in the overall severity of MR.

7.4.2 Determinants of Improvement in Early- versus Late-systolic Functional MR

Different factors might operate at different period of systolic phase that determine the severity of functional MR. In previous studies, it has been observed that in patients with globally dilated LV and severely impaired LV systolic function, the early-systolic peak was greater than the late-systolic one (64). On the other hand, in patients with localized inferior myocardial infarction where there was no obvious LV global remodeling but presence of local LV remodeling, the late-systolic peak was greater than the early-systolic one (65). These early observations suggested that the early-systolic MR is closely related to the amount of global LV remodeling, while the late-systolic MR is more likely to be contributed by mitral apparatus deformation as a result of local LV remodeling.

Understandably, during early-systole, the dilated LV causes papillary muscle displacement, which exerts significant tethering forces on the mitral leaflets, resulting in restricted leaflet motion and incomplete leaflets closure. During late-systole, when the LV segments with earlier activation already contracted, the delayed LV segments were left behind the contracting ventricle, resulting in more severe local remodeling and valvular deformation.

Previous studies have suggested that factors might have explained the reduction of functional MR by CRT. These include LV reverse remodeling (151, 164), improvement of papillary muscle dyssynchrony (120-122), increase in ventricular closing force (90) and augmented long-axis myocardial function (168, 198). Of note, these studies did not attempt to measure and segregate early- from late-systolic MR, while the determinants of functional MR were not established statistically, but rather only descriptive observations of improvement in MR and other parameters of cardiac

function. The current study with a much larger sample size revealed that although the severity of global dyssynchrony determined the amount of both early- and late-systolic MR, other determinants were different in different phases of MR.

During early-systole, the presence of LV dilatation will cause outward displacement of papillary muscles which exerts significant tethering force on the mitral leaflets and results in incomplete leaflets closure. Therefore, significant LV reverse remodeling will reduce the amount of LV mid-cavity dilatation and diminish mitral leaflet tethering, leading to the decreased early-systolic MR.

In contrast, during late-systole when the contractile LV segments have completed most of the systolic motion, the hypokinetic or akinetic LV segments are lagged behind resulting in localized remodeling. This will result in increased mitral valve deformation and consequently development of late-systolic functional MR. CRT may decrease mitral valve deformation by increasing LV closing force (90) and decreasing inter-papillary muscle dyssynchrony (120-122), giving rise to the reduction in late-systolic MR.

Interestingly, improvement of LV systolic dyssynchrony has shown to exert a positive impact in both early- and late-systolic MR in the present study. A previous study has shown that CRT achieves resynchronization by homogenously delaying systolic contraction to a later timing (151). It is likely that reduction of LV systolic dyssynchrony with improvement of both global and regional coordination of contraction which in turn will decrease the distortion of mitral apparatus geometry and facilitate simultaneous closure of mitral leaflets. Furthermore, with improvement

of systolic synchronicity, the concerted systolic force development will be enhanced as segments are recruited to contract in a similar timing. This will be reflected by an increased mitral valve coaptation force and shortened regurgitant period (90).

In conclusion, CRT reduced both early- and late-systolic functional MR in patients with evidence of pre-pacing MR. The improvement of early-systolic MR was determined by the extent of LV reverse remodeling while those of late-systolic MR was determined by the decrease in mitral valve tenting area. Furthermore, LV systolic dyssynchrony is another independent determinant of improvement of both early- and late-systolic MR.

SECTION IV

SUMMARY

CHAPTER 8 SUMMARY

8.1 Pathogenesis of Functional Mitral Regurgitation (MR) in Systolic Heart Failure

Functional MR broadly denotes abnormal function of normal leaflets in the context of impaired left ventricular (LV) systolic function. It is frequently observed in patients with congestive heart failure and severely affects cardiovascular mortality and morbidity (33, 34).

The primary mechanism of functional MR is believed to be the imbalance between the tethering force and the closing force which is initiated by global and regional LV remodeling in systolic heart failure (87). The presence of remodeling causes alterations in the normal geometric relationship between the ventricle and mitral valve apparatus by displacing the papillary muscles apically and/or outward, which results in tethering of the mitral leaflets and apical displacement of the coaptation zone (91-94). On the other hand, the impaired contraction of myocardium occurring in systolic heart failure with LV remodeling further disturbs the balance by decreasing the ventricular closing force (62, 87). Furthermore, multiple factors are suggested to be involved in the pathogenesis of this force imbalance, including LV remodeling and dysfunction (62, 85, 86, 91, 92, 94), leaflet tenting (83, 101), annular dilation and dysfunction (11, 102-106), as well as mechanical dyssynchrony (84, 125). Consequently, these changes lead to the deformation of the mitral valve apparatus and reduction in the coaptation area of the leaflets.

8.2 LV Systolic Dyssynchrony as a Determinant of the Severity of Functional MR

LV systolic mechanical dyssynchrony describes the uncoordinated contraction among different regions of the heart due to the difference in timing to reach the maximal movement or deformation during systole. It is commonly observed in patients with congestive heart failure, irrespective of the QRS duration on surface ECG. The prevalence is about 70% in wide QRS and more than one third in narrow QRS complexes (143-145). The presence of significant systolic dyssynchrony not only reduces the efficiency of LV systolic contraction, but also associates with a higher risk of cardiac events (186).

LV intraventricular dyssynchrony induces discoordinated contraction between different LV segments that the regional wall contractions are not effectively converted to pressure build-up in the LV but rather cause substantial blood volume shifts within the LV cavity. This will give rise to a decrease in LV contraction efficiency and the rate of pressure rise during systole (+dp/dt) that reduces the closing forces acting on the mitral leaflets (90). Secondly, dyssynchrony between the LV segments supporting the papillary muscles will produce uncoordinated regional LV mechanical activation in these segments, resulting in geometric changes in mitral leaflet attachments and implying tethering of the mitral leaflets (120). Thirdly, asynchronous contraction of the LV basal segments may render a non-simultaneous contraction of mitral annulus and adjacent LV walls, associated with the annular dilation and deformation where the leaflet tethering will be further compounded (128). In the current study, although mitral valvular tenting was the strongest determinant of MR severity, the existence of significant intraventricular mechanical

dyssynchrony was also found to be an independent factor that had an incremental predictive value over the mitral valve deformation. In the presence of significant valvular tenting, severe functional MR was observed in 77% of the patients with mechanical dyssynchrony and in 59% of those without. Therefore, it is indicated that functional and geometric changes induced by LV intraventricular dyssynchrony in systolic heart failure could affect the severity of functional MR.

It has been postulated that both LV global dyssynchrony which calculates all the LV segments and regional dyssynchrony which only reflects the inter-papillary muscle delay are involved in the pathogenesis of functional MR. However, previous studies only reported the association between MR and the inter-papillary muscle contraction delay (125) or the delay among the eight segments adjacent to papillary muscles which could have included the contribution of global and/or regional dyssynchrony (84). In the present study, both LV global dyssynchrony which measured the maximal difference in the time to peak systolic velocity (Ts) among the 12 LV segments (Ts-Dif) and regional dyssynchrony which measured the difference in Ts between the LV segments underlying papillary muscles (APM-PPM delay) were investigated and compared. As a result, global dyssynchrony had a larger correlation coefficient with the severity of functional MR than inter-papillary muscle dyssynchrony, though the latter was also found to be associated with MR in univariate analysis. Nevertheless, by using multivariate analysis, global but not regional dyssynchrony was the independent determinant of MR severity, in addition to the mitral valvular deformation. Therefore, it appears that functional MR is not only determined by the uncoordinated motion generated from the two papillary

muscles, but rather different LV segments with dyssynchronous motion in concert contribute to the development of functional MR.

8.3 LV Remodeling, Myocardial Deformation and Functional MR

The progression of heart failure is characterized by progressive LV remodeling, which is defined as the change in size, shape and function of the LV that occurs in response to pathological stimuli. LV remodeling after myocardial infarction or in early stage of dilated cardiomyopathy has been regarded as the initial event for the development of functional MR (85, 86, 91, 92, 94). In ischemic and nonischemic cardiomyopathy, LV remodeling causes functional MR through annular dilation, papillary muscle displacement, leaflet tethering, reduced myocardial contractility, as well as systolic dyssynchrony. Although the mitral leaflet tenting appeared predominant in previous studies (83, 84) and this study as well to determine the severity of functional MR, it should be regarded as the common pathway attributed by various factors including LV remodeling. It has been demonstrated in prior studies that the tethering force increases with the more spherical ventricle and therefore the presence of functional MR in heart failure is dependent on alterations in LV shape (91, 92, 94).

Functional MR is increasingly recognized as a ventricular disease rather than a valvular problem, where myocardial performance accompanied by LV remodeling will provoke more research interests and clinical implications. Our current study observed that despite comparable ejection fraction between the two groups, more severe functional MR was associated with further impairment in short-axis myocardial deformation and greater extent of LV remodeling, in particular in terms

of short-axis dimension. In addition, the extent of LV remodeling was related to the degree of myocardial systolic impairment. This differential change in myocardial deformation implies that higher degree of functional MR is associated with more severe ventricular disease which can not be identified by ejection fraction. On the other hand, functional MR as a complication of LV dilation and systolic dysfunction, can further aggravate LV remodeling by overloading the ventricle. Therefore, a vicious cycle is formed between LV remodeling and functional MR which leads to deterioration of heart failure and poor prognosis.

8.4 Favorable Effects on Functional MR Caused by Cardiac Resynchronization Therapy (CRT)

CRT has been proposed as an effective device therapy in patients with drug refractory heart failure presented with systolic dyssynchrony (146). It improves symptoms, exercise capacity and quality of life, induces LV reverse remodeling as well as decreases mortality and heart failure hospitalization (148-152, 154, 155). Reduction of functional MR acutely or in the long-term after CRT have also been demonstrated by a number of studies (90, 120-122, 152, 155, 166). In the present study, apart from the conventional measurement of total MR volume, the changes in different phases of MR after CRT were particularly analyzed. It was found that reduction of both early- and late-systolic MR occurred at three months after the therapy, in contrast to a previous study with much smaller population (n=19) which reported only the improvement in early-systolic MR.

Furthermore, the predictors of early- and late-systolic MR reduction after CRT were investigated. Consequently, the improvement of LV systolic dyssynchrony was an

independent determinant for both early- and late-systolic MR reduction. Diminished systolic dyssynchrony improves global and regional coordination of contraction that may decrease the distortion of mitral apparatus geometry and increase mitral valve coaptation force. This corroborates the findings in previous studies that reduction of functional MR after CRT was associated with decreased mechanical dyssynchrony (120-122), increased closing force (90), improved mitral valve deformation (121, 122), and LV reverse remodeling (152). However, these studies did not attempt to measure early- from late-systolic MR separately, nor predictor of MR improvement was identified. In addition to mechanical dyssynchrony, the improvement of early-systolic MR was also determined by the extent of LV reverse remodeling while the reduction of late-systolic MR by the improvement of mitral valve deformation. It could be explained by that LV reverse remodeling reduces the amount of LV mid-cavity dilatation and diminishes mitral leaflet tethering, whereas increased LV closing force and decreased inter-papillary muscle dyssynchrony causes the change in mitral leaflet tenting by correcting the localized remodeling of the hypokinetic or akinetic LV segments that "left behind" the contracting ventricle.

8.5 Contribution of MR Reduction to LV Reverse Remodeling after CRT

Despite the compelling beneficial effects of CRT on improving clinical status, cardiac function, reverse remodeling and prognosis, approximately 30% of patients treated with CRT do not respond to treatment when evaluated by composite clinical and/or echocardiographic endpoints (172). A number of factors could result in lack of response, such as ischemic etiology of heart failure, baseline mechanical dyssynchrony and LV end-diastolic diameter (173, 174). Some previous studies also related the severity of pre-pacing MR to responses after CRT (174-176).

Unfortunately, the extent of LV reverse remodeling after CRT was not reported in most of them. However, baseline MR severity appeared not to be a determinant of the change in LVESV in our current study.

On the other hand, the present study showed the association between changes in MR severity and volumetric responses to CRT, similar to the findings of previous studies (151, 173). In responders, MR was reduced significantly after CRT; however in non-responders, the extent of MR reduction was much less or remained unchanged. Moreover, we observed that the degree of LV reverse remodeling was the greatest in patients with significant MR reduction after CRT, moderate in those with no or only mild MR at baseline and the least in those without MR reduction. Understandably, the improvement of functional MR could be an important component underlying the favorable hemodynamic changes and gain in systolic function due to volume unloading effect in the LV and pressure offload in the left atrium after CRT (196, 197). In patients who have no or mild MR at baseline, LV reverse remodeling is achieved by a more synchronous timing of LV contraction, resulting in improved forward systolic force and increased ejection fraction. In patients who have significant pre-pacing functional MR, the beneficial effect will be augmented through the change of MR. The reverse remodeling process will be accelerated by an additional offload effect caused by MR reduction. However, in patients without improvement of MR, the process of LV reverse remodeling will be slowed or even reversed by the volume overload caused by the persistent MR after CRT.

REFERENCES

1. Perloff JK, Roberts WC. The mitral apparatus. Functional anatomy of mitral regurgitation. *Circulation* 1972;**46**(2):227-239.

2. Walmsley R. Anatomy of human mitral valve in adult cadaver and comparative anatomy of the valve. *Br Heart J* 1978;**40**(4):351-366.

3. Ormiston JA, Shah PM, Tei C, Wong M. Size and motion of the mitral valve annulus in man. I. A two-dimensional echocardiographic method and findings in normal subjects. *Circulation* 1981;**64**(1):113-120.

4. Tsakiris AG, von BG, Rastelli GC, Bourgeois MJ, Titus JL, Wood EH. Size and motion of the mitral valve annulus in anesthetized intact dogs. *J Appl Physiol* 1971;**30**(5):611-618.

5. Levine RA, Triulzi MO, Harrigan P, Weyman AE. The relationship of mitral annular shape to the diagnosis of mitral valve prolapse. *Circulation* 1987;**75**(4):756-767.

6. Levine RA, Handschumacher MD, Sanfilippo AJ, Hagege AA, Harrigan P, Marshall JE, Weyman AE. Three-dimensional echocardiographic reconstruction of the mitral valve, with implications for the diagnosis of mitral valve prolapse. *Circulation* 1989;**80**(3):589-598.

7. Silverman ME, Hurst JW. The mitral complex. Interaction of the anatomy, physiology, and pathology of the mitral annulus, mitral valve leaflets, chordae tendineae, and papillary muscles. *Am Heart J* 1968;**76**(3):399-418.

8. Ormiston JA, Shah PM, Tei C, Wong M. Size and motion of the mitral valve annulus in man. II. Abnormalities in mitral valve prolapse. *Circulation* 1982;**65**(4):713-719.

9. Toumanidis ST, Sideris DA, Papamichael CM, Moulopoulos SD. The role of mitral annulus motion in left ventricular function. *Acta Cardiol* 1992;**47**(4):331-348.

10. Rushmer RF., Finlayson BL., Nash AA. Movements of the mitral valve. *Circ Res* 1956;**4**(3):337-342.

11. Ahmad RM, Gillinov AM, McCarthy PM, Blackstone EH, pperson-Hansen C, Qin JX, Agler D, Shiota T, Cosgrove DM. Annular geometry and motion in human ischemic mitral regurgitation: novel assessment with three-dimensional echocardiography and computer reconstruction. *Ann Thorac Surg* 2004;**78**(6):2063-2068.

12. Davis PK, Kinmonth JB. The movements of the annulus of the mitral valve. *J Cardiovasc Surg (Torino)* 1963;**4**:427-431.

13. Chiechi MA, Lees WM, Thompson R. Functional anatomy of the normal mitral valve. *J Thorac Surg* 1956;**32**(3):378-398.

14. Ranganathan N, Lam JH, Wigle ED, Silver MD. Morphology of the human mitral valve. II. The value leaflets. *Circulation* 1970;**41**(3):459-467.

15. Lam JH, Ranganathan N, Wigle ED, Silver MD. Morphology of the human mitral valve. I. Chordae tendineae: a new classification. *Circulation* 1970;**41**(3):449-458.

16. Fenster MS, Feldman MD. Mitral regurgitation: an overview. *Curr Probl Cardiol* 1995;**20**(4):193-280.

17. Luther RR, Meyers SN. Acute mitral insufficiency secondary to ruptured chrodae tendineae. *Arch Intern Med* 1974;**134**(3):568.

18. Voci P, Bilotta F, Caretta Q, Mercanti C, Marino B. Papillary muscle perfusion pattern. A hypothesis for ischemic papillary muscle dysfunction. *Circulation* 1995;**91**(6):1714-1718.

19. Semafuko WE, Bowie WC. Papillary muscle dynamics: in situ function and responses of the papillary muscle. *Am J Physiol* 1975;**228**(6):1800-1807.

20. Marzilli M, Sabbah HN, Lee T, Stein PD. Role of the papillary muscle in opening and closure of the mitral valve. *Am J Physiol* 1980;**238**(3):H348-H354.

21. Rayhill SC, Daughters GT, Castro LJ, Niczyporuk MA, Moon MR, Ingels NB, Jr., Stadius ML, Derby GC, Bolger AF, Miller DC. Dynamics of normal and ischemic canine papillary muscles. *Circ Res* 1994;**74**(6):1179-1187.

22. Tsakiris AG, Sturm RE, Wood EH. Experimental studies on the mechanisms of closure of cardiac valves with use of roentgen videodensitometry. *Am J Cardiol* 1973;**32**(2):136-143.

23. Tsakiris AG, Gordon DA, Mathieu Y, Irving L. Motion of both mitral valve leaflets: a cineroentgenographic study in intact dogs. *J Appl Physiol* 1975;**39**(3):359-366.

24. Tsakiris AG, Rastelli GC, Amorim DS, Titus JL, Wood EH. Effect of experimental papillary muscle damage on mitral valve closure in intact anesthetized dogs. *Mayo Clin Proc* 1970;**45**(4):275-285.

25. Laniado S, Yellin EL, Miller H, Frater RW. Temporal relation of the first heart sound to closure of the mitral valve. *Circulation* 1973;**47**(5):1006-1014.

26. Tsakiris AG, Gordon DA, Padiyar R, Frechette D. Relation of mitral valve opening and closure to left atrial and ventricular pressures in the intact dog. *Am J Physiol* 1978;**234**(2):H146-H151.

27. Carpentier A. Cardiac valve surgery--the "French correction". *J Thorac Cardiovasc Surg* 1983;**86**(3):323-337.

28. Le HC, Thys DM. Ischemic mitral regurgitation. *Semin Cardiothorac Vasc Anesth* 2006;**10**(1):73-77.

29. Spinale FG, Ishihra K, Zile M, DeFryte G, Crawford FA, Carabello BA. Structural basis for changes in left ventricular function and geometry because of chronic mitral regurgitation and after correction of volume overload. *J Thorac Cardiovasc Surg* 1993;**106**(6):1147-1157.

30. Corin WJ, Monrad ES, Murakami T, Nonogi H, Hess OM, Krayenbuehl HP. The relationship of afterload to ejection performance in chronic mitral regurgitation. *Circulation* 1987;**76**(1):59-67.

31. Zile MR, Gaasch WH, Levine HJ. Left ventricular

stress-dimension-shortening relations before and after correction of chronic aortic and mitral regurgitation. *Am J Cardiol* 1985;**56**(1):99-105.

32. Mukherjee R, Brinsa TA, Dowdy KB, Scott AA, Baskin JM, Deschamps AM, Lowry AS, Escobar GP, Lucas DG, Yarbrough WM, Zile MR, Spinale FG. Myocardial infarct expansion and matrix metalloproteinase inhibition. *Circulation* 2003;**107**(4):618-625.

33. Trichon BH, Felker GM, Shaw LK, Cabell CH, O'Connor CM. Relation of frequency and severity of mitral regurgitation to survival among patients with left ventricular systolic dysfunction and heart failure. *Am J Cardiol* 2003;**91**(5):538-543.

34. Koelling TM, Aaronson KD, Cody RJ, Bach DS, Armstrong WF. Prognostic significance of mitral regurgitation and tricuspid regurgitation in patients with left ventricular systolic dysfunction. *Am Heart J* 2002;**144**(3):524-529.

35. Lamas GA, Mitchell GF, Flaker GC, Smith SC, Jr., Gersh BJ, Basta L, Moye L, Braunwald E, Pfeffer MA. Clinical significance of mitral regurgitation after acute myocardial infarction. Survival and Ventricular Enlargement Investigators. *Circulation* 1997;**96**(3):827-833.

36. Lehmann KG, Francis CK, Dodge HT. Mitral regurgitation in early myocardial infarction. Incidence, clinical detection, and prognostic implications. TIMI Study Group. *Ann Intern Med* 1992;**117**(1):10-17.

37. O'Connor CM, Hathaway WR, Bates ER, Leimberger JD, Sigmon KN, Kereiakes DJ, George BS, Samaha JK, Abbottsmith CW, Candela RJ, Topol EJ, Califf RM. Clinical characteristics and long-term outcome of patients in whom congestive heart failure develops after thrombolytic therapy for acute myocardial infarction: development of a predictive model. *Am Heart J* 1997;**133**(6):663-673.

38. Tcheng JE, Jackman JD, Jr., Nelson CL, Gardner LH, Smith LR, Rankin JS, Califf RM, Stack RS. Outcome of patients sustaining acute ischemic mitral regurgitation during myocardial infarction. *Ann Intern Med* 1992;**117**(1):18-24.

39. Pellizzon GG, Grines CL, Cox DA, Stuckey T, Tcheng JE, Garcia E,

Guagliumi G, Turco M, Lansky AJ, Griffin JJ, Cohen DJ, Aymong E, Mehran R, O'Neill WW, Stone GW. Importance of mitral regurgitation inpatients undergoing percutaneous coronary intervention for acute myocardial infarction: the Controlled Abciximab and Device Investigation to Lower Late Angioplasty Complications (CADILLAC) trial. *J Am Coll Cardiol* 2004;**43**(8):1368-1374.

40. Bursi F, Enriquez-Sarano M, Nkomo VT, Jacobsen SJ, Weston SA, Meverden RA, Roger VL. Heart failure and death after myocardial infarction in the community: the emerging role of mitral regurgitation. *Circulation* 2005;**111**(3):295-301.

41. Bhatnagar SK, al Yusuf AR. Significance of a mitral regurgitation systolic murmur complicating a first acute myocardial infarction in the coronary care unit--assessment by colour Doppler flow imaging. *Eur Heart J* 1991;**12**(12):1311-1315.

42. Barzilai B, Gessler C, Jr., Perez JE, Schaab C, Jaffe AS. Significance of Doppler-detected mitral regurgitation in acute myocardial infarction. *Am J Cardiol* 1988;**61**(4):220-223.

43. Vicente VT, Valdes CM, Garcia AA, Soria AF, Fernandez PJ, Perez LF, Roldan CD. [Mitral valve insufficiency in acute myocardial infarction. Assessment with pulsed and coded Doppler color]. *Arch Inst Cardiol Mex* 1991;**61**(2):117-121.

44. van Dantzig JM, Delemarre BJ, Koster RW, Bot H, Visser CA. Pathogenesis of mitral regurgitation in acute myocardial infarction: importance of changes in left ventricular shape and regional function. *Am Heart J* 1996;**131**(5):865-871.

45. Ma HH, Honma H, Munakata K, Hayakawa H. Mitral insufficiency as a complication of acute myocardial infarction and left ventricular remodeling. *Jpn Circ J* 1997;**61**(11):912-920.

46. Feinberg MS, Schwammenthal E, Shlizerman L, Porter A, Hod H, Friemark D, Matezky S, Boyko V, Mandelzweig L, Vered Z, Behar S, Sagie A. Prognostic significance of mild mitral regurgitation by color Doppler echocardiography in acute myocardial infarction. *Am J Cardiol*

2000;**86**(9):903-907.

47. Neskovic AN, Marinkovic J, Bojic M, Popovic AD. Early predictors of mitral regurgitation after acute myocardial infarction. *Am J Cardiol* 1999;**84**(3):329-32, A8.

48. Golia G, Anselmi M, Rossi A, Cicoira MA, Tinto M, Marino P, Zardini P. Relationship between mitral regurgitation and myocardial viability after acute myocardial infarction: their impact on prognosis. *Int J Cardiol* 2001;**78**(1):81-90.

49. Alam M, Thorstrand C, Rosenhamer G. Mitral regurgitation following first-time acute myocardial infarction--early and late findings by Doppler echocardiography. *Clin Cardiol* 1993;**16**(1):30-34.

50. Tada H, Tamai J, Takaki H, Ohnishi E, Okano Y, Yoshioka T. Mild mitral regurgitation reduces exercise capacity in patients with idiopathic dilated cardiomyopathy. *Int J Cardiol* 1997;**58**(1):41-45.

51. Grigioni F, Enriquez-Sarano M, Zehr KJ, Bailey KR, Tajik AJ. Ischemic mitral regurgitation: long-term outcome and prognostic implications with quantitative Doppler assessment. *Circulation* 2001;**103**(13):1759-1764.

52. Grigioni F, Detaint D, Avierinos JF, Scott C, Tajik J, Enriquez-Sarano M. Contribution of ischemic mitral regurgitation to congestive heart failure after myocardial infarction. *J Am Coll Cardiol* 2005;**45**(2):260-267.

53. Ishikawa T, Sumita S, Kimura K, Kuji N, Nakayama R, Nagura T, Miyazaki N, Tochikubo O, Usui T, Kashiwagi M, . Critical PQ interval for the appearance of diastolic mitral regurgitation and optimal PQ interval in patients implanted with DDD pacemakers. *Pacing Clin Electrophysiol* 1994;**17**(11 Pt 2):1989-1994.

54. Ishikawa T, Kimura K, Nihei T, Usui T, Kashiwagi M, Ishii M. Relationship between diastolic mitral regurgitation and PQ intervals or cardiac function in patients implanted with DDD pacemakers. *Pacing Clin Electrophysiol* 1991;**14**(11 Pt 2):1797-1802.

55. Ishikawa T, Kimura K, Miyazaki N, Tochikubo O, Usui T, Kashiwagi M, Ishii

M. Diastolic mitral regurgitation in patients with first-degree atrioventricular block. *Pacing Clin Electrophysiol* 1992;**15**(11 Pt 2):1927-1931.

56. Panidis IP, Ross J, Munley B, Nestico P, Mintz GS. Diastolic mitral regurgitation in patients with atrioventricular conduction abnormalities: a common finding by Doppler echocardiography. *J Am Coll Cardiol* 1986;**7**(4):768-774.

57. Nof E, Glikson M, Bar-Lev D, Gurevitz O, Luria D, Eldar M, Schwammenthal E. Mechanism of diastolic mitral regurgitation in candidates for cardiac resynchronization therapy. *Am J Cardiol* 2006;**97**(11):1611-1614.

58. Borgenhagen DM, Serur JR, Gorlin R, Adams D, Sonnenblick EH. The effects of left ventricular load and contractility on mitral regurgitant orifice size and flow in the dog. *Circulation* 1977;**56**(1):106-113.

59. Yellin EL, Yoran C, Sonnenblick EH, Gabbay S, Frater RW. Dynamic changes in the canine mitral regurgitant orifice area during ventricular ejection. *Circ Res* 1979;**45**(5):677-683.

60. Yoran C, Yellin EL, Becker RM, Gabbay S, Frater RW, Sonnenblick EH. Dynamic aspects of acute mitral regurgitation: effects of ventricular volume, pressure and contractility on the effective regurgitant orifice area. *Circulation* 1979;**60**(1):170-176.

61. Shiota T, Jones M, Teien DE, Yamada I, Passafini A, Ge S, Sahn DJ. Dynamic change in mitral regurgitant orifice area: comparison of color Doppler echocardiographic and electromagnetic flowmeter-based methods in a chronic animal model. *J Am Coll Cardiol* 1995;**26**(2):528-536.

62. Hung J, Otsuji Y, Handschumacher MD, Schwammenthal E, Levine RA. Mechanism of dynamic regurgitant orifice area variation in functional mitral regurgitation: physiologic insights from the proximal flow convergence technique. *J Am Coll Cardiol* 1999;**33**(2):538-545.

63. Schwammenthal E, Chen C, Benning F, Block M, Breithardt G, Levine RA. Dynamics of mitral regurgitant flow and orifice area. Physiologic application of the proximal flow convergence method: clinical data and experimental testing. *Circulation* 1994;**90**(1):307-322.

64. Fukuda S, Grimm R, Song JM, Kihara T, Daimon M, Agler DA, Wilkoff BL, Natale A, Thomas JD, Shiota T. Electrical conduction disturbance effects on dynamic changes of functional mitral regurgitation. *J Am Coll Cardiol* 2005;**46**(12):2270-2276.

65. Schwammenthal E, Popescu AC, Popescu BA, Freimark D, Hod H, Eldar M, Feinberg MS. Mechanism of mitral regurgitation in inferior wall acute myocardial infarction. *Am J Cardiol* 2002;**90**(3):306-309.

66. Lafitte S, Bordachar P, Lafitte M, Garrigue S, Reuter S, Reant P, Serri K, Lebouffos V, Berrhouet M, Jais P, Haissaguerre M, Clementy J, Roudaut R, DeMaria AN. Dynamic ventricular dyssynchrony: an exercise-echocardiography study. *J Am Coll Cardiol* 2006;**47**(11):2253-2259.

67. Lancellotti P, Lebrun F, Pierard LA. Determinants of exercise-induced changes in mitral regurgitation in patients with coronary artery disease and left ventricular dysfunction. *J Am Coll Cardiol* 2003;**42**(11):1921-1928.

68. Lebrun F, Lancellotti P, Pierard LA. Quantitation of functional mitral regurgitation during bicycle exercise in patients with heart failure. *J Am Coll Cardiol* 2001;**38**(6):1685-1692.

69. Lancellotti P, Melon P, Sakalihasan N, Waleffe A, Dubois C, Bertholet M, Pierard LA. Effect of cardiac resynchronization therapy on functional mitral regurgitation in heart failure. *Am J Cardiol* 2004;**94**(11):1462-1465.

70. Lancellotti P, Stainier PY, Lebois F, Pierard LA. Effect of dynamic left ventricular dyssynchrony on dynamic mitral regurgitation in patients with heart failure due to coronary artery disease. *Am J Cardiol* 2005;**96**(9):1304-1307.

71. Ennezat PV, Gal B, Kouakam C, Marquie C, LeTourneau T, Klug D, Lacroix D, Logeart D, Cohen-Solal A, Dennetiere S, Van BE, Deklunder G, Asseman P, de GP, Kacet S, Lejemtel TH. Cardiac resynchronisation therapy reduces functional mitral regurgitation during dynamic exercise in patients with chronic heart failure: an acute echocardiographic study. *Heart* 2006;**92**(8):1091-1095.

72. Bordachar P, Lafitte S, Reuter S, Serri K, Garrigue S, Laborderie J, Reant P,

Jais P, Haissaguerre M, Roudaut R, Clementy J. Echocardiographic assessment during exercise of heart failure patients with cardiac resynchronization therapy. *Am J Cardiol* 2006;**97**(11):1622-1625.

73. Ennezat PV, Marechaux S, Le TT, Lamblin N, Bauters C, Van BE, Gal B, Kacet S, Asseman P, Deklunder G, Lejemtel TH, de GP. Myocardial asynchronism is a determinant of changes in functional mitral regurgitation severity during dynamic exercise in patients with chronic heart failure due to severe left ventricular systolic dysfunction. *Eur Heart J* 2006;**27**(6):679-683.

74. Lancellotti P, Troisfontaines P, Toussaint AC, Pierard LA. Prognostic importance of exercise-induced changes in mitral regurgitation in patients with chronic ischemic left ventricular dysfunction. *Circulation* 2003;**108**(14):1713-1717.

75. Lancellotti P, Gerard PL, Pierard LA. Long-term outcome of patients with heart failure and dynamic functional mitral regurgitation. *Eur Heart J* 2005;**26**(15):1528-1532.

76. Pierard LA, Lancellotti P. The role of ischemic mitral regurgitation in the pathogenesis of acute pulmonary edema. *N Engl J Med* 2004;**351**(16):1627-1634.

77. Ogawa S, Hubbard FE, Mardelli TJ, Dreifus LS. Cross-sectional echocardiographic spectrum of papillary muscle dysfunction. *Am Heart J* 1979;**97**(3):312-321.

78. Godley RW, Wann LS, Rogers EW, Feigenbaum H, Weyman AE. Incomplete mitral leaflet closure in patients with papillary muscle dysfunction. *Circulation* 1981;**63**(3):565-571.

79. Otsuji Y, Gilon D, Jiang L, He S, Leavitt M, Roy MJ, Birmingham MJ, Levine RA. Restricted diastolic opening of the mitral leaflets in patients with left ventricular dysfunction: evidence for increased valve tethering. *J Am Coll Cardiol* 1998;**32**(2):398-404.

80. Glasson JR, Komeda M, Daughters GT, Bolger AF, Karlsson MO, Foppiano LE, Hayase M, Oesterle SN, Ingels NB, Jr., Miller DC. Early systolic mitral leaflet "loitering" during acute ischemic mitral regurgitation. *J Thorac*

Cardiovasc Surg 1998;**116**(2):193-205.

81. Lai DT, Tibayan FA, Myrmel T, Timek TA, Dagum P, Daughters GT, Liang D, Ingels NB, Jr., Miller DC. Mechanistic insights into posterior mitral leaflet inter-scallop malcoaptation during acute ischemic mitral regurgitation. *Circulation* 2002;**106**(12 Suppl 1):I40-I45.

82. Myrmel T, Lai DT, Lo S, Timek TA, Liang D, Miller DC, Ingels NB, Jr., Daughters GT. Ischemia-induced malcoaptation of scallops within the posterior mitral leaflet. *J Heart Valve Dis* 2002;**11**(6):823-829.

83. Yiu SF, Enriquez-Sarano M, Tribouilloy C, Seward JB, Tajik AJ. Determinants of the degree of functional mitral regurgitation in patients with systolic left ventricular dysfunction: A quantitative clinical study. *Circulation* 2000;**102**(12):1400-1406.

84. Agricola E, Oppizzi M, Galderisi M, Pisani M, Meris A, Pappone C, Margonato A. Role of regional mechanical dyssynchrony as a determinant of functional mitral regurgitation in patients with left ventricular systolic dysfunction. *Heart* 2006;**92**(10):1390-1395.

85. Otsuji Y, Handschumacher MD, Schwammenthal E, Jiang L, Song JK, Guerrero JL, Vlahakes GJ, Levine RA. Insights from three-dimensional echocardiography into the mechanism of functional mitral regurgitation: direct in vivo demonstration of altered leaflet tethering geometry. *Circulation* 1997;**96**(6):1999-2008.

86. Otsuji Y, Handschumacher MD, Liel-Cohen N, Tanabe H, Jiang L, Schwammenthal E, Guerrero JL, Nicholls LA, Vlahakes GJ, Levine RA. Mechanism of ischemic mitral regurgitation with segmental left ventricular dysfunction: three-dimensional echocardiographic studies in models of acute and chronic progressive regurgitation. *J Am Coll Cardiol* 2001;**37**(2):641-648.

87. He S, Fontaine AA, Schwammenthal E, Yoganathan AP, Levine RA. Integrated mechanism for functional mitral regurgitation: leaflet restriction versus coapting force: in vitro studies. *Circulation* 1997;**96**(6):1826-1834.

88. Kaul S, Spotnitz WD, Glasheen WP, Touchstone DA. Mechanism of ischemic

mitral regurgitation. An experimental evaluation. *Circulation* 1991;**84**(5):2167-2180.

89. Otsuji Y, Kumanohoso T, Yoshifuku S, Matsukida K, Koriyama C, Kisanuki A, Minagoe S, Levine RA, Tei C. Isolated annular dilation does not usually cause important functional mitral regurgitation: comparison between patients with lone atrial fibrillation and those with idiopathic or ischemic cardiomyopathy. *J Am Coll Cardiol* 2002;**39**(10):1651-1656.

90. Breithardt OA, Sinha AM, Schwammenthal E, Bidaoui N, Markus KU, Franke A, Stellbrink C. Acute effects of cardiac resynchronization therapy on functional mitral regurgitation in advanced systolic heart failure. *J Am Coll Cardiol* 2003;**41**(5):765-770.

91. Kono T, Sabbah HN, Stein PD, Brymer JF, Khaja F. Left ventricular shape as a determinant of functional mitral regurgitation in patients with severe heart failure secondary to either coronary artery disease or idiopathic dilated cardiomyopathy. *Am J Cardiol* 1991;**68**(4):355-359.

92. Kono T, Sabbah HN, Rosman H, Alam M, Jafri S, Goldstein S. Left ventricular shape is the primary determinant of functional mitral regurgitation in heart failure. *J Am Coll Cardiol* 1992;**20**(7):1594-1598.

93. Kono T, Sabbah HN, Rosman H, Alam M, Jafri S, Stein PD, Goldstein S. Mechanism of functional mitral regurgitation during acute myocardial ischemia. *J Am Coll Cardiol* 1992;**19**(5):1101-1105.

94. Sabbah HN, Kono T, Rosman H, Jafri S, Stein PD, Goldstein S. Left ventricular shape: a factor in the etiology of functional mitral regurgitation in heart failure. *Am Heart J* 1992;**123**(4 Pt 1):961-966.

95. Gorman JH, III, Gorman RC, Plappert T, Jackson BM, Hiramatsu Y, St John-Sutton MG, Edmunds LH, Jr. Infarct size and location determine development of mitral regurgitation in the sheep model. *J Thorac Cardiovasc Surg* 1998;**115**(3):615-622.

96. Kumanohoso T, Otsuji Y, Yoshifuku S, Matsukida K, Koriyama C, Kisanuki A, Minagoe S, Levine RA, Tei C. Mechanism of higher incidence of ischemic mitral regurgitation in patients with inferior myocardial infarction:

quantitative analysis of left ventricular and mitral valve geometry in 103 patients with prior myocardial infarction. *J Thorac Cardiovasc Surg* 2003;**125**(1):135-143.

97. Gorman RC, McCaughan JS, Ratcliffe MB, Gupta KB, Streicher JT, Ferrari VA, St John-Sutton MG, Bogen DK, Edmunds LH, Jr. Pathogenesis of acute ischemic mitral regurgitation in three dimensions. *J Thorac Cardiovasc Surg* 1995;**109**(4):684-693.

98. Agricola E, Oppizzi M, Maisano F, De BM, Schinkel AF, Torracca L, Margonato A, Melisurgo G, Alfieri O. Echocardiographic classification of chronic ischemic mitral regurgitation caused by restricted motion according to tethering pattern. *Eur J Echocardiogr* 2004;**5**(5):326-334.

99. Watanabe N, Ogasawara Y, Yamaura Y, Yamamoto K, Wada N, Kawamoto T, Toyota E, Akasaka T, Yoshida K. Geometric differences of the mitral valve tenting between anterior and inferior myocardial infarction with significant ischemic mitral regurgitation: quantitation by novel software system with transthoracic real-time three-dimensional echocardiography. *J Am Soc Echocardiogr* 2006;**19**(1):71-75.

100. Messas E, Guerrero JL, Handschumacher MD, Conrad C, Chow CM, Sullivan S, Yoganathan AP, Levine RA. Chordal cutting: a new therapeutic approach for ischemic mitral regurgitation. *Circulation* 2001;**104**(16):1958-1963.

101. Nesta F, Otsuji Y, Handschumacher MD, Messas E, Leavitt M, Carpentier A, Levine RA, Hung J. Leaflet concavity: a rapid visual clue to the presence and mechanism of functional mitral regurgitation. *J Am Soc Echocardiogr* 2003;**16**(12):1301-1308.

102. Tibayan FA, Rodriguez F, Zasio MK, Bailey L, Liang D, Daughters GT, Langer F, Ingels NB, Jr., Miller DC. Geometric distortions of the mitral valvular-ventricular complex in chronic ischemic mitral regurgitation. *Circulation* 2003;**108 Suppl 1**:II116-II121.

103. Green GR, Dagum P, Glasson JR, Daughters GT, Bolger AF, Foppiano LE, Berry GJ, Ingels NB, Jr., Miller DC. Mitral annular dilatation and papillary muscle dislocation without mitral regurgitation in sheep. *Circulation*

1999;**100**(19 Suppl):II95-102.

104. Watanabe N, Ogasawara Y, Yamaura Y, Wada N, Kawamoto T, Toyota E, Akasaka T, Yoshida K. Mitral annulus flattens in ischemic mitral regurgitation: geometric differences between inferior and anterior myocardial infarction: a real-time 3-dimensional echocardiographic study. *Circulation* 2005;**112**(9 Suppl):I458-I462.

105. Flachskampf FA, Chandra S, Gaddipatti A, Levine RA, Weyman AE, Ameling W, Hanrath P, Thomas JD. Analysis of shape and motion of the mitral annulus in subjects with and without cardiomyopathy by echocardiographic 3-dimensional reconstruction. *J Am Soc Echocardiogr* 2000;**13**(4):277-287.

106. De SR, Wolf I, Mottl-Link S, Hoda R, Mikhail B, Sack FU, Meinzer HP, Hagl S. A clinical study of annular geometry and dynamics in patients with ischemic mitral regurgitation: new insights into asymmetrical ring annuloplasty. *Eur J Cardiothorac Surg* 2006;**29**(3):355-361.

107. He S, Lemmon JD, Jr., Weston MW, Jensen MO, Levine RA, Yoganathan AP. Mitral valve compensation for annular dilatation: in vitro study into the mechanisms of functional mitral regurgitation with an adjustable annulus model. *J Heart Valve Dis* 1999;**8**(3):294-302.

108. Hung J, Papakostas L, Tahta SA, Hardy BG, Bollen BA, Duran CM, Levine RA. Mechanism of recurrent ischemic mitral regurgitation after annuloplasty: continued LV remodeling as a moving target. *Circulation* 2004;**110**(11 Suppl 1):II85-II90.

109. Magne J, Pibarot P, Dagenais F, Hachicha Z, Dumesnil JG, Senechal M. Preoperative posterior leaflet angle accurately predicts outcome after restrictive mitral valve annuloplasty for ischemic mitral regurgitation. *Circulation* 2007;**115**(6):782-791.

110. Zhu F, Otsuji Y, Yotsumoto G, Yuasa T, Ueno T, Yu B, Koriyama C, Hamasaki S, Biro S, Kisanuki A, Minagoe S, Levine RA, Sakata R, Tei C. Mechanism of persistent ischemic mitral regurgitation after annuloplasty: importance of augmented posterior mitral leaflet tethering. *Circulation* 2005;**112**(9 Suppl):I396-I401.

111. Kuwahara E, Otsuji Y, Iguro Y, Ueno T, Zhu F, Mizukami N, Kubota K, Nakashiki K, Yuasa T, Yu B, Uemura T, Takasaki K, Miyata M, Hamasaki S, Kisanuki A, Levine RA, Sakata R, Tei C. Mechanism of recurrent/persistent ischemic/functional mitral regurgitation in the chronic phase after surgical annuloplasty: importance of augmented posterior leaflet tethering. *Circulation* 2006;**114**(1 Suppl):I529-I534.

112. Jouan J, Tapia M, Cook C, Lansac E, Acar C. Ischemic mitral valve prolapse: mechanisms and implications for valve repair. *Eur J Cardiothorac Surg* 2004;**26**(6):1112-1117.

113. Tei C, Sakamaki T, Shah PM, Meerbaum S, Kondo S, Shimoura K, Corday E. Mitral valve prolapse in short-term experimental coronary occlusion: a possible mechanism of ischemic mitral regurgitation. *Circulation* 1983;**68**(1):183-189.

114. Izumi S, Miyatake K, Beppu S, Park YD, Nagata S, Kinoshita N, Sakakibara H, Nimura Y. Mechanism of mitral regurgitation in patients with myocardial infarction: a study using real-time two-dimensional Doppler flow imaging and echocardiography. *Circulation* 1987;**76**(4):777-785.

115. Miller GE, Jr., Kerth WJ, Gerbode F. Experimental papillary muscle infarction. *J Thorac Cardiovasc Surg* 1968;**56**(5):611-616.

116. Mittal AK, Langston M, Jr., Cohn KE, Selzer A, Kerth WJ. Combined papillary muscle and left ventricular wall dysfunction as a cause of mitral regurgitation. An experimental study. *Circulation* 1971;**44**(2):174-180.

117. Matsuzaki M, Yonezawa F, Toma Y, Miura T, Katayama K, Fujii T, Kohtoku N, Otani N, Ono S, Tateno S, . [Experimental mitral regurgitation in ischemia-induced papillary muscle dysfunction]. *J Cardiol Suppl* 1988;**18**:121-6, discussion.

118. Messas E, Guerrero JL, Handschumacher MD, Chow CM, Sullivan S, Schwammenthal E, Levine RA. Paradoxic decrease in ischemic mitral regurgitation with papillary muscle dysfunction: insights from three-dimensional and contrast echocardiography with strain rate measurement. *Circulation* 2001;**104**(16):1952-1957.

119. Khankirawatana B, Khankirawatana S, Mahrous H, Porter TR. Assessment of papillary muscle function using myocardial velocity gradient derived from tissue Doppler echocardiography. *Am J Cardiol* 2004;**94**(1):45-49.

120. Kanzaki H, Bazaz R, Schwartzman D, Dohi K, Sade LE, Gorcsan J, III. A mechanism for immediate reduction in mitral regurgitation after cardiac resynchronization therapy: insights from mechanical activation strain mapping. *J Am Coll Cardiol* 2004;**44**(8):1619-1625.

121. Ypenburg C, Lancellotti P, Tops LF, Bleeker GB, Holman ER, Pierard LA, Schalij MJ, Bax JJ. Acute effects of initiation and withdrawal of cardiac resynchronization therapy on papillary muscle dyssynchrony and mitral regurgitation. *J Am Coll Cardiol* 2007;**50**(21):2071-2077.

122. Ypenburg C, Lancellotti P, Tops LF, Boersma E, Bleeker GB, Holman ER, Thomas JD, Schalij MJ, Pierard LA, Bax JJ. Mechanism of improvement in mitral regurgitation after cardiac resynchronization therapy. *Eur Heart J* 2008;**29**(6):757-765.

123. Erlebacher JA, Barbarash S. Intraventricular conduction delay and functional mitral regurgitation. *Am J Cardiol* 2001;**88**(1):A7, 83-A7, 86.

124. Maurer G, Torres MA, Corday E, Haendchen RV, Meerbaum S. Two-dimensional echocardiographic contrast assessment of pacing-induced mitral regurgitation: relation to altered regional left ventricular function. *J Am Coll Cardiol* 1984;**3**(4):986-991.

125. Soyama A, Kono T, Mishima T, Morita H, Ito T, Suwa M, Kitaura Y. Intraventricular dyssynchrony may play a role in the development of mitral regurgitation in dilated cardiomyopathy. *J Card Fail* 2005;**11**(8):631-637.

126. van dL, V, Germans T, van DJ, Zwanenburg JJ, Spreeuwenberg M, Marcus JT, Kamp O, Gotte MJ, van Rossum AC. The effect of left bundle branch block on left ventricular remodeling, dyssynchrony and deformation of the mitral valve apparatus: an observational cardiovascular magnetic resonance imaging study. *Int J Cardiovasc Imaging* 2007;**23**(4):529-536.

127. Langer F, Tibayan FA, Rodriguez F, Timek T, Zasio MK, Liang D, Daughters GT, Ingels NB, Miller DC. Altered mitral valve kinematics with

atrioventricular and ventricular pacing. *J Heart Valve Dis* 2005;**14**(3):286-294.

128. Szymanski P, Klisiewicz A, Hoffman P. Asynchronous movement of mitral annulus: an additional mechanism of ischaemic mitral regurgitation. *Clin Cardiol* 2007;**30**(10):512-516.

129. D'Andrea A, Caso P, Cuomo S, Scarafile R, Salerno G, Limongelli G, Di SG, Severino S, Ascione L, Calabro P, Romano M, Romano G, Santangelo L, Maiello C, Cotrufo M, Calabro R. Effect of dynamic myocardial dyssynchrony on mitral regurgitation during supine bicycle exercise stress echocardiography in patients with idiopathic dilated cardiomyopathy and 'narrow' QRS. *Eur Heart J* 2007;**28**(8):1004-1011.

130. Keren G, Bier A, Strom JA, Laniado S, Sonnenblick EH, Lejemtel TH. Dynamics of mitral regurgitation during nitroglycerin therapy: a Doppler echocardiographic study. *Am Heart J* 1986;**112**(3):517-525.

131. Stevenson LW, Bellil D, Grover-McKay M, Brunken RC, Schwaiger M, Tillisch JH, Schelbert HR. Effects of afterload reduction (diuretics and vasodilators) on left ventricular volume and mitral regurgitation in severe congestive heart failure secondary to ischemic or idiopathic dilated cardiomyopathy. *Am J Cardiol* 1987;**60**(8):654-658.

132. Heinle SK, Tice FD, Kisslo J. Effect of dobutamine stress echocardiography on mitral regurgitation. *J Am Coll Cardiol* 1995;**25**(1):122-127.

133. Levine AB, Muller C, Levine TB. Effects of high-dose lisinopril-isosorbide dinitrate on severe mitral regurgitation and heart failure remodeling. *Am J Cardiol* 1998;**82**(10):1299-301, A10.

134. Hamilton MA, Stevenson LW, Child JS, Moriguchi JD, Walden J, Woo M. Sustained reduction in valvular regurgitation and atrial volumes with tailored vasodilator therapy in advanced congestive heart failure secondary to dilated (ischemic or idiopathic) cardiomyopathy. *Am J Cardiol* 1991;**67**(4):259-263.

135. Lowes BD, Gill EA, Abraham WT, Larrain JR, Robertson AD, Bristow MR, Gilbert EM. Effects of carvedilol on left ventricular mass, chamber geometry, and mitral regurgitation in chronic heart failure. *Am J Cardiol*

1999;**83**(8):1201-1205.

136. Capomolla S, Febo O, Gnemmi M, Riccardi G, Opasich C, Caporotondi A, Mortara A, Pinna GD, Cobelli F. Beta-blockade therapy in chronic heart failure: diastolic function and mitral regurgitation improvement by carvedilol. *Am Heart J* 2000;**139**(4):596-608.

137. Braun J, Bax JJ, Versteegh MI, Voigt PG, Holman ER, Klautz RJ, Boersma E, Dion RA. Preoperative left ventricular dimensions predict reverse remodeling following restrictive mitral annuloplasty in ischemic mitral regurgitation. *Eur J Cardiothorac Surg* 2005;**27**(5):847-853.

138. Hung J, Guerrero JL, Handschumacher MD, Supple G, Sullivan S, Levine RA. Reverse ventricular remodeling reduces ischemic mitral regurgitation: echo-guided device application in the beating heart. *Circulation* 2002;**106**(20):2594-2600.

139. Moainie SL, Guy TS, Gorman JH, III, Plappert T, Jackson BM, St John-Sutton MG, Edmunds LH, Jr., Gorman RC. Infarct restraint attenuates remodeling and reduces chronic ischemic mitral regurgitation after postero-lateral infarction. *Ann Thorac Surg* 2002;**74**(2):444-449.

140. Menicanti L, Di DM, Frigiola A, Buckberg G, Santambrogio C, Ranucci M, Santo D. Ischemic mitral regurgitation: intraventricular papillary muscle imbrication without mitral ring during left ventricular restoration. *J Thorac Cardiovasc Surg* 2002;**123**(6):1041-1050.

141. Kaza AK, Patel MR, Fiser SM, Long SM, Kern JA, Tribble CG, Kron IL. Ventricular reconstruction results in improved left ventricular function and amelioration of mitral insufficiency. *Ann Surg* 2002;**235**(6):828-832.

142. Liel-Cohen N, Guerrero JL, Otsuji Y, Handschumacher MD, Rudski LG, Hunziker PR, Tanabe H, Scherrer-Crosbie M, Sullivan S, Levine RA. Design of a new surgical approach for ventricular remodeling to relieve ischemic mitral regurgitation: insights from 3-dimensional echocardiography. *Circulation* 2000;**101**(23):2756-2763.

143. Yu CM, Lin H, Zhang Q, Sanderson JE. High prevalence of left ventricular systolic and diastolic asynchrony in patients with congestive heart failure and

normal QRS duration. *Heart* 2003;**89**(1):54-60.

144. Bleeker GB, Schalij MJ, Molhoek SG, Verwey HF, Holman ER, Boersma E, Steendijk P, van der Wall EE, Bax JJ. Relationship between QRS duration and left ventricular dyssynchrony in patients with end-stage heart failure. *J Cardiovasc Electrophysiol* 2004;**15**(5):544-549.

145. Ghio S, Constantin C, Klersy C, Serio A, Fontana A, Campana C, Tavazzi L. Interventricular and intraventricular dyssynchrony are common in heart failure patients, regardless of QRS duration. *Eur Heart J* 2004;**25**(7):571-578.

146. Hunt SA, Abraham WT, Chin MH, Feldman AM, Francis GS, Ganiats TG, Jessup M, Konstam MA, Mancini DM, Michl K, Oates JA, Rahko PS, Silver MA, Stevenson LW, Yancy CW. 2009 Focused update incorporated into the ACC/AHA 2005 Guidelines for the Diagnosis and Management of Heart Failure in Adults A Report of the American College of Cardiology Foundation/American Heart Association Task Force on Practice Guidelines Developed in Collaboration With the International Society for Heart and Lung Transplantation. *J Am Coll Cardiol* 2009;**53**(15):e1-e90.

147. Cazeau S, Ritter P, Bakdach S, Lazarus A, Limousin M, Henao L, Mundler O, Daubert JC, Mugica J. Four chamber pacing in dilated cardiomyopathy. *Pacing Clin Electrophysiol* 1994;**17**(11 Pt 2):1974-1979.

148. Cazeau S, Leclercq C, Lavergne T, Walker S, Varma C, Linde C, Garrigue S, Kappenberger L, Haywood GA, Santini M, Bailleul C, Daubert JC. Effects of multisite biventricular pacing in patients with heart failure and intraventricular conduction delay. *N Engl J Med* 2001;**344**(12):873-880.

149. Abraham WT, Fisher WG, Smith AL, DeLurgio DB, Leon AR, Loh E, Kocovic DZ, Packer M, Clavell AL, Hayes DL, Ellestad M, Trupp RJ, Underwood J, Pickering F, Truex C, McAtee P, Messenger J. Cardiac resynchronization in chronic heart failure. *N Engl J Med* 2002;**346**(24):1845-1853.

150. Gras D, Leclercq C, Tang AS, Bucknall C, Luttikhuis HO, Kirstein-Pedersen A. Cardiac resynchronization therapy in advanced heart failure the multicenter InSync clinical study. *Eur J Heart Fail* 2002;**4**(3):311-320.

151. Yu CM, Chau E, Sanderson JE, Fan K, Tang MO, Fung WH, Lin H, Kong SL, Lam YM, Hill MR, Lau CP. Tissue Doppler echocardiographic evidence of reverse remodeling and improved synchronicity by simultaneously delaying regional contraction after biventricular pacing therapy in heart failure. *Circulation* 2002;**105**(4):438-445.

152. St John Sutton MG, Plappert T, Abraham WT, Smith AL, DeLurgio DB, Leon AR, Loh E, Kocovic DZ, Fisher WG, Ellestad M, Messenger J, Kruger K, Hilpisch KE, Hill MR. Effect of cardiac resynchronization therapy on left ventricular size and function in chronic heart failure. *Circulation* 2003;**107**(15):1985-1990.

153. Bradley DJ, Bradley EA, Baughman KL, Berger RD, Calkins H, Goodman SN, Kass DA, Powe NR. Cardiac resynchronization and death from progressive heart failure: a meta-analysis of randomized controlled trials. *JAMA* 2003;**289**(6):730-740.

154. Bristow MR, Saxon LA, Boehmer J, Krueger S, Kass DA, De MT, Carson P, DiCarlo L, DeMets D, White BG, DeVries DW, Feldman AM. Cardiac-resynchronization therapy with or without an implantable defibrillator in advanced chronic heart failure. *N Engl J Med* 2004;**350**(21):2140-2150.

155. Cleland JG, Daubert JC, Erdmann E, Freemantle N, Gras D, Kappenberger L, Tavazzi L. The effect of cardiac resynchronization on morbidity and mortality in heart failure. *N Engl J Med* 2005;**352**(15):1539-1549.

156. Saxon LA, De MT, Schafer J, Chatterjee K, Kumar UN, Foster E. Effects of long-term biventricular stimulation for resynchronization on echocardiographic measures of remodeling. *Circulation* 2002;**105**(11):1304-1310.

157. Zhang Q, Fung JW, Auricchio A, Chan JY, Kum LC, Wu LW, Yu CM. Differential change in left ventricular mass and regional wall thickness after cardiac resynchronization therapy for heart failure. *Eur Heart J* 2006;**27**(12):1423-1430.

158. Yu CM, Bleeker GB, Fung JW, Schalij MJ, Zhang Q, van der Wall EE, Chan YS, Kong SL, Bax JJ. Left ventricular reverse remodeling but not clinical

improvement predicts long-term survival after cardiac resynchronization therapy. *Circulation* 2005;**112**(11):1580-1586.

159. Duncan A, Wait D, Gibson D, Daubert JC. Left ventricular remodelling and haemodynamic effects of multisite biventricular pacing in patients with left ventricular systolic dysfunction and activation disturbances in sinus rhythm: sub-study of the MUSTIC (Multisite Stimulationin Cardiomyopathies) trial. *Eur Heart J* 2003;**24**(5):430-441.

160. Brandt RR, Reiner C, Arnold R, Sperzel J, Pitschner HF, Hamm CW. Contractile response and mitral regurgitation after temporary interruption of long-term cardiac resynchronization therapy. *Eur Heart J* 2006;**27**(2):187-192.

161. Vinereanu D, Bleasdale R, Turner M, Frenneaux MP, Fraser AG. Comparison of left ventricular-biventricular pacing on ventricular synchrony, mitral regurgitation, and global left ventricular function in patients with severe chronic heart failure. *Am J Cardiol* 2004;**94**(4):519-521.

162. Bordachar P, Lafitte S, Reuter S, Garrigue S, Sanders P, Roudaut R, Jais P, Haissaguerre M, Clementy J. Biventricular pacing and left ventricular pacing in heart failure: similar hemodynamic improvement despite marked electromechanical differences. *J Cardiovasc Electrophysiol* 2004;**15**(12):1342-1347.

163. Rao RK, Kumar UN, Schafer J, Viloria E, De LD, Foster E. Reduced ventricular volumes and improved systolic function with cardiac resynchronization therapy: a randomized trial comparing simultaneous biventricular pacing, sequential biventricular pacing, and left ventricular pacing. *Circulation* 2007;**115**(16):2136-2144.

164. Sutton MG, Plappert T, Hilpisch KE, Abraham WT, Hayes DL, Chinchoy E. Sustained reverse left ventricular structural remodeling with cardiac resynchronization at one year is a function of etiology: quantitative Doppler echocardiographic evidence from the Multicenter InSync Randomized Clinical Evaluation (MIRACLE). *Circulation* 2006;**113**(2):266-272.

165. Delnoy PP, Ottervanger JP, Luttikhuis HO, Elvan A, Misier AR, Beukema WP, van Hemel NM. Comparison of usefulness of cardiac resynchronization

therapy in patients with atrial fibrillation and heart failure versus patients with sinus rhythm and heart failure. *Am J Cardiol* 2007;**99**(9):1252-1257.

166. Yu CM, Chan YS, Zhang Q, Yip GW, Chan CK, Kum LC, Wu L, Lee AP, Lam YY, Fung JW. Benefits of cardiac resynchronization therapy for heart failure patients with narrow QRS complexes and coexisting systolic asynchrony by echocardiography. *J Am Coll Cardiol* 2006;**48**(11):2251-2257.

167. Madaric J, Vanderheyden M, Van LC, Verhamme K, Feys A, Goethals M, Verstreken S, Geelen P, Penicka M, De BB, Bartunek J. Early and late effects of cardiac resynchronization therapy on exercise-induced mitral regurgitation: relationship with left ventricular dyssynchrony, remodelling and cardiopulmonary performance. *Eur Heart J* 2007;**28**(17):2134-2141.

168. Vinereanu D, Turner MS, Bleasdale RA, Mumford CE, Cinteza M, Frenneaux MP, Fraser AG. Mechanisms of reduction of mitral regurgitation by cardiac resynchronization therapy. *J Am Soc Echocardiogr* 2007;**20**(1):54-62.

169. Macioce R, Cappelli F, Demarchi G, Lilli A, Ricciardi G, Pieragnoli P, Colella A, Michelucci A, Porciani MC, Padeletti L. Resynchronization of mitral valve annular segments reduces functional mitral regurgitation in cardiac resynchronization therapy. *Minerva Cardioangiol* 2005;**53**(4):329-333.

170. Naqvi TZ, Rafique AM, Swerdlow C, Verma S, Siegel RJ, Tolstrup K, Kerwin W, Goodman J, Gallik D, Gang E, Peter CT. Predictors of reduction in mitral regurgitation in patients undergoing cardiac resynchronisation treatment. *Heart* 2008;**94**(12):1580-1588.

171. Goland S, Rafique AM, Mirocha J, Siegel RJ, Naqvi TZ. Reduction in mitral regurgitation in patients undergoing cardiac resynchronization treatment: assessment of predictors by two-dimensional radial strain echocardiography. *Echocardiography* 2009;**26**(4):420-430.

172. Yu CM, Wing-Hong FJ, Zhang Q, Sanderson JE. Understanding nonresponders of cardiac resynchronization therapy--current and future perspectives. *J Cardiovasc Electrophysiol* 2005;**16**(10):1117-1124.

173. Yu CM, Fung WH, Lin H, Zhang Q, Sanderson JE, Lau CP. Predictors of left ventricular reverse remodeling after cardiac resynchronization therapy for

heart failure secondary to idiopathic dilated or ischemic cardiomyopathy. *Am J Cardiol* 2003;**91**(6):684-688.

174. az-Infante E, Mont L, Leal J, Garcia-Bolao I, Fernandez-Lozano I, Hernandez-Madrid A, Perez-Castellano N, Sitges M, Pavon-Jimenez R, Barba J, Cavero MA, Moya JL, Perez-Isla L, Brugada J. Predictors of lack of response to resynchronization therapy. *Am J Cardiol* 2005;**95**(12):1436-1440.

175. Cabrera-Bueno F, Garcia-Pinilla JM, Pena-Hernandez J, Jimenez-Navarro M, Gomez-Doblas JJ, Barrera-Cordero A, zueta-Rodriguez J, de Teresa-Galvan E. Repercussion of functional mitral regurgitation on reverse remodelling in cardiac resynchronization therapy. *Europace* 2007;**9**(9):757-761.

176. Reuter S, Garrigue S, Barold SS, Jais P, Hocini M, Haissaguerre M, Clementy J. Comparison of characteristics in responders versus nonresponders with biventricular pacing for drug-resistant congestive heart failure. *Am J Cardiol* 2002;**89**(3):346-350.

177. Daubert JC, Ritter P, Le BH, Gras D, Leclercq C, Lazarus A, Mugica J, Mabo P, Cazeau S. Permanent left ventricular pacing with transvenous leads inserted into the coronary veins. *Pacing Clin Electrophysiol* 1998;**21**(1 Pt 2):239-245.

178. Ritter P, Padeletti L, Gillio-Meina L, Gaggini G. Determination of the optimal atrioventricular delay in DDD pacing. Comparison between echo and peak endocardial acceleration measurements. *Europace* 1999;**1**(2):126-130.

179. Zoghbi WA, Enriquez-Sarano M, Foster E, Grayburn PA, Kraft CD, Levine RA, Nihoyannopoulos P, Otto CM, Quinones MA, Rakowski H, Stewart WJ, Waggoner A, Weissman NJ. Recommendations for evaluation of the severity of native valvular regurgitation with two-dimensional and Doppler echocardiography. *J Am Soc Echocardiogr* 2003;**16**(7):777-802.

180. Quinones MA, Otto CM, Stoddard M, Waggoner A, Zoghbi WA. Recommendations for quantification of Doppler echocardiography: a report from the Doppler Quantification Task Force of the Nomenclature and Standards Committee of the American Society of Echocardiography. *J Am Soc Echocardiogr* 2002;**15**(2):167-184.

181. Schiller NB, Shah PM, Crawford M, DeMaria A, Devereux R, Feigenbaum H, Gutgesell H, Reichek N, Sahn D, Schnittger I, . Recommendations for quantitation of the left ventricle by two-dimensional echocardiography. American Society of Echocardiography Committee on Standards, Subcommittee on Quantitation of Two-Dimensional Echocardiograms. *J Am Soc Echocardiogr* 1989;**2**(5):358-367.

182. Yu CM, Yang H, Lau CP, Wang Q, Wang S, Lam L, Sanderson JE. Regional left ventricle mechanical asynchrony in patients with heart disease and normal QRS duration: implication for biventricular pacing therapy. *Pacing Clin Electrophysiol* 2003;**26**(2 Pt 1):562-570.

183. Pai RG, Gill KS. Amplitudes, durations, and timings of apically directed left ventricular myocardial velocities: II. Systolic and diastolic asynchrony in patients with left ventricular hypertrophy. *J Am Soc Echocardiogr* 1998;**11**(2):112-118.

184. Yu CM, Fung JW, Zhang Q, Chan CK, Chan YS, Lin H, Kum LC, Kong SL, Zhang Y, Sanderson JE. Tissue Doppler imaging is superior to strain rate imaging and postsystolic shortening on the prediction of reverse remodeling in both ischemic and nonischemic heart failure after cardiac resynchronization therapy. *Circulation* 2004;**110**(1):66-73.

185. Yu CM, Gorcsan J, III, Bleeker GB, Zhang Q, Schalij MJ, Suffoletto MS, Fung JW, Schwartzman D, Chan YS, Tanabe M, Bax JJ. Usefulness of tissue Doppler velocity and strain dyssynchrony for predicting left ventricular reverse remodeling response after cardiac resynchronization therapy. *Am J Cardiol* 2007;**100**(8):1263-1270.

186. Bader H, Garrigue S, Lafitte S, Reuter S, Jais P, Haissaguerre M, Bonnet J, Clementy J, Roudaut R. Intra-left ventricular electromechanical asynchrony. A new independent predictor of severe cardiac events in heart failure patients. *J Am Coll Cardiol* 2004;**43**(2):248-256.

187. Song JM, Fukuda S, Kihara T, Shin MS, Garcia MJ, Thomas JD, Shiota T. Value of mitral valve tenting volume determined by real-time three-dimensional echocardiography in patients with functional mitral regurgitation. *Am J Cardiol* 2006;**98**(8):1088-1093.

188. Bax JJ, Bleeker GB, Marwick TH, Molhoek SG, Boersma E, Steendijk P, van der Wall EE, Schalij MJ. Left ventricular dyssynchrony predicts response and prognosis after cardiac resynchronization therapy. *J Am Coll Cardiol* 2004;**44**(9):1834-1840.

189. Bax JJ, Marwick TH, Molhoek SG, Bleeker GB, van EL, Boersma E, Steendijk P, van der Wall EE, Schalij MJ. Left ventricular dyssynchrony predicts benefit of cardiac resynchronization therapy in patients with end-stage heart failure before pacemaker implantation. *Am J Cardiol* 2003;**92**(10):1238-1240.

190. Tibayan FA, Lai DT, Timek TA, Dagum P, Liang D, Daughters GT, Ingels NB, Miller DC. Alterations in left ventricular torsion in tachycardia-induced dilated cardiomyopathy. *J Thorac Cardiovasc Surg* 2002;**124**(1):43-49.

191. Meluzin J, Spinarova L, Hude P, Krejci J, Poloczkova H, Podrouzkova H, Pesl M, Orban M, Dusek L, Korinek J. Left ventricular mechanics in idiopathic dilated cardiomyopathy: systolic-diastolic coupling and torsion. *J Am Soc Echocardiogr* 2009;**22**(5):486-493.

192. Sengupta PP, Korinek J, Belohlavek M, Narula J, Vannan MA, Jahangir A, Khandheria BK. Left ventricular structure and function: basic science for cardiac imaging. *J Am Coll Cardiol* 2006;**48**(10):1988-2001.

193. Greenbaum RA, Ho SY, Gibson DG, Becker AE, Anderson RH. Left ventricular fibre architecture in man. *Br Heart J* 1981;**45**(3):248-263.

194. Nagueh SF, McFalls J, Meyer D, Hill R, Zoghbi WA, Tam JW, Quinones MA, Roberts R, Marian AJ. Tissue Doppler imaging predicts the development of hypertrophic cardiomyopathy in subjects with subclinical disease. *Circulation* 2003;**108**(4):395-398.

195. Kosmala W, Plaksej R, Strotmann JM, Weigel C, Herrmann S, Niemann M, Mende H, Stork S, Angermann CE, Wagner JA, Weidemann F. Progression of left ventricular functional abnormalities in hypertensive patients with heart failure: an ultrasonic two-dimensional speckle tracking study. *J Am Soc Echocardiogr* 2008;**21**(12):1309-1317.

196. Bach DS, Bolling SF. Improvement following correction of secondary mitral

regurgitation in end-stage cardiomyopathy with mitral annuloplasty. *Am J Cardiol* 1996;**78**(8):966-969.

197. Bax JJ, Braun J, Somer ST, Klautz R, Holman ER, Versteegh MI, Boersma E, Schalij MJ, van der Wall EE, Dion RA. Restrictive annuloplasty and coronary revascularization in ischemic mitral regurgitation results in reverse left ventricular remodeling. *Circulation* 2004;**110**(11 Suppl 1):II103-II108.

198. Karvounis HI, Dalamaga EG, Papadopoulos CE, Karamitsos TD, Vassilikos V, Paraskevaidis S, Styliadis IH, Parharidis GE, Louridas GE. Improved papillary muscle function attenuates functional mitral regurgitation in patients with dilated cardiomyopathy after cardiac resynchronization therapy. *J Am Soc Echocardiogr* 2006;**19**(9):1150-1157.